UiT The Arctic University of Norway

Faculty of Science and Technology

Department of Geosciences

Pre-Last Glacial Maximum glaciations in the Barents Sea: seismic investigations

Nikolitsa Alexandropoulou

A dissertation for the degree of Philosophiae Doctor - June 2024

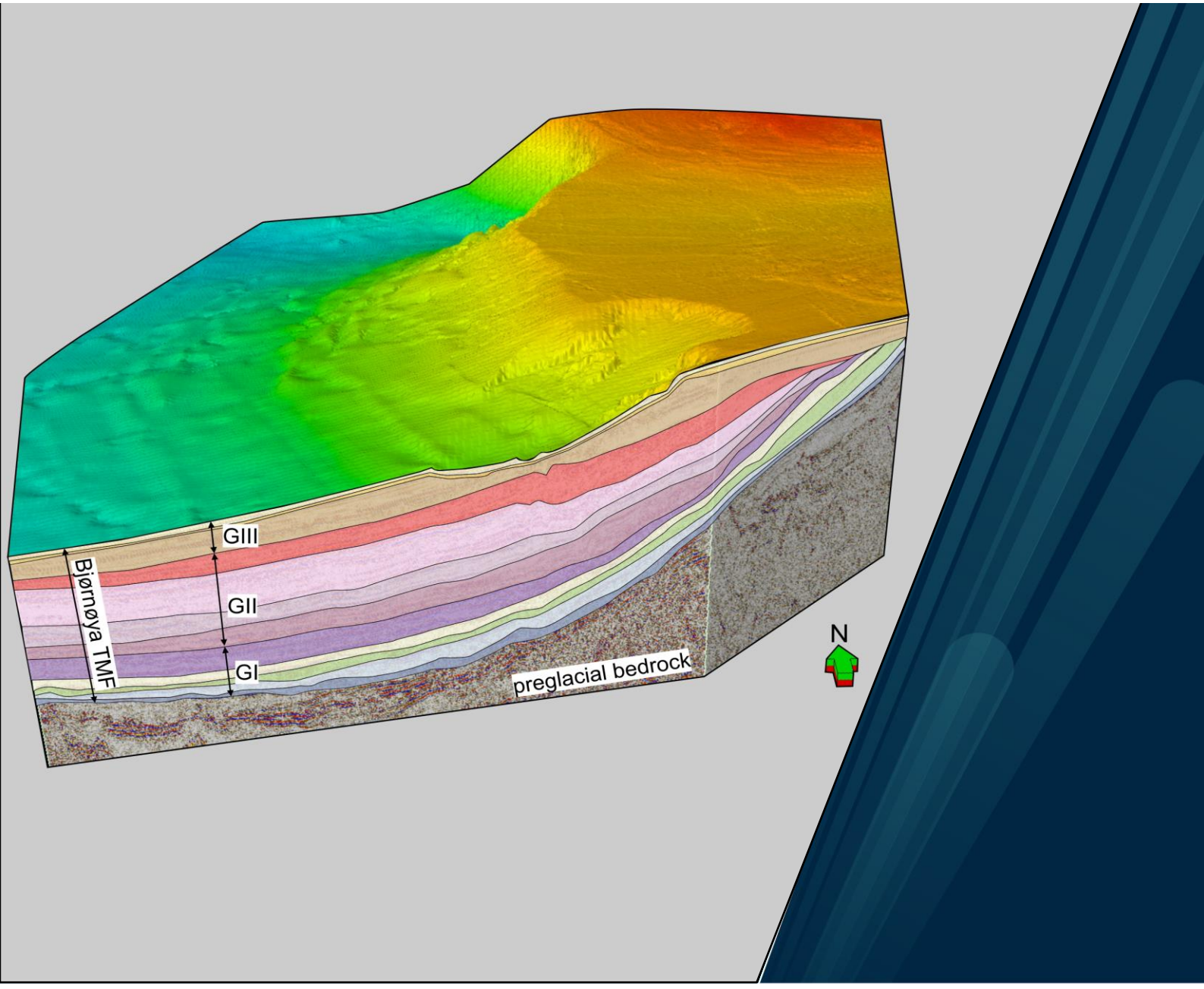

Pre-Last Glacial Maximum glaciations in the Barents Sea: seismic investigations

Nikolitsa Alexandropoulou

A dissertation for the degree of Philosophiae Doctor

UiT The Arctic University of Norway

Faculty of Science and Technology

Department of Geosciences

June 2024

UiT The Arctic University of Norway

Supervisors:

Professor Emerita Karin Andreassen (main supervisor)
Department of Geosciences
Faculty of Science and Technology
UiT The Arctic University of Norway, Tromsø, Norway

Assoc. Professor Monica Winsborrow (co-supervisor)
Department of Geosciences
Faculty of Science and Technology
UiT The Arctic University of Norway, Tromsø, Norway

Assoc. Professor Andreia Aletia Plaza-Faverola (co-supervisor)
Department of Geosciences
Faculty of Science and Technology
UiT The Arctic University of Norway, Tromsø, Norway

Front page image: Composite profile crossing the Bjørnøya (Bear Island) Trough-Mouth Fan, southwestern Barents Sea showing the seismic stratigraphy of the Plio-Pleistocene glacigenic sediment (Fiedler and Faleide 1996; Paper 1).

Preface

The work forming the basis for this PhD thesis was carried out at the Department of Geosciences, UiT The Arctic University of Norway, Tromsø (UiT), under the supervision of Professor Karin Andreassen (main supervisor), Assoc. Prof. Monica Winsborrow (co-supervisor/medveileder) and Assoc. Prof. Andreia Aletia Plaza-Faverola (co-supervisor/biveileder). I worked on this doctoral degree thesis from 2014 to 2023, including two maternity leaves in 2015-2016 and 2018-2019. The PhD was funded by the Department of Geosciences at the UiT.

The position was connected to the research group in Polar Marine Geology and Geophysics at the Department of Geosciences, UiT and was affiliated to the Norwegian Research Council funded Centre of Excellence in Arctic Gas Hydrate, Environment and Climate (CAGE), hosted at the same department. The project was part of the Research School "Arctic Marine Geology and Geophysics" (AMGG), which was organized by UiT in collaboration with The Norwegian Polar Institute, The University Centre in Svalbard (UNIS) and The Geological Survey of Norway (NGU). It was also connected to the national Norwegian research schools "Climate Dynamics (ResClim)" and "Changing climates in the coupled earth system (CHESS)". As a doctoral candidate at the Department of Geosciences, 25% of the four-year funded period was dedicated to duty work. During my PhD period, I had the opportunity to participate in four research cruises, on board RV *Helmer Hanssen* and RV *Kronprins Haakon*. In one of them, together with the cruise leader-main PhD supervisor Karin Andreassen, we acquired 2D seismic lines on the Yermak Plateau and along western Svalbard (Andreassen, 2017) that formed an important contribution to this thesis. These lines targeted areas which either lacked data or where existing data was of poor quality.

This thesis consists of an introduction and three scientific papers, focusing on refining the seismic stratigraphic framework along the western Svalbard-Barents Sea margin and improving our understanding of the chronology, extent, and dynamics of pre-Last Glacial Maximum glaciations in the western Svalbard-Barents Sea. The three papers are:

Paper 1. Alexandropoulou, N., Winsborrow, M., Andreassen, K., Plaza-Faverola, A., Dessandier, P. A., Mattingsdal, R., Baeten, N., Knies, J., 2021. A Continuous Seismostratigraphic Framework for the Western Svalbard-Barents Sea Margin over the Last 2.7 Ma: Implications for the Late Cenozoic Glacial History of the Svalbard-Barents Sea Ice Sheet. Front. Earth Sci. 9, 327. https://doi.org/10.3389/feart.2021.656732.

Paper 2. Reconstruction of the southwestern Barents Sea Ice Sheet over the last ~200 ka reveals variations in glacial dynamics during the Late Saalian and Weichselian glaciations (in prep., to be submitted)

Paper 3. Glacial tectonics, fluid flow and gas hydrates on the Bjørnøyrenna Ice Stream bed, SW Barents Sea (in prep., to be submitted)

The work presented in this PhD thesis has already contributed to the wider scientific community. This includes contributions to two studies modelling the glacial erosion of the Eurasian Ice Sheet complex over the entire last glacial cycle (Patton et al., 2022;Patton et al., in review), to which I contributed thickness maps and equivalent sediment volumes deposited along the western Barents Sea margin from ~1.5 to ~0.2 Ma and over the last ~0.2 Ma. These were used to constrain numerical ice sheet model simulations of glacial erosion. Additionally, I contributed to a study of Early Pleistocene glaciations of the Barents Sea (Bellwald et al., in review), including extending the seismic stratigraphy of the western Svalbard margin from Paper 1 to available exploration wellbores (7216-11-1S, 7117/9-1, 7117/9-2, and 7218/11-1) located on the outer continental shelf of Bjørnøyrenna (Bear Island Trough). The chronostratigraphic framework presented in Paper 1 was also used during the selection of drilling sites for the Integrated Ocean Drilling Program (IODP) exp. 403 that will sail summer 2024 (IODP proposal 985; Lucchi et al., 2023).

These collaborations have resulted in co-authorship of the following research papers:

Patton, H., Hubbard, A., Heyman, J., **Alexandropoulou, N.**, Lasabuda, A.P.E., Stroeven, A.P., Hall, A. M., Winsborrow, M., Sugden, D. E., Kleman, J., Andreassen, K., 2022. The extreme yet transient nature of glacial erosion. Nat. Commun. 13 (1), 1–14. https://doi.org/10.1038/s41467-022-35072-0

Winsborrow, M.C.M., Patton, H., Esteves, M., and **Alexandropoulou, N.** (2022). "Chapter 32 - The Eurasian Arctic: glacial landforms prior to the Last Glacial Maximum (before 29ka)," in *European Glacial Landscapes,* eds. D. Palacios, P.D. Hughes, J.M. García-Ruiz & N. Andrés. Elsevier), 233-240. https://doi.org/10.1016/B978-0-12-823498-3.00037-6

Bellwald, B., Maharjan, D., Planke, S., Winsborrow, M., Rydningen, T. A., **Alexandropoulou, N.**, Myklebust, R. (in review). Major tunnel valleys and sedimentation changes document extensive Early Pleistocene glaciations of the Barents Sea. Nature Communications Earth & Environment.

Patton, H., **Alexandropoulou, N.**, Lasabuda, A. P. E., Knies, J., Andreassen, K., Winsborrow, M., Laberg, J. S., Hubbard, A. (in review). Glacial erosion and Quaternary landscape development of the Eurasian Arctic. Earth-Science Reviews.

Acknowledgments

I would like to express my gratitude to my three supervisors, Karin Andreassen, Monica Winsborrow, and Andreia Plaza-Faverola for all their support, guidance, and inspiration during my PhD journey. Special thanks go to my co-authors whom I had the privilege to work with during this PhD. I would also like to acknowledge Johan Petter Nystuen and Jan Inge Faleide for introducing me to the seismic stratigraphy of the western Svalbard-Barents Sea continental margin. My warmest thanks to my friends and colleagues for all the good times and their support throughout the PhD years. Finally, I would like to express my heartfelt gratitude to my dear family, Γιώργο, Πάνο and Αναστασία, for being a constant source of inspiration and hope.

Abbreviations

BGHSZ: base of the gas hydrate stability zone

Bjørnøya: Bear Island

Bjørnøyrenna: Bear Island Trough

BSIS: Barents Sea Ice Sheet

GHSZ: gas hydrate stability zone

IODP: Integrated Ocean Drilling Program

ka: thousand years

LGM: Last Glacial Maximum

Ma: million years

MeBo: Meeresboden-Bohrgerät (seabed drilling rig)

MIS: Marine Isotope Stages

MPT: Middle Pleistocene transition

MSGL: mega-scale glacial lineation

NPD: Norwegian Offshore Directorate (previously Norwegian Petroleum Directorate)

ODP: Ocean Drilling Program

RMS: root-mean square

TMF: Through Mouth Fan

WAIS: West Antarctic Ice Sheet

Table of Contents

1. Introduction 1

1.1. Rationale 1

1.2. Continental slope records as archives of multiple pre-Last Glacial Maximum glacial-interglacial cycles 2

1.3. Seismic stratigraphy of the Svalbard-Barents Sea margin 3

1.4. Current knowledge of Barents Sea Ice Sheet- extent, evolution and dynamics 5

2. Thesis aim and key objectives 11

3. Scientific approach and study area 11

4. Datasets 11

4.1. 2D seismic dataset 11

4.2. 3D seismic datasets 12

4.3. Boreholes 12

5. Methods 14

5.1. Seismostratigraphic correlation 14

5.2. Seismic stratigraphy 16

5.3. 3D seismic attributes 16

5.4. Gas hydrate modelling 17

6. Summary of research papers 18

6.1. Paper 1 18

6.2. Paper 2 19

6.3. Paper 3 19

7. Synthesis 21

7.1. Long term evolution of the Svalbard-Barents Sea margin 21

7.2. Extent and dynamics of pre-Last Glacial Maximum Barents Sea Ice Sheets over the last 200 ka 23

7.3. Interactions between the Barents Sea Ice Sheets and gas hydrate systems 25

7.4. Future research 29

8. References 31

9. Research papers 39

1. Introduction

1.1. Rationale

Over the past decades, ice loss has represented the largest contributor to global sea level rise, with the Greenland and Antarctic ice sheets together contributing a global sea level rise of 20.9 mm between 1971 and 2018 (Fox-Kemper et al., 2021). This mass loss, and associated sea level rise, is predicted to continue throughout this century under all emission scenarios. There remain, however, large uncertainties around these predictions, often stemming from incomplete understanding of the processes of the observed ice sheet changes. Here palaeo records may play an important role, for contextualising the observational record and testing projection models.

This thesis focusses on the former Barents Sea Ice Sheet (BSIS), the northernmost ice sheet comprising the former Eurasian ice sheet complex. This ice sheet glaciated the epicontinental Barents Sea multiple times over the last ~2.7 million years. Studying the record of past changes of the BSIS is valuable for several reasons. Firstly, like the present-day West Antarctic Ice Sheet (WAIS), the BSIS was a marine-based ice sheet, meaning that its bed was largely grounded below sea level. Such ice sheet settings are widely considered to be particularly sensitive to climatic-driven change (e.g., Joughin and Alley, 2011), thus gaining a longer-term understanding of the processes, rates and drivers of marine-based ice sheet change can contribute to better prediction of future change. Secondly, the ready availability of high-resolution marine geophysical datasets from the Norwegian Barents Sea offers a perhaps unique potential to gain insights into the spatial and temporal variations in glacial dynamics occurring at the ice sheet bed over multiple glacial-interglacial cycles.

A growing body of marine geophysical and sedimentological records from the continental shelf has provided a refined picture of the sensitivity, behaviour, and geological imprint of the palaeo marine-based BSIS (e.g., Landvik et al., 1998; Dowdeswell and Cofaigh, 2002; Dowdeswell and Elverhøi, 2002; Ottesen et al., 2008; Winsborrow et al., 2010; Andreassen et al., 2014; Bjarnadottir et al., 2014; Patton et al., 2015; Piasecka et al., 2016; Esteves et al., 2017; Hogan et al., 2017; Newton and Huuse, 2017; Dowdeswell et al., 2021; Bellwald et al., 2023; Montelli et al., 2023). These reconstructions are based on glacial-geological evidence from the continental shelf, and are restricted to the most recent Late Weischelian glacial and in particular its retreat, due to extensive glacial erosion erasing much of the sedimentological and geomorphological record of pre-LGM glaciations. This PhD thesis

focuses on pre-Late Weichselian glaciations and the evolution of past BSIS's over the last ~2.7 Ma.

1.2. Continental slope records as archives of multiple pre-Last Glacial Maximum glacial-interglacial cycles

The extensive glacial erosion of the Barents Sea shelf has led to the formation of large submarine trough mouth fans (TMFs) along its northern and western margins. These formed at the mouth of cross-shelf troughs, where ice streams, narrow arteries of the ice sheet that flow an order of magnitude faster than the surrounding ice (e.g., Anandakrishnan et al., 1998; Bennett, 2003), supplied large volumes of eroded material to the outer shelf, which was often remobilised downslope as glacigenic debris flows on the continental slope. Along the western and northern Barents Sea margins, TMFs are archives recording the long-term evolution of the BSIS, its timing, extent, vigour and erosional capability over repeated glacial-interglacial cycles over the last ~2.7 Ma (e.g., Knies et al., 2009; Mattingsdal et al., 2014; Batchelor et al., 2019). As such they provide valuable constraints to numerical ice sheet models and insight into the coupled climate-ocean-cryosphere systems and landscape/seafloor evolution over Quaternary timescales (e.g., Patton et al., 2015; Patton et al., 2016; Patton et al., 2022). The Bjørnøya TMF, by far the largest fan along the western Svalbard-Barents Sea margin (Figure 1), is located on the southwestern Barents Sea margin. It consists of a ~3.5 km thick sedimentary succession and a volume of ~340,000 km^3 (Fiedler and Faleide, 1996) that covers ~2.7 Ma of glacial fluctuations across the Barents Sea shelf. These sedimentary archives can, however, only be fully utilized if there is sufficient geophysical data to characterize their volume, distribution and sedimentological properties; and perhaps most importantly, a stratigraphic and chronological framework to constrain the timing of their deposition.

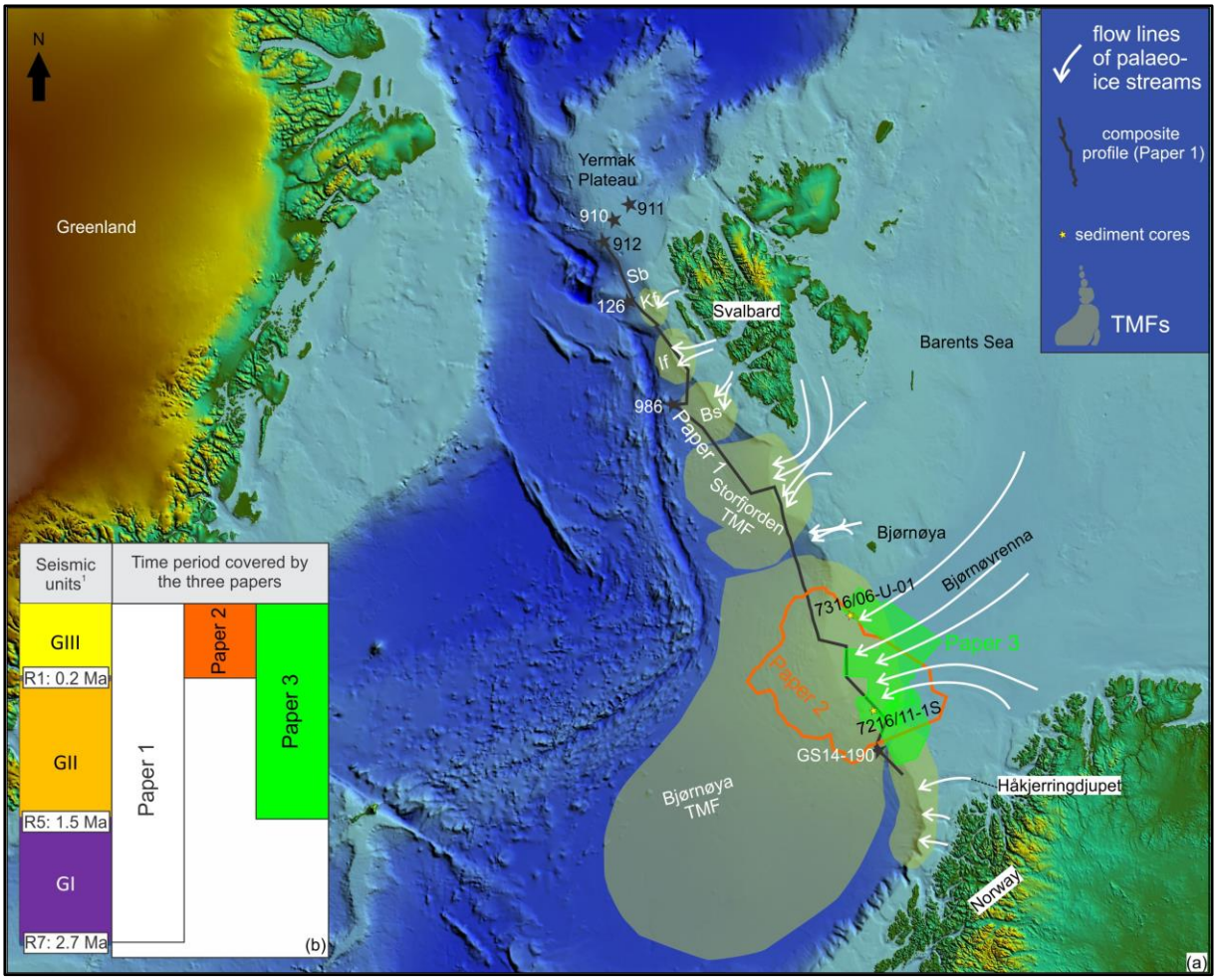

Figure 1. (a) Basemap showing the study areas for the three papers (black bold line, Paper 1; orange outline, Paper 2; bright green area, Paper 3). Background bathymetry from the International Bathymetric Chart of the Arctic Ocean (IBCAO, version 4.0) (Jakobsson et al., 2020). Trough-mouth fans (TMF; green shaded polygons): Vorren and Laberg (1997); Torbjørn Dahlgren et al. (2005). (b) Periods that the three papers cover respectively. [1]Faleide et al. (1996).

1.3. Seismic stratigraphy of the Svalbard-Barents Sea margin

In the past 30 years, there have been many attempts to develop Plio-Pleistocene stratigraphic frameworks for parts of the western Svalbard-Barents Sea margin, based on available boreholes and seismic dataset coverage (e.g., Vorren et al., 1991; Faleide et al., 1996; Fiedler and Faleide, 1996; Hjelstuen et al., 1996; Laberg and Vorren, 1996b; Laberg and Vorren, 1996a; Ryseth et al., 2003; Geissler and Jokat, 2004). The first attempt to combine the local seismic stratigraphies from different TMFs along the western Svalbard-Barents Sea margin into one was made by Faleide et al. (1996). This combined seismic stratigraphic framework is composed of three main seismic units GI-GIII, and seven regional seismic reflections R7-R1 along the western margin (Faleide et al., 1996). The R7 seismic reflection was interpreted to mark the base of the glacial deposits (Figure 2). Later, another seismic stratigraphic framework was established by Geissler and Jokat (2004), this time covering the

northern Barents Sea margin. This stratigraphic framework was based on the three Ocean Drilling Program (ODP) Sites (910, 911,912) located on the Yermak Plateau (Figure 1) divided into three seismic units YP-1, YP-2, and YP-3 (Eiken and Hinz, 1993; Geissler and Jokat, 2004) (Figure 2). The base of unit YP-3 was assigned an age of ~2.7 Ma based on the chronostratigraphic framework of ODP Site 911 (Myhre et al., 1995: palaeomagnetic data; Sato and Kameo, 1996: biostratigraphic data) and represents the base of the glacial deposits. Additional seismic horizons within YP-3 unit were further identified by Mattingsdal et al. (2014) (Figure 2). The ages of the internal seismic horizons within the YP-3 were assigned by tying seismic to the three ODP sites on Yermak Plateau (910, 911, 912). A close correspondence of both seismic units GI-GIII (west) and YP-3 (north) is indicated by the similar ages of the R7 seismic reflection on the western Barents Sea margin and the YP2-YP3 boundary on the Yermak Plateau (Figure 2).

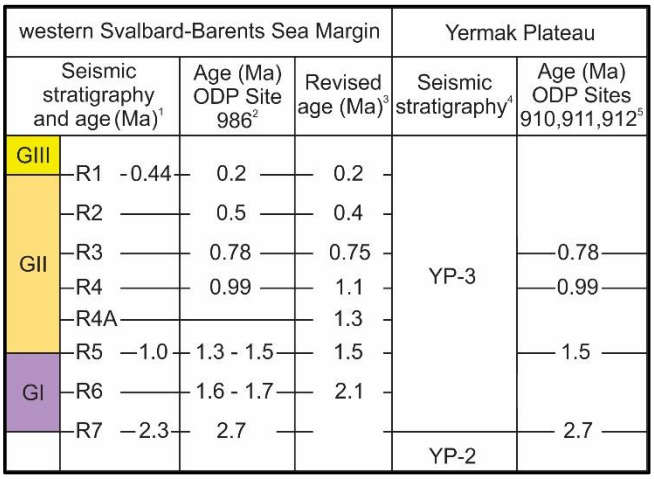

Figure 2. Correlation between the seismic stratigraphy of the western Barents Sea-Svalbard margin and Yermak Plateau together with the published age estimates for the seismic reflections. [1]Faleide et al. (1996); [2]Jansen et al. (1996); Channell et al. (1999); Eidvin and Nagy (1999); Forsberg et al. (1999); Butt et al. (2000); Knies et al. (2009); [3]Rebesco et al. (2014); [4]Geissler and Jokat (2004); [5]Myhre et al. (1995); Knies et al. (2009); Mattingsdal et al. (2014) (modified from Paper 1).

Despite such indications that these two separate seismic stratigraphic frameworks (R1 to R7 seismic reflections and YP-units), covering different parts of the continental margin, are comparable, attempts to combine these have been hampered by inconsistent chronologies between the sparse boreholes along the margin and limited seismic surveys necessary to by-pass problematic areas and correlate between the available boreholes. This lack of a continuous chronostratigraphic framework has also hindered attempts to provide a coherent reconstruction of paleoenvironmental variations along the entire western Svalbard-Barents Sea margin based on paleontological studies from the ODP sites on Yermak Plateau (ODP Site 910, 911, 912) and offshore west Svalbard (ODP 986). It is this knowledge gap that this thesis addresses. The

focus of the three papers presented herein is the western Svalbard-Barents Sea margin (Figure 1), where, in recent years, the combination of exceptional coverage of 2D/3D seismic and borehole data on the outer continental shelf/upper slope of the western Svalbard-Barents Sea margin and offshore western Svalbard, and new chronological constraints on the sedimentary sequences, has allowed us to develop a new continuous seismostratigraphic framework for the entire margin. This framework is then employed to advance knowledge of the Quaternary evolution of the Barents Sea continental margin and to reconstruct the glacial history of past BSIS's over the last ~2.7 Ma.

1.4. Current knowledge of Barents Sea Ice Sheet- extent, evolution and dynamics

Based on the existing seismic stratigraphy and literature, the glacial history of the western Barents Sea margin is divided into three glacial periods, GI (ca. ~2.7-1.5 Ma), GII (ca. ~1.5-0.2 Ma) and GIII period (ca. <~0.2 Ma). The onset of the GI period is interpreted to coincide with the onset of large-scale glaciations in the northern Barents Sea at around ~2.7 Ma (e.g., Knies et al., 2009). The timing is consistent with the intensification of the Northern Hemisphere glaciations around ~2.7 Ma ago, evidenced by major pulses of ice-rafted debris (IRD) from the Nordic Seas and North Atlantic (Shackleton et al., 1984; Flesche Kleiven et al., 2002; Knies et al., 2009), and by a global ice volume increase (Flesche Kleiven et al., 2002) inferring synchronous ice sheet development on Greenland, Barents Sea, Scandinavia and North America.

GII period is characterized by glacial expansion accompanied by large-scale waxing and waning of the BSIS and intensive periods of glacial erosion across the Barents Sea. More specifically, glacial intensification at around 1.5 Ma resulted in ice cover expansion across the wider Barents Sea and to the shelf-edge, at least part of the Western Svalbard-Barents Sea margin (e.g., Andreassen et al., 2004; Andreassen et al., 2007b; Andreassen and Winsborrow, 2009; Laberg et al., 2012; Rebesco et al., 2014). This intensification of glaciation is inferred by massive glacigenic debris flows and IRD along the western Svalbard margin (Solheim et al., 1998; Butt et al., 2000; Mattingsdal et al., 2014; Rebesco et al., 2014), and enhanced IRD supply in the Molloy Basin, Fram Strait (Gruetzner et al., 2022) while for the southwestern Barents Sea shelf edge glaciations are indicated by mega-scale glacial lineations (MSGLs) formed by grounded ice (Andreassen et al., 2004; Andreassen et al., 2007b; Andreassen and Winsborrow, 2009).

Finaly, the GIII period was affected by two major glacial periods, the Late Saalian (~200-130 ka) and the Weichselian (<~123 ka). The Late Saalian Glaciation (MIS 6; ~200-130 ka) is inferred to be the most extensive glaciation, with significant ice cover onshore in Northern Russia (e.g., Svendsen et al., 2004; Batchelor et al., 2019), whilst during the Weichselian glaciation (<123 ka), each of the three major readvances (Early, Middle, and Late Weichselian) was successively less extensive along its eastern margin (e.g., Svendsen et al., 2004; Vorren et al., 2011; Batchelor et al., 2019). The lateral extension of the BSIS was directly affected by the subglacial landscape. Its lateral extend varied significantly on the mainly terrestrial eastern margin, whilst along the western and northern margins the bathymetric barrier of the shelf edge constrained the maximum possible ice extent over multiple advances (e.g., Svendsen et al., 2004; Winsborrow et al., 2022) (Figure 3). However, the timing of the maximum lateral extent of the BSIS and the EISC did not coincide with the maximum extent of the Laurentide Ice Sheet. There are indications that the Laurentide Ice Sheet reached its maximum extent during the LGM whilst the EISC obtained its maximum lateral extent during the Late Saalian. This is inferred by a combination of climate and ice-sheet modelling (e.g., Colleoni et al., 2014; Liakka et al., 2016; Wekerle et al., 2016), glacial isostatic adjustment (GIA) modelling (e.g., Lambeck et al., 2006; Lambeck et al., 2010), and North Atlantic IRD observation (e.g., Obrochta et al., 2014).

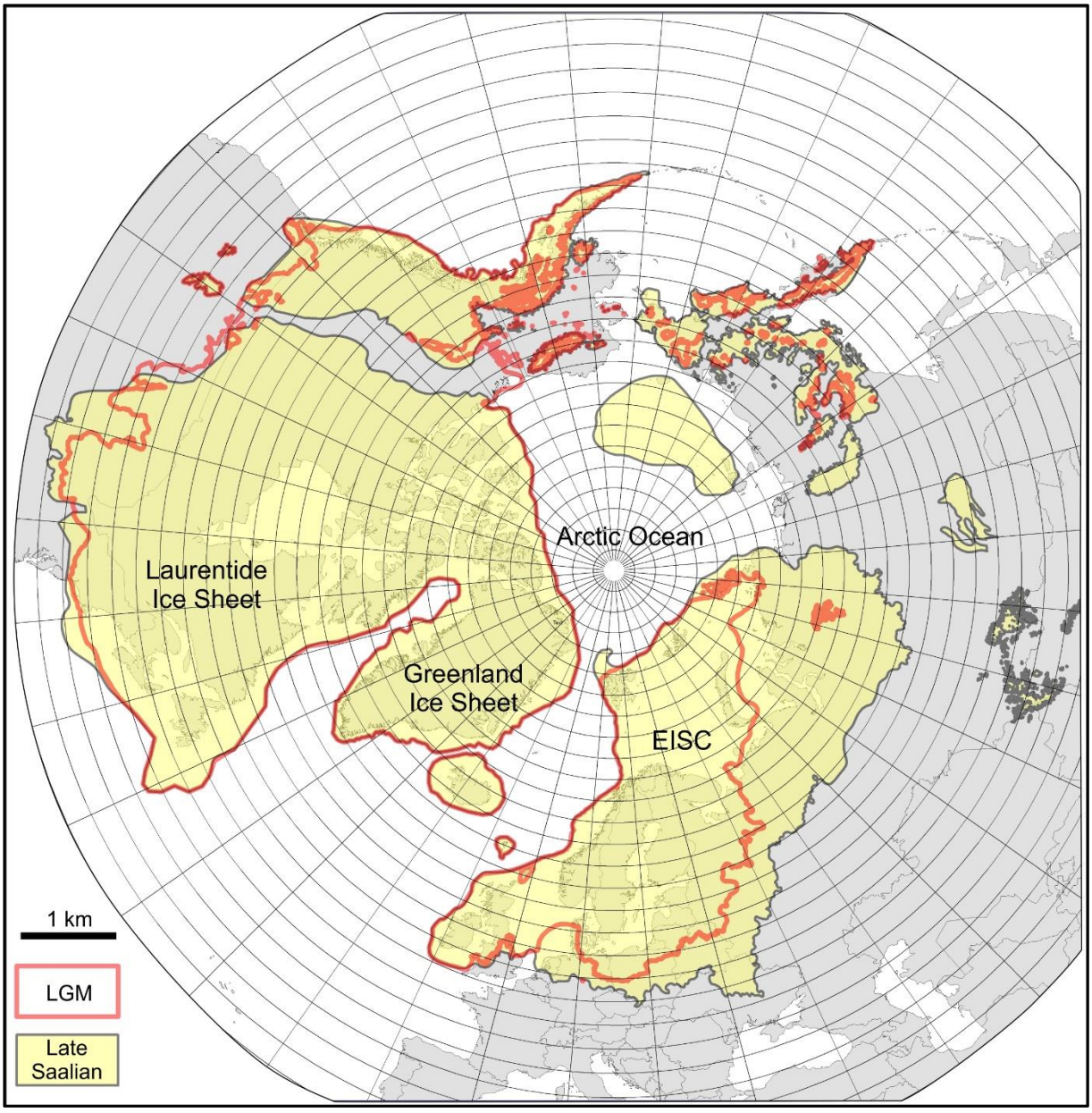

Figure 3. Comparison of the ice sheet extension on the Northern Hemisphere between (a) the Last Glacial Maximum (~26.5 ka ago) and (b) the Late Saalian (peak of MIS 6) glacial maximum (~140 ka ago) (modified from Batchelor et al., 2019). EISC: Eurasian Ice Sheet Complex. MIS: Marine isotope stages

Across the Barents Sea, several ice streams operated over the last ~2.7 Ma. Bjørnøyrenna (Figure 1) was the main drainage outlet of the former Barents Sea ice sheets. During the Plio-Pleistocene, Bjørnøyrenna was frequently reoccupied by ice streams, as inferred by observations of landforms such as MSGLs on buried beds of the Bjørnøyrenna (e.g., Andreassen et al., 2004; Andreassen et al., 2007b; Andreassen and Winsborrow, 2009). Bjørnøyrenna Ice Stream drained extensive portions of the central and southern Barents Sea shelf during the LGM (Patton et al., 2015) and is regarded as an analogue for contemporary ice streams in West Antarctica.

Multiple ice advances across the Bjørnøyrenna have sculptured the landscape over the last ~1.5 Ma. As a result, several glaciotectonic landforms, formed by deformation of rocks and/or sediments due to the overriding or pushing of ice, are preserved within the remaining subglacial till deposits formed beneath the Bjørnøyrenna palaeo-ice stream. The degree of subglacial frictional resistance is known to play a fundamental role in the ice stream stability (Whillans and Van Der Veen, 1993; MacAyeal et al., 1995; Whillans et al., 2001), and is highly dependent on their basal thermal regime (e.g., Stokes et al., 2007; Greenwood et al., 2022). In recent decades the increasing coverage of 3D seismic datasets in the southwestern Barents Sea has provided the ability to image, and study these buried glacial landforms in the Bjørnøyrenna. 3D seismic datasets (Figure 4c) have revealed glacial landforms on the buried beds, such as extensive chains of glacitectonic megablocks and rafts emplaced within thick tills deposits and aligned with streamlined bedforms indicative of ice streaming (Figure 5b) (Andreassen et al., 2004; Andreassen et al., 2007b; Andreassen and Winsborrow, 2009). These seismic observations are supported by the discovery of a 15-25 m thick glacitectonically rafted block of consolidated Cretaceous bedrock embedded in very stiff, Late Weichselian till within 7316/06-U-01 geotechnical borehole on the northern flank of the ice stream bed (Sættem et al., 1992) (Figures 1, 5c). Until now there is no published research linking the sediment megablocks and raft to their source depressions.

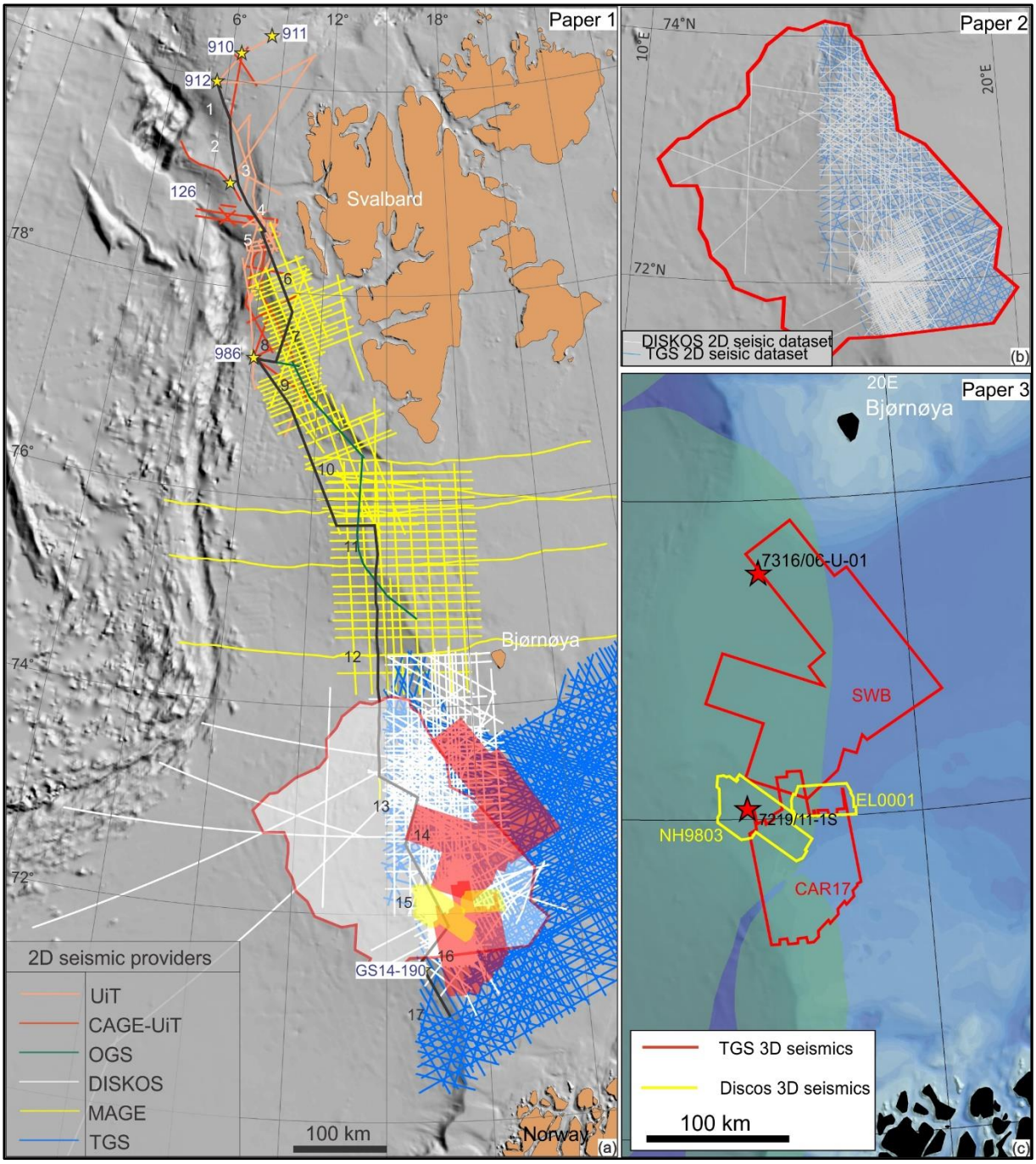

Figure 4. (a) Basemap presenting 2D seismic dataset and composite seismic profile used to derive the new seismic stratigraphic framework in Paper 1. Yellow stars: location of the core sites. ODP Sites: 910, 911, 912, 986. MeBo Site: 126. Piston core: GS14-190. CAGE-UiT: Centre for Arctic Gas Hydrate, Environment and Climate-UiT The Arctic University of Norway in Tromsø. OGS: National Institute of Oceanography and Applied Geophysics, Trieste, Italy. Diskos: Norwegian Diskos National Data Repository (NDR) database. MAGE: Russian Joint Stock Company 'Marine Arctic Geological Expedition'. TGS: TGS-NOPEC Geophysical Company Pty Ltd. (b) 2D seismic data that have been used in Paper 2. Background bathymetry from the International Bathymetric Chart of the Arctic Ocean (IBCAO, version 3.0) (Jakobsson et al., 2012). (c) Basemap shows the outline of the 3D seismic dataset used in Paper 3 extending across the outer continental shelf of the Bjørnøyrenna. Background bathymetry from the International Bathymetric Chart of the Arctic Ocean (IBCAO, version 3.0) (Jakobsson et al., 2012). Through-mouth fans: Vorren and Laberg (1997); Torbjørn Dahlgren et al. (2005).

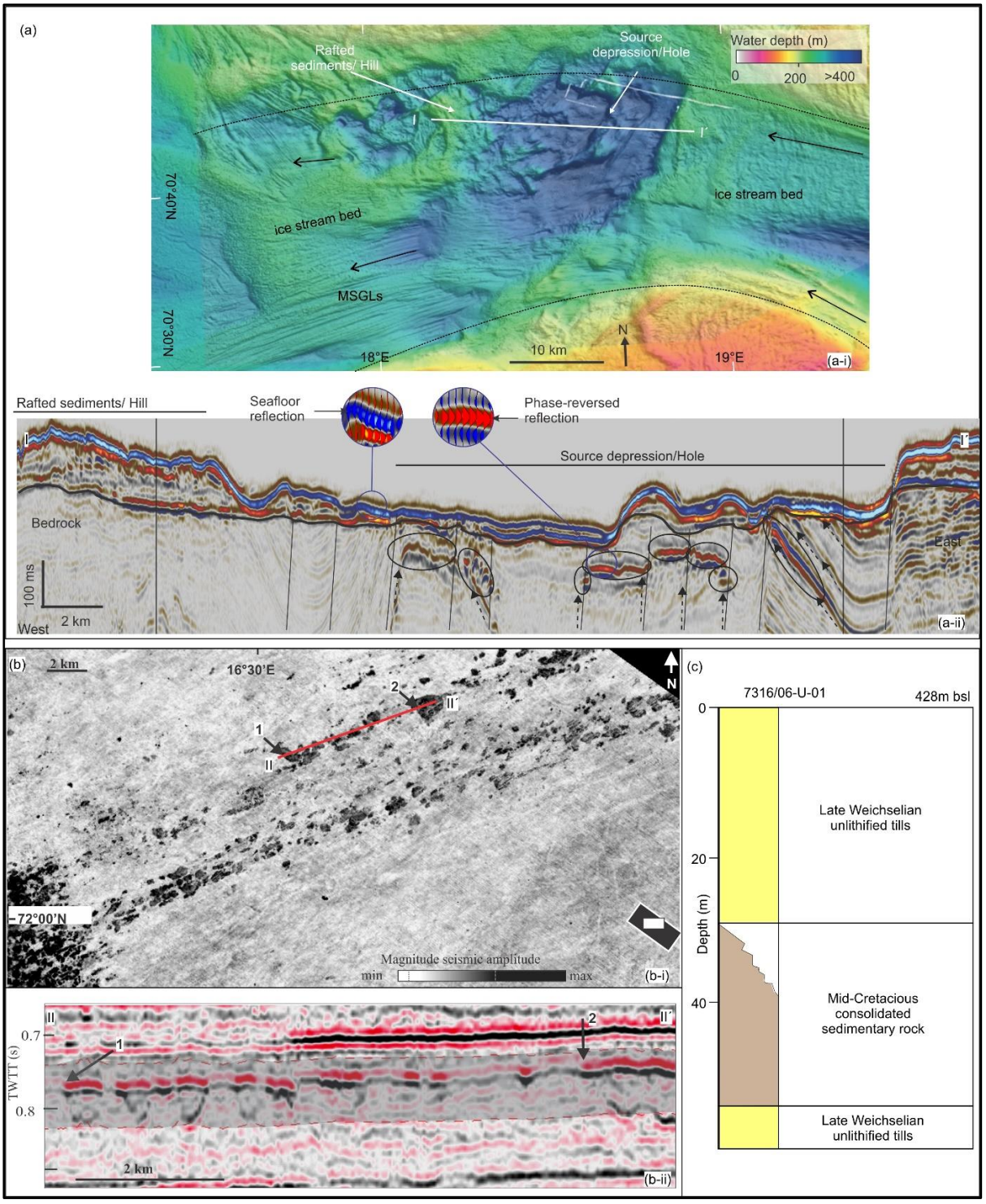

Figure 5. (a) (a-i) A hill-hole pair formed in an area where there are indications of free gas within glacial and preglacial strata and vertical faults beneath the source depression acting as gas migration pathways from deep reservoirs (modified from Winsborrow et al., 2016). (a-ii) Seismic profile (its location is indicated in Figure 5a-i) crossing the hill-hole pair, the fault system and phase-reversed reflections (modified from Winsborrow et al., 2016) (b) (b-i) RMS amplitude map, calculated for the shaded layer in Figure b-ii, shows sediment block chains within the Pleistocene glacigenic sediment across the outer shelf of the Bjørnøyrenna and the palaeo-shelf break (modified from Andreassen et al., 2004). (b-ii) Seismic profile II-II´ (see location in Figure 5b-i) crosses one of the sediment block chains (dark grey areas in Figure 5b-i). (c) Overview of borehole 7316/06-U-01 lithology (location in Figure 1) (modified from Sættem et al., 1992) where a 15-25m thick block of consolidated Cretaceous bedrock was found within a very stiff, Late Weichselian till layer.

2. Thesis aim and key objectives

The main aim of this PhD is to improve our understanding of the evolution and dynamics of pre-LGM Barents Sea glaciations. This is achieved by the following three key objectives:

- Refine and extend the existing seismic stratigraphic framework for the western Svalbard-Barents Sea margin over the past ~2.7 Ma (Paper 1).
- Reconstruct the extent and dynamics of former ice sheets of the western Barents Sea margin during the Late Saalian and Weichselian glaciations (Paper 2).
- Investigate the interaction of glacial processes, fluid flow and gas hydrates in the southwestern Barents Sea over successive periods of ice advance and retreat (Paper 3).

3. Scientific approach and study area

This thesis uses a seismic stratigraphic approach to investigate long-term glacial evolution along the western Svalbard-Barents Sea margin. The primary database for this work comprises 2D and 3D seismic reflection data available from industry and academia, used to constrain the volume, distribution and nature of glacigenic sediments deposited along the Svalbard-Barents Sea margin, and borehole data used to assess the age of these sediments (Figure 4).

4. Datasets

4.1. 2D seismic dataset

A large number of 2D seismic reflection profiles acquired over the last 34 years, both by industry and academia, extend along the entire western Svalbard-Barents Sea margin and were used in Papers 1 and 2 of this thesis (Figures 4a, 4b). The vertical resolution (~1/4 of the dominant wavelength λ) of the 2D seismic data varies from 10 to 15 m close to the seafloor and up to 25-30 m near the base of the glacigenic sediments. New 2D high-resolution seismic lines (CAGE-UiT; Figure 4a) were also acquired along the western Svalbard continental margin and Yermak Plateau for the purpose of this thesis, to help update the seismic correlation between the ODP Sites 986 (western Svalbard margin) and 910, 911, 912 on the Yermak Plateau (Andreassen, 2017). These lines were designed to either fill in data gaps or to provide improved data quality to existing lines. These 2D high-resolution seismic lines have a vertical resolution

(~1/4 of the dominant wavelength, λ) of ~3–5 m at the seafloor, and ~11–15 m at the base of the glacigenic sediments.

4.2. 3D seismic datasets

Four industry 3D seismic surveys were used in Paper 3 of this thesis (Figures 4a, 4c). These 3D seismic datasets were provided by the Norwegian Offshore Directorate (previously NPD) (EL0001, NH9803) and the TGS company (SWB, CAR17). The EL0001 seismic survey covers an area of 903 km^2, and the NH9803 an area of 2050 km^2. The more recently available 3D seismic surveys SWB and CAR17 cover 14226 km^2 and 5930 km^2 respectively, extending across a much larger part of the outer shelf and upper slope of outer Bjørnøyrenna (Figure 4c). For the glacigenic sediments a 2000 m s^{-1} average interval velocity is assumed (e.g., Fiedler and Faleide, 1996). The vertical resolution of the 3D seismic dataset (~1/4 of the dominant wavelength, λ) varies from 35 m (14 Hz dominant frequency) to 16 m (30 Hz dominant frequency). The 3D seismic data allowed us to visualize the subsurface in three dimensions. With relatively high spatial sampling (12.5 m) and 3D migration techniques, the horizontal resolution theoretically reached 12 m (e.g., Andreassen et al., 2007a).

4.3. Boreholes

For this PhD thesis, 12 age fix-points from six available sediment cores were used in Paper 1, providing a robust, consistent chronology for the western Svalbard-Barents Sea margin (Figures 1, 4a, 6). The six available sediment cores are the following: ODP Sites 910, 911, 912 on Yermak Plateau, ODP Site 986 west of Svalbard, MeBo (Meeresboden-Bohrgerät) site (MeBo Site 126) on Vestnesa Ridge, and a piston core site (GS14190-01PC; hereafter referred to as GS14-190) on the Bjørnøya TMF.

Core sites	Longitude	Latitude	Location	Water depth (m)
ODP 910A[a]	80°15.882 N	6°35.405 E	Yermak Plateau	556.4
ODP 911A[a]	80°28.466 N	8°13.640 E	Yermak Plateau	901.6
ODP 912A[a]	79°57.557' N	5°27.360' E	Yermak Plateau	556.4
ODP 986C[b]	77°20.431' N	9°04.664' E	west Svalbard	2051.5
MeBo 126[c]	78°59.806' N	6°57.808' E	Vestnesa Ridge	1207
GS14-190[d]	71°28.53' N	16°9.9' E	SW Barents Sea	949

Figure 6. Details of core sites displayed in Figure 1. [a]Myhre et al. (1995); [b]Jansen et al. (1996); [c]Bohrmann et al. (2017); [d]Knies et al. (2018).

The ODP Sites 910, 911 and 912 were retrieved during Summer 1993, on the Yermak Plateau (Myhre et al., 1995). These ODP Sites were selected to study trends in Neogene and Quaternary sediment accumulation on the Yermak Plateau and to investigate the glacial history of the Arctic gateway (Myhre et al., 1995). Sediments recovered at Site 912 are predominantly very dark grey, unlithified, slightly to moderately bioturbated silty clays and clayey silts of Pliocene to Quaternary age (Myhre et al., 1995). The sediments recovered at Site 911 consist primarily of unlithified, homogeneous, very dark grey clayey silts and silty clays of Quaternary and Pliocene age (Myhre et al., 1995). Finally, the sequence recovered at Site 910 consists of very firm, nearly homogeneous, silty clays and clayey silts, predominantly very dark grey (Myhre et al., 1995). The Yermak Plateau crest is characterized by persistent erosion and as a result, based on the age model established by Mattingsdal et al. (2014), ODP Site 912 covers sediments that extend only over the last 1.95 Ma (Myhre et al., 1995), whilst ODP Sites 910 and 911 cover sediments older than 1.95 Ma. A Late Miocene age for the base of ODP Sites 911 and 910 has been assigned by Mattingsdal et al. (2014), providing the first complete late Neogene record for the marginal Arctic Ocean.

In 1995, ODP Site 986 west of Svalbard was drilled (Jansen et al., 1996), with a maximum penetration of 964.6 mbsf (68% overall core recovery). An age of ~3.2 Ma has been assigned for the base of ODP 986 (Knies et al., 2009). The recovered sediments predominantly consist of fine- to medium-grained siliclastics with varying amounts of gravel (Jansen et al., 1996). A key objective for this site was to improve the age control of the R7-R1 seismic stratigraphy by Faleide et al. (1996). All the seismic sequences defined by Faleide et al. (1996) were penetrated at the site. Prior to the drilling of the site, age estimates were only available for R7 and R1 seismic reflections (Faleide et al., 1996). Initial age estimates for ODP Site 986 were made using paleomagnetic (Channell et al., 1999), biostratigraphic (Eidvin and Nagy, 1999) and Sr-isotope data (Forsberg et al., 1999), with much emphasis placed on the magnetic stratigraphy due to poor biostratigraphic constraints. However, although ODP Site 986 has been a key borehole for seismic stratigraphy of the western Barents Sea-Svalbard margin, due to discrepancy between the biostratigraphy and the paleomagnetic/Sr-data the age estimates from this well are somewhat uncertain.

Piston core GS14-190 was retrieved from the upper continental slope on the southwestern Barents Sea margin in ~949 m water depth (Knies et al., 2018). The core length is 1,380 cm and the age of the core was estimated by linear interpolation to be ~74 ka (supplementary material in Paper 1). The recovered sediments consist of hemipelagic, silty-

clay mud intercalated with IRD or dropstones with occasional signs of lamination, and intervals of more heterogenous facies with higher amounts of coarse sand (Knies et al., 2018).

Finally, in summer 2016, MeBo 126 was drilled on the Vestnesa Ridge, offshore west of Svalbard, as a reference site for seismic chronostratigraphic frameworks (Bohrmann et al., 2017; Dessandier et al., 2021). It reached 62.50 mbsf (42% core recovery) (Bohrmann et al., 2017). The age at its base was estimated to ca. 424 ka based on $\delta^{18}O$ values (MIS 12/11 transition) (Dessandier et al., 2021).

5. Methods

5.1. Seismostratigraphic correlation

In Paper 1, 12 pronounced seismic horizons within the glacigenic sediments were traced and mapped along a composite seismic profile, between Yermak Plateau and the Bjørnøya TMF (Figures 1, 7b). These seismic horizons character varies from depositional, continuous sedimentary reflections to erosional unconformities, and as such they are not necessarily timelines. The age assignments from ~0.074 to 2.7 Ma of these seismic horizons were derived from selected age fix-points from available core sites to which seismic ties were possible. In addition to the age fix-points derived from the available sediment cores, a seismic horizon representing the first occurrences of large erosional furrows on both the western and eastern slopes of the southern Yermak Plateau, interpreted as iceberg ploughmarks (Mattingsdal et al., 2014). This seismic reflection has been assigned an age of ~1.5 Ma and is equivalent to the R5 reflection by Faleide et al. (1996) (Mattingsdal et al., 2014).

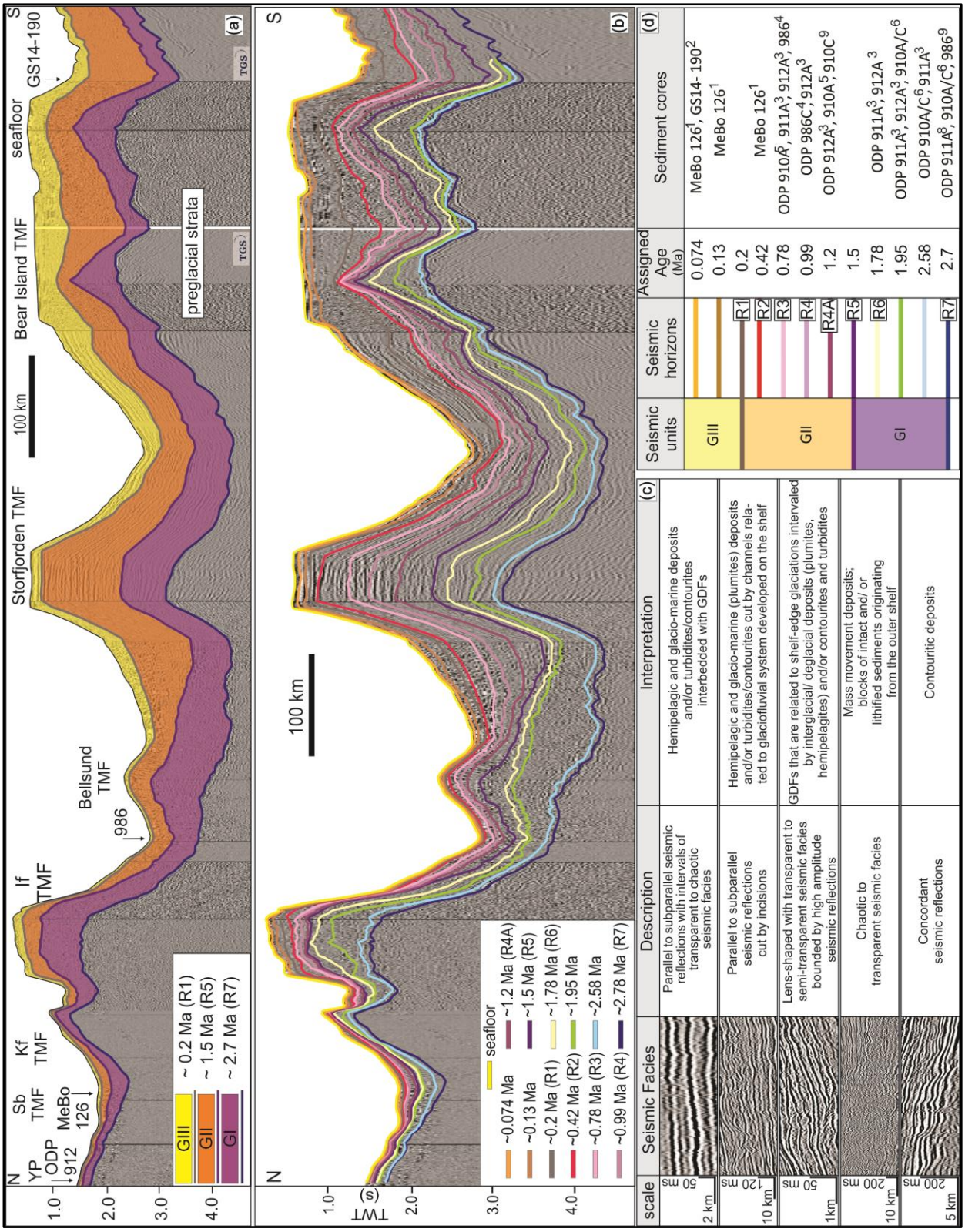

Figure 7. (a) Composite profile along the western Svalbard-Barents Sea margin (location in Figure 1) showing the three GI-GIII seismic units (modified from Paper 1). (b) Composite profile along the western Svalbard-Barents Sea margin (location in Figure 1) showing the new seismic stratigraphy presented in Paper 1. The seismic stratigraphy is correlated with the western Barents Sea seismic stratigraphy by Faleide et al. (1996) and Rebesco et al. (2014). I–III: selected points along the composite profile for estimating the sedimentation rates (see Figures 8d-8f). (c) Characteristic seismic facies observed along the western Svalbard-Barents Sea margin over the last ~2.7 Ma together with their interpretation (modified from Paper 1). GDFs:

glacigenic debris flow deposits. (d) Table presenting the age-fix points on which the seismostratigraphic framework in Paper 1 is based. Seismic units and seismic reflections R7-R1 along the western Svalbard-Barents Sea margin correlated with the seismic stratigraphy by Faleide et al. (1996) and Jansen et al. (1996). [1]Dessandier et al. (2021), [2]Paper 1, [3]Myhre et al. (1995), [4]Channell et al. (1999), [5]Knies et al. (2007), [6]Mattingsdal et al. (2014), [7]Faleide et al. (1996); Fiedler and Faleide (1996), [8]Sato and Kameo (1996), [9]Channell et al. (1999); Knies et al. (2009).

5.2. Seismic stratigraphy

Seismic stratigraphy is used to correlate sedimentary strata at depth by seismic data analysis. It provides the necessary tools to reconstruct the glacial history of the BSIS by revealing unconformity-bounded seismic sequences along the western Svalbard-Barents Sea margin. Clinoform analysis and seismic facies analysis were applied within the mapped seismic sequences (Mitchum and Vail, 1977; Mitchum et al., 1977). Clinoform analysis was applied to define stacking patterns and reconstruct the evolution of the shelf-edge (e.g., Gilbert, 1885; Barrell, 1912; Rich, 1951). The geometry of the clinoforms and the seismic facies of the seismic sequences may vary spatially and temporally, reflecting variations in several factors such as grain size, sediment distribution, sedimentation rate, and accommodation space. The seismic facies units were interpreted in terms of environmental setting such as sedimentary processes, depositional environments, sediment source and geological setting (Mitchum and Vail, 1977) in order to reconstruct the southwestern Barents Sea pre-LGM ice sheets. Seismic facies analysis within the mapped seismic sequences was based on defined seismic reflection parameters, such as reflection configuration, continuity, amplitude, and frequency (Mitchum et al., 1977). Seismic stratigraphy was used in Papers 1-3.

5.3. 3D seismic attributes

One of the key advantages of 3D seismic datasets are that they provide the opportunity to image the internal structure of sedimentary packages. Calculation of 3D seismic attributes is a powerful means of visualising different aspects of these sediments. In this thesis the root-mean-square (RMS) amplitude attribute was found to be most useful. RMS amplitude was calculated for stratigraphically defined windows within the 3D seismic data. Within these volumes the amplitude values are squared before averaged and taken square root of, enhancing the high amplitudes. In affect what the RMS amplitude map does is to visually enhance subsurface characteristics and specific geobodies within the defined window of analysis which have a seismic amplitude that is significantly higher from that of the surrounding sediment. It is thus an effective method to highlight features such as glacitectonic sediment blocks (e.g., Andreassen et al., 2004; Andreassen et al., 2007a; Andreassen and Winsborrow, 2009) of a

different sediment type (much higher product of density and velocity) compared to the surrounding sediments.

5.4. Gas hydrate modelling

Paper 3 examines the interactions between gas hydrates and glacial tectonic processes. An important tool in this work was theoretical modelling of gas hydrate stability zone variations. Gas hydrates may form within the so-called gas hydrate stability zone (GHSZ) when there is an adequate supply of gas (mainly methane) and water under appropriate pressure, temperature, and salinity conditions (e.g., Sloan, 1998; Sloan Jr and Koh, 2007). The parameters that determine the thickness of GHSZ are bottom water temperature, hydrostatic pressure, geothermal gradient, composition of the hydrate forming gas and formation water salinity (e.g., Sloan, 1998; Sloan Jr and Koh, 2007). In Paper 3, the gas hydrate stability field was calculated both for past glacial/interglacial periods and for the present day conditions (Sloan Jr and Koh, 2007). For the past glacial/interglacial periods, former ice thickness (Andreassen et al., 2017; Sejrup et al., 2022) and subglacial temperature (Patton et al., 2016; Andreassen et al., 2017) estimates were required from the published papers mentioned above.

6. Summary of research papers

6.1. Paper 1

A Continuous Seismostratigraphic Framework for the Western Svalbard-Barents Sea Margin Over the Last 2.7 Ma: Implications for the Late Cenozoic Glacial History of the Svalbard-Barents Sea Ice Sheet (Frontiers in Earth Science, VOL. 9, 10.3389/feart.2021.656732)

In paper 1, by establishing a set of reliable age fix-points from available boreholes along the margin, we used a large 2-D seismic database to extend this consistent chronology from the Yermak Plateau and offshore western Svalbard, southwards to the Bjørnøya TMF, southwestern Barents Sea margin. By doing so, we established a high-resolution, continuous seismostratigraphic framework that for the first time, connects the over 1,000 km long western Svalbard-Barents Sea margin and covers the last ~2.7 million years (Ma). We divided the seismic stratigraphy along the continental margin into three seismic units, and 12 regionally correlated seismic reflections, each with an estimated age assignment. We demonstrate one potential application of this framework by reconstructing the BSIS evolution from the intensification of the northern hemisphere glaciation at ~2.7 Ma to the Weichselian glaciations. Through seismic facies distribution and sedimentation rate fluctuations along the margin we distinguish the three following phases of glacial development phase 1-phase 3.

A clear two-step onset to glacial intensification is documented in the region during phase 1 (between ~2.7 and 1.5 Ma). The start of this period (between ~2.7 and 2.58 Ma) is characterized by glacial expansion across Svalbard, followed by glacial advances beyond Svalbard to the northwestern Barents Sea (between ~1.95 and 1.78 Ma). The first indication of shelf-edge glaciation is recorded on the Sjubrebanken TMF, northwestern Barents Sea, after ~2.58 Ma. Phase 2 is characterized by glacial intensification for the whole Barents Sea-Svalbard region, with widespread shelf-edge glaciations recorded at around ~1.5 Ma, supported by seismic facies and variations in sedimentation rates. Phase 3 is characterized once again by a regional glacial intensification inferred by a dramatic increase in sedimentation rates on the western Barents Sea margin. This phase encompasses the Early Saalian (~0.4 and 0.2 Ma), Late Saalian (~0.2 and 0.13 Ma), and Weichselian (<~0.123 Ma) periods. The presented framework allows for the sediments deposited on the slope during the last two glacial cycles (Late Saalian and Weichselian) to be separated stratigraphically for the first time.

6.2. Paper 2

Reconstruction of the southwestern Barents Sea Ice Sheet over the last ~200 ka reveals variations in glacial dynamics during the Late Saalian and Weichselian glaciations (in prep., to be submitted)

Paper 2 focuses on the Late Saalian-Weichselian seismic stratigraphy of the southwestern Barents Sea margin over the last ~200 ka. For the first time, we separated the sediments deposited during the following ice sheet advances: the Late Saalian (~200-130 ka), and the two comprising the Last Glacial Cycle (LGC), the Early Weichselian (~130-74 ka), and Middle-Late Weichselian (<~74 ka) across both the outer continental shelf and the upper-middle continental slope on the southwestern Barents Sea margin. This separation allowed for the first time to study variations in glacial dynamics and ice sheet configuration between the Late Saalian and Weichselian glaciations on the southwestern Barents Sea margin.

Our data show a pronounced reduction both in the sedimentation rates on the upper-middle Bjørnøya fan from ~620 cm ka^{-1} during the Late Saalian to ~53 cm ka^{-1} during the Middle-Late Weichselian, and the lateral extension of sediment depocentres. This reduction is accompanied by a change in seismic stacking configuration from progradational stacking patterns in the Late Saalian unit to an aggradational stacking configuration of the Weichselian units. We suggest at least one ice advance to the palaeo-shelf edge during the Late Saalian period, characterized by several fluctuations in the position of the ice margin during that period, supported by seismic facies analysis of the outer continental shelf and upper-middle fan units, and the distribution and thickness of the sediment depocentres. Additionally, one ice advance to the palaeo-shelf break during the Early Weichselian, and at least two ice advances during the Middle-Late Weichselian are inferred by our data, one during the Middle Weichselian and one during the Late Weichselian (LGM).

6.3. Paper 3

Glacial tectonics, fluid flow and gas hydrates on the Bjørnøyrenna Ice Stream bed, SW Barents Sea (in prep., to be submitted)

This paper aims to test the hypothesis of subglacial gas hydrate regulation of palaeo-ice stream flow on the Bjørnøyrenna palaeo-ice stream beds, southwestern Barents Sea and their link to the formation of glaciotectonic landforms. Within the GII and GIII sediment packages deposited over the last ~1.5 Ma, large depressions have been identified on several of the buried

palaeo shelf surfaces. The deepest depressions, recorded on the R5 and R1 surface, are up to 5 km wide and ~130 m deep and are eroded into either the westward dipping units of the GI-GII glacigenic sediment packages or the Palaeocene-Eocene bedrock. Based on their clear erosion cutting into the underlying strata, and their long-axis alignment with the inferred palaeo-ice flow direction, the depressions are interpreted to have formed at the base of palaeo-ice streams by removing sediments/bedrock from the subglacial strata.

Additionally, long chains of sediment megablocks and rafts are recorded downstream of the large depressions located within the palaeo shelf strata. The accordant orientation of the MSGLs with the sediment block chains and the source depression long-axes, supports an interpretation of the large depressions as the source for the observed sediment megablocks and rafts. We, therefore, suggest that the observed morphology of depressions, sediment blocks/rafts and MSGLs record the operation of ice streams on the outer shelf that have eroded, transported and then deposited large blocks of underlying sediment and bedrock.

The presence of gas accumulations below these depressions both at shallow and deep stratigraphic levels, accompanied by faults and dipping permeable layers acting as potential fluid flow pathways, indicate an active fluid migration system, suggesting a spatial relationship between fluid flow and gas accumulations. Under glacial conditions, migrating gas entering the region of gas hydrate stability zone beneath the ice sheet would have resulted in gas hydrate formation. The gas hydrates are assumed to have formed in patches, localized in areas of porous sediments and around faults and fractures. In these areas, the presence of gas hydrate would have increased the shear strength of the subglacial sediment, promoting glacitectonism, in line with Winsborrow et al. (2016). Based on our observation, we suggest a link between the gas hydrates and the glaciotectonic landforms assuming the presence of subglacial gas hydrate-driven sticky spots.

7. Synthesis

7.1. Long term evolution of the Svalbard-Barents Sea margin

This PhD thesis focuses on the Late Cenozoic evolution of the western Svalbard-Barents Sea margin and how it was affected by the waxing and waning of multiple Barents Sea Ice Sheets over the Quaternary. The work takes advantage of an extensive 2D and 3D seismic dataset and age-fix points on new and existing sediment cores in the study area to refine the existing seismic stratigraphy of the western Svalbard-Barents Sea margin and thereby improve our understanding of sedimentary processes and glacial evolution along the margin.

Refinement of the stratigraphic framework of the western Svalbard-Barents Sea margin (Paper 1) allows us to compare the Quaternary glacial history along the entire margin and reconstruct in greater detail the configuration and dynamics of the numerous glacial advances across the continental shelf. In Paper 1 a clear two-step, Svalbard-focused, onset to glacial intensification in the Barents Sea around ~2.7 Ma is suggested based on sedimentation rate (Figure 8d) and seismic facies variations (Figure 7). This interpretation is consistent with previous studies (e.g., Forsberg et al., 1999; Butt et al., 2000; Laberg et al., 2010; Knies et al., 2014; Mattingsdal et al., 2014), however, those studies could not resolve the subsequent pause in glacial build-up (between ~2.58 and 1.95 Ma), followed by a second period of intensification (between ~1.95 and 1.78 Ma), where ice began to extend beyond Svalbard, as indicated by the sedimentation rate (Figures 8a, 8d) and seismic facies data presented in Paper 1.

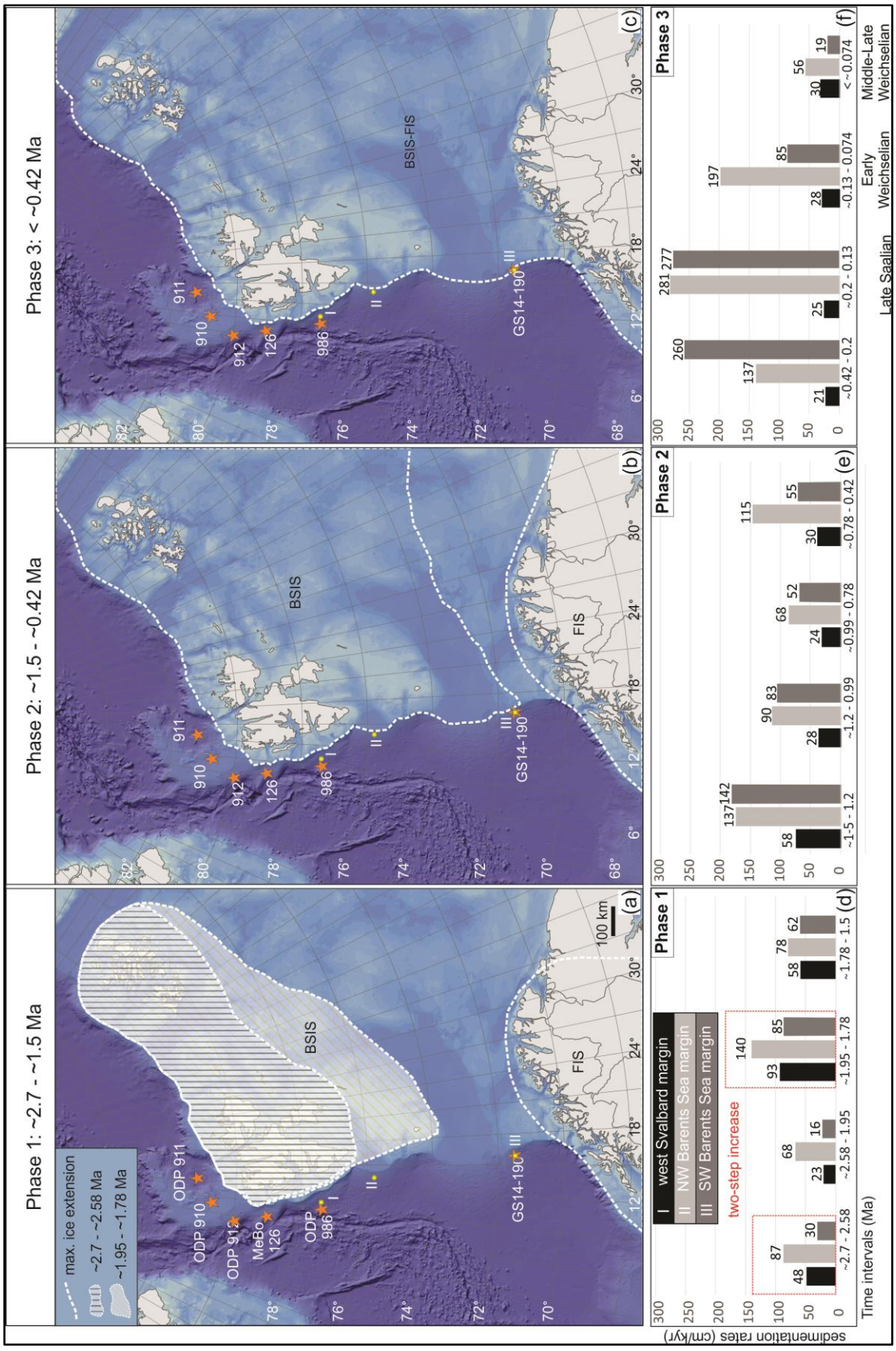

Figure 8. (a-c) Variations of the lateral extension of the BSIS and the FIS over the last ~2.7 Ma (modified from Paper 1). BSIS: Barents Sea Ice Sheet; FIS: Fennoscandian Ice Sheet. (d–f) Sedimentation rate plots show variations in sedimentation rates on selected points I–III over the past ~2.7 Ma (modified from Paper 1).

A robust, consistent chronostratigraphic framework also facilitates comparison between the western Svalbard-Barents Sea margin and other glaciated Northern Hemisphere margins such as those in the wider circum-Atlantic region. A Similar pause in glacial build-up to that observed in the western Svalbard-Barents Sea margin (Paper 1) is also suggested for Greenland, Scandinavia and North America. The initial ice sheet development at ~2.7 Ma in Greenland and Scandinavia was followed by a pause in glacial build-up inferred by a reduction in IRD fluxes in the circum-Atlantic region between ~2.5 and 1.55 Ma indicative of an interval characterized by less severe glaciations (Fronval and Jansen, 1996) and/or stabilized ice margins (Knies et al., 2009). A similar pattern is also suggested for the Greenland and North American Ice Sheets where the initial ice sheet development at ~2.72– 2.75 Ma (e.g., Jansen et al., 2000; Flesche Kleiven et al., 2002) was followed by an interval characterized by a suggested absence of huge ice masses from northern Greenland at ~2.4 Ma based palaeontological data (Funder et al., 2001) and from western Canadian Arctic between ~<2.0 and 1.8 Ma based on palaeo-magnetostratigraphic data (Barendregt and Irving, 1998). A gradual Northern Hemisphere glacial intensification was suggested, similar to what we suggest for the Barents Sea area (Paper 1), inferring a more regional climatic control of the Northern Hemisphere glaciations.

7.2. Extent and dynamics of pre-Last Glacial Maximum Barents Sea Ice Sheets over the last 200 ka

The refined high-resolution seismic stratigraphic framework (Paper 1) allows for the first time the differentiation of the sediments deposited on the slope during the Late Saalian and Weichselian periods (<200 ka) (Figure 9), revealing a significant reduction both in sedimentation rates on the upper-middle fan, from the Late Saalian to the Middle-Late Weichselian, and the lateral extension of the sediment depocentres on the Bjørnøya TMF (Figures 9a, 9b). These observations are in accordance with previous suggestions that the dynamics and extents of the Late Saalian and the Weichselian BSIS were very different (e.g., Solheim et al., 1998; Pope et al., 2016). Based on our work, the Late Saalian period is characterized by extremely high sediment input to the continental margin, which is consistent with a larger catchment area than during the Weichselian period and a Kara Sea-focused ice sheet in line with Svendsen et al. (2004) reconstructions. Our observations also show for the first time interbeds of ice proximal glaciomarine sediment within the till deposits, especially during the latest stages of the Late Saalian period (lower U1B), accompanied by an increase in thickness and lateral restriction of the depocentres to the upper fan (Figure 9a). We interpret these interbeds of ice proximal glaciomarine sediment within the till deposits to have been

deposited by a highly dynamic Late Saalian glaciation during its early stages, characterized by repeated advances and retreats from the shelf-edge. This suggests that the early stages of the Late Saalian glaciation were characterised by multiple advances and retreats until the maximum ice sheet extent/thickness was obtained. Once the BSIS obtained its maximum extent and thickness in the southwestern Barents Sea (Figure 9a), it became more stable experiencing fewer advances and retreats to the shelf edge. A long-lasting Late Saalian ice margin at the shelf edge has been suggested by Pope et al. (2016) based on sediment cores and 2D seismic data located on the deeper part of the fan. The absence in the studies of Pope et al. (2016) of indications for the highly dynamic ice marginal fluctuations that we see in our records likely reflects the strategic position of our datasets covering the upper fan where the depocentres are restricted (Figure 9a) recording the nuances in the ice sheet development that are unlikely to be recorded in the distal parts of the fan as studied by Pope et al. (2016).

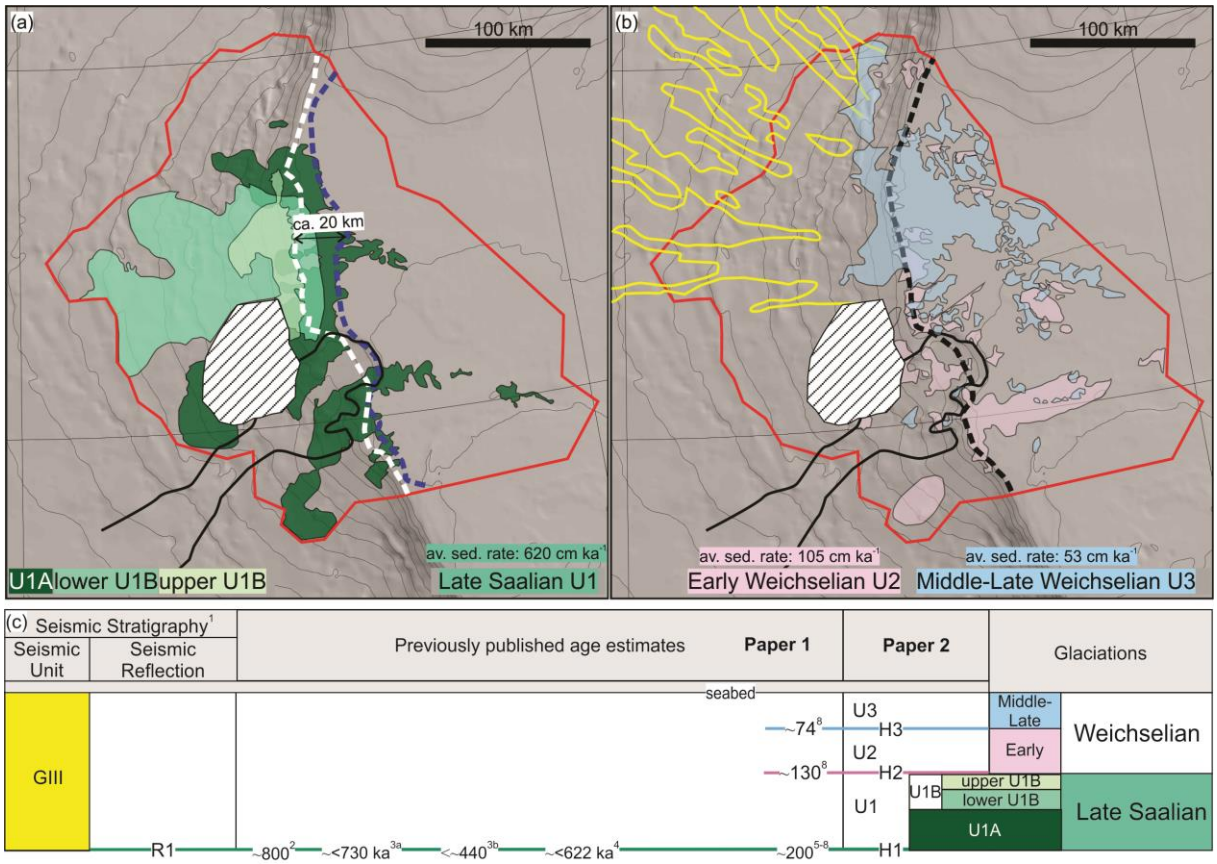

Figure 9. (a) Variations in lateral extension of the Bjørnøya TMF depocentres during the Late Saalian period. Thick blue dashed line: shelf-break position of the top horizon for U1A unit. Thick white dashed line: shelf-break position of the top horizon for U1B unit. (b) Shifts of the depocentres during the Early (U2) and Middle-Late (U3) Weichselian period. Shelf-break position of the top horizon for U2 and U3 units represented by a thick black dashed line, coinciding with the present-day shelf break. The yellow polylines represent glacigenic debris flows estimated to have been deposited during the Last Glacial Maximum (modified from Pope et al., 2018). The black line indicated the outline of the Bjørnøya palaeo landslide scar (modified from Pope et al., 2018). The white-striped polygon indicates the area with no available 2D seismic datasets. (c)

Published age estimates for the seismic reflections at the base and within the GIII seismic unit and correlation with Paper 2.[1]Faleide et al. (1996); Fiedler and Faleide (1996), [2]Vorren et al. (1990); Vorren et al. (1991), [3]Sættem et al. (1992): [3a]dating result based on magnetopolarity (Sættem et al., 1992), [3b]dating result based on aminostratigraphy (Sættem et al., 1992), [4]Laberg and Vorren (1996b), [5]Elverhøi et al. (1995), [6]Butt et al. (2000), [7]Rebesco et al. (2014), [8]paper 1. av. sed. rate: average sedimentation rate. (modified from Paper 2).

The subsequent Weichselian glaciations show a gradual decrease in sedimentation rates on the Bjørnøya TMF (Figure 9b), with the northwestern Barents Sea margin still characterized by relatively higher rates compared to the rest of the margin (Paper 1; Figure 8f). This is consistent with a central-Barents Sea-focused ice sheet with a smaller ice catchment area than during the Late Saalian (e.g., Svendsen et al., 2004) and also indicates higher erosion capacity of the BSIS in the northern Barents Sea during the Weichselian period. Changes in glacial dynamics, accompanied by an eastward shift in ice sheet nucleation (e.g., Svendsen et al., 2004) and more extensive cold-based ice characterized by little ice movement (e.g., Kleman and Hättestrand, 1999; Patton et al., 2016; Lien et al., 2022) during the Weichselian period may be potential factors that caused the decline in erosion rates in the southwestern sector of the BSIS catchment area from Late Saalian to Weichselian glaciations (Paper 2). In contrast to the EISC, the Laurentide Ice Sheet is inferred to have obtained its maximum lateral extent during the LGM (e.g., Colleoni et al., 2014; Obrochta et al., 2014; Liakka et al., 2016; Rohling et al., 2017). There are evidence inferring an interaction between the two largest ice sheets in the northern hemisphere, the Laurentide and the EISC. The asymmetric growth between the Laurentide Ice Sheet and the EISC during the Late Saalian and the LGM with the Laurentide Ice Sheet to be larger during the Late Saalian and the EISC during the LGM, may had consequences on the atmospheric circulation (e.g., Colleoni et al., 2011) resulting in shifting positions of jet streams delivering precipitations to the Eurasian Arctic (Liakka et al., 2016).

7.3. Interactions between the Barents Sea Ice Sheets and gas hydrate systems

The basal thermal regime of an ice stream is one of the most important factors in determining subglacial processes, and as such controls highly the spatial patterns of glacial erosion. Basal thermal regimes are classified as warm-based, cold-based and mixed thermal regimes. In the glacial landform record warm-based ice is identified by the presence of landforms indicating fast ice flow and bed deformation such as MSGLs (e.g., Stokes et al., 2007; Greenwood et al., 2021). Whilst cold-based ice is characterized by subdued subglacial landforms related to little ice movement, debris entrainment and deposition (Hall and Glasser,

2003; Kleman and Glasser, 2007). Mixed thermal regimes are characterized by the presence of landforms associated with warm- and cold-based ice, such as glaciotectonic landforms (e.g., hill-hole pairs and rafted sediment blocks) (e.g., Andreassen and Winsborrow, 2009; Winsborrow et al., 2016; Greenwood et al., 2021). One of the features that can be related to mixed thermal regimes are ice stream sticky spots. Sticky spots are localised patches of enhanced basal friction on otherwise well-lubricated, weak ice stream beds (e.g., Stokes et al., 2007). They may vary spatially and temporally, affecting the ice stream flow velocity and longevity (e.g., Alley, 1993; Anandakrishnan and Alley, 1997; Stokes et al., 2007). Changes in the "stiffness" of subglacial sediments have been suggested as one potential cause of ice stream sticky spots. Such change in sediment properties is usually considered a result of subglacial meltwater supply and/or routing variations or basal freeze-on (e.g., Sættem et al., 1996; Christoffersen and Tulaczyk, 2003; Andreassen et al., 2004; Andreassen and Winsborrow, 2009). However, an alternative theory hypothesises subglacial gas-hydrate formation as a mechanism for desiccating and stiffening subglacial sediments (e.g., Durham et al., 2003; Winters et al., 2004; Hyodo et al., 2013), which is suggested to promote ice stream sticky spot development (Winsborrow et al., 2016; Bellwald et al., 2023). Gas hydrates are ice-like crystalline compounds of gas (mainly methane with small amounts of other gases) and water, occurring naturally at low temperatures in permafrost regions and in relatively high pressure regimes in the oceans (e.g., Sloan Jr and Koh, 2007).

Extensive indications of glacitectonism in form of sediment block chains within the Pleistocene glacigenic sediment across the outer shelf of the Bjørnøyrenna and the palaeo-shelf break on the southwestern Barents Sea (Figure 5b) has been previously reported by Andreassen et al. (2004); Andreassen et al. (2007b); Andreassen and Winsborrow (2009) providing evidence that there were cold-bed patches on beds of the Bjørnøyrenna ice stream. Due to limited 3D coverage in the Bjørnøyrenna, the source of these sediment block chains has not been identified yet. Recently acquired 3D seismic data covering a large part of outer Bjørnøyrenna (Figures 4a, 4c) offers the unique opportunity to investigate the potential sources of theses glacitectonically displaced materials, the associated subglacial glaciotectonic processes, and their potential link to fluid flow and subglacial gas hydrates. In Paper 3, large depressions were documented on several of the buried palaeo shelf surfaces within the GII and GIII sediment packages, depressions up to 5 km wide and ~130 m deep. Downstream of these large depressions, long chains of sediment megablocks and rafts were recorded within the palaeo shelf strata. The similar orientation of the MSGLs as the long axes of the source

depressions and sediment block chains located on the downstream area, supports an interpretation of the large depressions as the source for the sediment megablocks and rafts. Similar glaciotectonic landforms related to sticky spots and mixed thermal regime have also been previously observed on palaeo-ice stream beds of the Håkjerringdjupet Ice Stream, located on the southwestern Barents Sea margin (Figure 1) (Winsborrow et al., 2016). The formation of such sticky spots was hypothesised to be due to subglacial gas hydrate desiccation of the sediments, based on the identification of glaciotectonic landforms on palaeo-ice stream beds, the location of which corresponds to evidence for fluid flow and shallow gas accumulations (Winsborrow et al., 2016; Bellwald et al., 2023).

For this PhD thesis, access to 3D seismic datasets on Bjørnøyrenna allowed us to look into the potential relationship between ice stream basal thermal regime, glacitectonics and subglacial gas hydrate formation. More specifically, in Paper 3, we test the hypothesis of subglacial gas hydrate regulation of palaeo-ice stream flow on the Bjørnøyrenna palaeo-ice stream beds and their link to the formation of glaciotectonic landforms. The presence of gas accumulations at shallow and deep stratigraphic levels where the source depressions are present, together with faults and dipping permeable layers acting as fluid flow pathways below these depressions, suggest an active fluid migration system, and a spatial relationship between fluid flow, gas accumulations and source depressions. Under glacial conditions, upwards migrating gas entering the gas hydrate stability zone beneath the ice sheet, would have resulted in subglacial gas hydrates formation in patches, ultimately increasing the sediment shear strength (e.g., Durham et al., 2003; Winters et al., 2004; Hyodo et al., 2013), and promoting ice stream sticky spot development (Winsborrow et al., 2016; Bellwald et al., 2023). Within our study area where the ice stream sticky spots were present, large depressions were formed as higher-strength subglacial sediment/bedrock were subsequently glacitectonically displaced from underlying lower-strength material, transported with the overlying ice, and then deposited in the downstream area forming sediment block chains. The areas where these glacitectonically landforms are observed coincide with areas of shallow gas accumulations, that would have been stable as gas hydrates under glacial conditions, supporting the hypothesis that subglacial gas hydrate patches increased the strength of gas hydrate-bearing sediments by desiccating them, and creating the high friction sticky spots on the ice stream bed that were subsequently glacitectonically displaced (Figure 10).

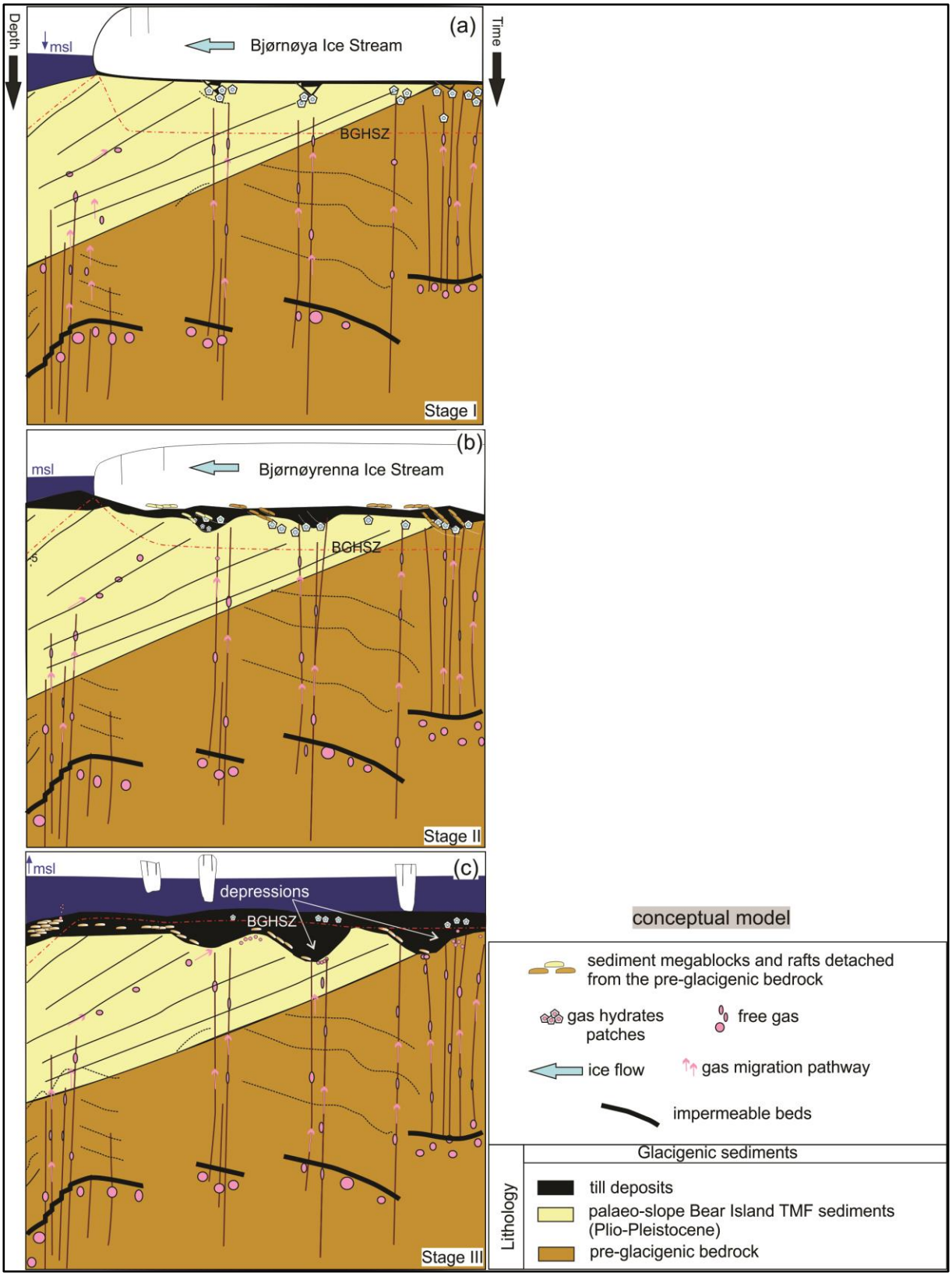

Figure 10. Conceptual model suggesting mechanisms involved in the formation of the depressions eroded in glacigenic sediments and bedrock. Brown lines: faults; msl: mean sea level; BGHSZ: base of the gas hydrate stability zone (modified from Paper 3).

This new knowledge is important as similar geological/glaciological settings are present today on other palaeo-ice stream beds such as in other places in the southwestern Barents Sea (e.g., Winsborrow et al., 2016; Bellwald et al., 2023) and in the central Alberta (e.g., Evans et al., 2021), and on contemporary ice streams such as in western Antarctica and Greenland. For the contemporary ice sheets, abundant gas hydrate accumulations are suggested to exist subglacially based on the presence of extensive sedimentary basins and modelling studies (e.g., Wadham et al., 2012; Wallmann et al., 2012; Wadham et al., 2019). From this perspective, subglacial gas-hydrate distribution is an important factor that should be included in attempts to model the future methane discharges and evolution of contemporary ice sheets in order to improve our understanding of their potential impacts on future global climate.

7.4. Future research

The new framework developed in Paper 1 works as a useful toolbox allowing direct comparison within the same time spans along the entire western Svalbard-Barents Sea margin that covers more than 1000 km distance over the last ~2.7 Ma. As demonstrated in this thesis, this framework has enormous value in elucidating the Quaternary evolution of the margin and adjacent continental shelf, and allowing comparison of this with other glaciated continental margins. It is with great excitement that I await IODP expedition 403 Eastern Fram Strait Palaeo-archive (FRAME) (Lucchi et al., 2023) that will take place in Summer 2024, where this framework will be tested, modified, and undoubtedly be improved by adding additional age fix-points. This will increase its reliability, especially on the southern part of the margin where there are currently limited age constraints. If successful, IODP Expedition 403 will also have the opportunity to extend the seismic stratigraphic framework back in time from ~2.7 Ma to ~5.8 Ma. This will offer the potential to study the pre-glacial evolution of the margin and wider Fram Strait ice-ocean-climate interactions.

Regarding the gas hydrate/glacial interactions (Paper 3), it would be interesting to investigate for similar evidence offshore other palaeo-ice sheets in similar settings with thermogenic reservoirs such as Greenland, Canadian Arctic. For example, to investigate possible connections with extensive glacitectonic landforms associated with the southern Laurentide ice sheet margin (e.g., Evans et al., 2021) and fluid flow from thermogenic reservoirs in these areas.

8. References

Alley, R.B. (1993). In search of ice-stream sticky spots. *Journal of Glaciology* 39**,** 447-454 10.3189/S0022143000016336.

Anandakrishnan, S., and Alley, R.B. (1997). Stagnation of Ice Stream C, West Antarctica by water piracy. *Geophysical Research Letters* 24**,** 265-268 https://doi.org/10.1029/96GL04016.

Anandakrishnan, S., Blankenship, D.D., Alley, R.B., and Stoffa, P.L. (1998). Influence of subglacial geology on the position of a West Antarctic ice stream from seismic observations. *Nature* 394**,** 62-65 10.1038/27889.

Andreassen, K. (2017). Cruise report CAGE 17-5. Marine geophysical cruise to the Yermak Plateau and western Svalbard continental margin. 28.

Andreassen, K., Hubbard, A., Winsborrow, M., Patton, H., Vadakkepuliyambatta, S., Plaza-Faverola, A., Gudlaugsson, E., Serov, P., Deryabin, A., Mattingsdal, R., Mienert, J., and Bünz, S. (2017). Massive blow-out craters formed by hydrate-controlled methane expulsion from the Arctic seafloor. *Science* 356**,** 948-953 10.1126/science.aal4500.

Andreassen, K., Nilssen, E.G., and Ødegaard, C.M. (2007a). Analysis of shallow gas and fluid migration within the Plio-Pleistocene sedimentary succession of the SW Barents Sea continental margin using 3D seismic data. *Geo-Marine Letters* 27**,** 155-171 10.1007/s00367-007-0071-5.

Andreassen, K., Nilssen, L.C., Rafaelsen, L., and Kuilman, L. (2004). Three-dimensional seismic data from the Barents Sea margin reveal evidence of past ice streams and their dynamics. *Geology* 32**,** 729-732 doi: 10.1130/g20497.1.

Andreassen, K., Odegaard, C.M., and Rafaelsen, B. (2007b). "Imprints of former ice streams, imaged and interpreted using industry three-dimensional seismic data from the south-western Barents Sea," in *Seismic Geomorphology: Applications to Hydrocarbon Exploration and Production*, eds. R.J. Davies, H.W. Posamentier, L.J. Wood & J.A. Cartwright.), 151-169.

Andreassen, K., and Winsborrow, M. (2009). Signature of ice streaming in Bjornoyrenna, Polar North Atlantic, through the Pleistocene and implications for ice-stream dynamics. *Annals of Glaciology* 50**,** 17-26.

Andreassen, K., Winsborrow, M.C.M., Bjamadottir, L.R., and Ruther, D.C. (2014). Ice stream retreat dynamics inferred from an assemblage of landforms in the northern Barents Sea. *Quaternary Science Reviews* 92**,** 246-257 10.1016/j.quascirev.2013.09.015.

Barendregt, R.W., and Irving, E. (1998). Changes in the extent of North American ice sheets during the late Cenozoic. *Canadian Journal of Earth Sciences* 35**,** 504-509 doi: 10.1139/e97-126.

Barrell, J. (1912). Criteria for the recognition of ancient delta deposits. *GSA Bulletin* 23**,** 377-446 10.1130/gsab-23-377.

Batchelor, C.L., Margold, M., Krapp, M., Murton, D.K., Dalton, A.S., Gibbard, P.L., Stokes, C.R., Murton, J.B., and Manica, A. (2019). The configuration of Northern Hemisphere ice sheets through the Quaternary. *Nature Communications* 10**,** 3713 10.1038/s41467-019-11601-2.

Bellwald, B., Maharjan, D., Planke, S., Winsborrow, M., Rydningen, T.A., Alexandropoulou, N., and Myklebust, R. (in review). Major tunnel valleys and sedimentation changes document extensive Early Pleistocene glaciations of the Barents Sea. . *Nature Communications Earth & Environment*.

Bellwald, B., Stokke, H., Winsborrow, M., Planke, S., Sættem, J., Lebedeva-Ivanova, N., Hafeez, A., Kurjanski, B., Myklebust, R., and Polteau, S. (2023). Structural and fluid-migration control on hill-hole pair formation: Evidence from high-resolution 3D seismic data from the SW Barents Sea. *Geomorphology* 420**,** 108502 https://doi.org/10.1016/j.geomorph.2022.108502.

Bennett, M.R. (2003). Ice streams as the arteries of an ice sheet: their mechanics, stability and significance. *Earth-Science Reviews* 61**,** 309-339 10.1016/s0012-8252(02)00130-7.

Bjarnadottir, L.R., Winsborrow, M.C.M., and Andreassen, K. (2014). Deglaciation of the central Barents Sea. *Quaternary Science Reviews* 92**,** 208-226 10.1016/j.quascirev.2013.09.012.

Bohrmann, G., Ahrlich, F., Bergenthal, M., Bünz, S., Düßmann, R., Ferreira, C., Freudenthal, T., Fröhlich, S., Hamann, K., Hong, W.-L., Hsu, C.-W., Johnson, J., Kaszemeik, K., Kausche, A., Klein, T., Lange, M., Lepland, A., Malnati, J., Meckel, S., Meyer-Schack, B., Noorlander, K.,

Panieri, G., P., T., , Reuter, M., Riedel, M., Rosiak, U., Schmidt, C., Schmidt, W., Seiter, C., Spagnoli, G., S., A., , Stange, N., Wallmann, K., Wintersteller, P., Wunsch, D., and Yao, H. (2017). R/V MARIA S. MERIAN Cruise Report MSM57, Gas Hydrate Dynamics at the Continental Margin of Svalbard, Reykjavik – Longyearbyen – Reykjavik, 29 July – 07 September 2016. *Berichte, MARUM – Zentrum für Marine Umweltwissenschaften, Fachbereich Geowissenschaften, Universität Bremen*, No. 314.

Butt, F.A., Elverhoi, A., Solheim, A., and Forsberg, C.F. (2000). Deciphering late Cenozoic development of the western Svalbard margin from ODP site 986 results. *Marine Geology* 169**,** 373-390 doi: 10.1016/s0025-3227(00)00088-8.

Channell, J.E.T., Smelror, M., Jansen, E., Higgins, S.M., Lehman, B., Eidvin, T., and Solheim, A. (1999). Age models for glacial fan deposits off East Greenland and Svalbard (ODP Site 986 and Site 987). *In: Raymo, M., Jansen, E., Blum, P., Herbert, T.D. (Eds.), Proceeding Ocean Drilling Program. Scientific Results* 162**,** 149-166.

Christoffersen, P., and Tulaczyk, S. (2003). Response of subglacial sediments to basal freeze-on 1. Theory and comparison to observations from beneath the West Antarctic Ice Sheet. *Journal of Geophysical Research: Solid Earth* 108 https://doi.org/10.1029/2002JB001935.

Colleoni, F., Liakka, J., Krinner, G., Jakobsson, M., Masina, S., and Peyaud, V. (2011). The sensitivity of the Late Saalian (140 ka) and LGM (21 ka) Eurasian ice sheets to sea surface conditions. *Climate Dynamics* 37**,** 531-553 10.1007/s00382-010-0870-7.

Colleoni, F., Masina, S., Cherchi, A., Navarra, A., Ritz, C., Peyaud, V., and Otto-Bliesner, B. (2014). Modeling Northern Hemisphere ice-sheet distribution during MIS 5 and MIS 7 glacial inceptions. *Clim. Past* 10**,** 269-291 10.5194/cp-10-269-2014.

Dessandier, P.-A., Knies, J., Plaza-Faverola, A., Labrousse, C., Renoult, M., and Panieri, G. (2021). Ice-sheet melt drove methane emissions in the Arctic during the last two interglacials. *Geology* 10.1130/g48580.1.

Dowdeswell, J.A., and Cofaigh, C.Ó. (2002). Glacier-influenced sedimentation on high-latitude continental margins: introduction and overview. *Geological Society, London, Special Publications* 203**,** 1-9 10.1144/gsl.Sp.2002.203.01.01.

Dowdeswell, J.A., and Elverhøi, A. (2002). The timing of initiation of fast-flowing ice streams during a glacial cycle inferred from glacimarine sedimentation. *Marine Geology* 188**,** 3-14 https://doi.org/10.1016/S0025-3227(02)00272-4.

Dowdeswell, J.A., Montelli, A., Akhmanov, G., Solovyeva, M., Terekhina, Y., Mironyuk, S., and Tokarev, M. (2021). Late Weichselian ice-sheet flow directions in the Russian northern Barents Sea from high-resolution imagery of submarine glacial landforms. *Geology* 49**,** 1484-1488 10.1130/g49252.1.

Durham, W.B., Kirby, S.H., Stern, L.A., and Zhang, W. (2003). The strength and rheology of methane clathrate hydrate. *Journal of Geophysical Research: Solid Earth* 108 https://doi.org/10.1029/2002JB001872.

Eidvin, E., and Nagy, J. (1999). Foraminiferal biostratigraphy of Pliocene deposits at Site 986, Svalbard margin. *In: Raymo, M., Jansen, E., Blum, P., Herbert, T.D. (Eds.), Proceeding Ocean Drilling Program. Scientific Results* 162**,** 3-17. doi:10.2973/odp.proc.sr.162.009.1999.

Eiken, O., and Hinz, K. (1993). Contourites in the Fram Strait. *Sedimentary Geology* 82**,** 15-32 https://doi.org/10.1016/0037-0738(93)90110-Q.

Elverhøi, A., Svendsen, J.I., Solheim, A., Andersen, E.S., Milliman, J., Mangerud, J., and Hooke, R.L. (1995). Late Quaternary Sediment Yield from the high Arctic Svalbard area. *Journal of Geology* 103**,** 1-17.

Esteves, M., Bjarnadóttir, L.R., Winsborrow, M.C.M., Shackleton, C.S., and Andreassen, K. (2017). Retreat patterns and dynamics of the Sentralbankrenna glacial system, central Barents Sea. *Quaternary Science Reviews* 169**,** 131-147 http://dx.doi.org/10.1016/j.quascirev.2017.06.004.

Evans, D.J.A., Phillips, E.R., and Atkinson, N. (2021). Glacitectonic rafts and their role in the generation of Quaternary subglacial bedforms and deposits. *Quaternary Research* 104**,** 101-135 10.1017/qua.2021.11.

Faleide, J.I., Solheim, A., Fiedler, A., Hjelstuen, B.O., Andersen, E.S., and Vanneste, K. (1996). Late Cenozoic evolution of the western Barents Sea-Svalbard continental margin. *Global and Planetary Change* 12**,** 53-74 doi: 10.1016/0921-8181(95)00012-7.

Fiedler, A., and Faleide, J.I. (1996). Cenozoic sedimentation along the southwestern Barents Sea margin in relation to uplift and erosion of the shelf. *Global and Planetary Change* 12**,** 75-93 doi: 10.1016/0921-8181(95)00013-5.

Flesche Kleiven, H., Jansen, E., Fronval, T., and Smith, T.M. (2002). Intensification of Northern Hemisphere glaciations in the circum Atlantic region (3.5–2.4 Ma) – ice-rafted detritus evidence. *Palaeogeography, Palaeoclimatology, Palaeoecology* 184**,** 213-223 https://doi.org/10.1016/S0031-0182(01)00407-2.

Forsberg, C.F., Solheim, A., Elverhoi, A., Jansen, E., Channell, J.E.T., and Andersen, E.S. (1999). 17. The depositional environment of the western Svalbard margin during the late Pliocene and the Pleistocene: Sedimentary facies changes at Site 986. *In: Raymo, M., Jansen, E., Blum, P., Herbert, T.D. (Eds.), Proceeding Ocean Drilling Program. Scientific Results* 162**,** 233-246.

Fox-Kemper, B., Hewitt, H.T., Xiao, C., Aðalgeirsdóttir, G., Drijfhout, S.S., Edwards, T.L., Golledge, N.R., Hemer, M., Kopp, R.E., Krinner, G., Mix, A., Notz, D., Nowicki, S., Nurhati, I.S., Ruiz, L., Sallée, J.-B., Slangen, A.B.A., and Yu, Y. (2021). "Ocean, Cryosphere and Sea Level Change," in *Climate Change 2021: The Physical Science Basis. Contribution of Working Group I to the Sixth Assessment Report of the Intergovernmental Panel on Climate Change, edited by: Masson-Delmotte, V., Zhai, P., Pirani, A., Connors, S. L., Péan, C., Berger, S., Caud, N., Chen, Y., Goldfarb, L., Gomis, M. I., Huang, M., Leitzell, K., Lonnoy, E., Matthews, J. B. R., Maycock, T. K., Waterfield, T., Yelekçį, O., Yu, R., and Zhou, B.*, ed. C. Intergovernmental Panel on Climate. (Cambridge: Cambridge University Press), 1211-1362.

Fronval, T., and Jansen, E. (1996). Late Neogene paleoclimates and paleoceanography in the Iceland-Norwegian Sea: evidence from the Iceland and Vøring Plateaus. In: Thiede, J., Myhre, A.M., Firth, J.V., Johnson, G.L., Ruddiman, W.F. (Eds.). *Proceeding Ocean Drilling Program. Scientific Results, vol.Ocean Drilling Program, College Station, TX.* 151**,** 455–468.

Funder, S., Bennike, O., Bocher, J., Israelson, C., Strand, K., Símonarson, L., Bennike, Israelson, J., Petersen, C., Simonarson, K., Bennike, D., Nv, D., and Bacher (2001). Late Pliocene Greenland -The Kap K0benhavn Formation in North Greenland. *Bulletin of the Geological Society of Denmark* 48**,** 117-134.

Geissler, W.H., and Jokat, W. (2004). A geophysical study of the northern Svalbard continental margin. *Geophysical Journal International* 158**,** 50-66 doi: 10.1111/j.1365-246X.2004.02315.x.

Gilbert, G.K. (1885). *The topographic features of lake shores.* US Government Printing Office.

Greenwood, S.L., Hughes, A.L.C., and Winsborrow, M.C.M. (2022). "Chapter 28 - The EISC evolution prior to the Last Glacial Maximum," in *European Glacial Landscapes*, eds. D. Palacios, P.D. Hughes, J.M. García-Ruiz & N. Andrés. Elsevier), 203-211.

Greenwood, S.L., Simkins, L.M., Winsborrow, M.C.M., and Bjarnadóttir, L.R. (2021). Exceptions to bed-controlled ice sheet flow and retreat from glaciated continental margins worldwide. *Sci Adv* 7 10.1126/sciadv.abb6291.

Gruetzner, J., Matthiessen, J., Geissler, W.H., Gebhardt, A.C., and Schreck, M. (2022). A revised core-seismic integration in the Molloy Basin (ODP Site 909): Implications for the history of ice rafting and ocean circulation in the Atlantic-Arctic gateway. *Global and Planetary Change* 215**,** 103876 https://doi.org/10.1016/j.gloplacha.2022.103876.

Hall, A.M., and Glasser, N.F. (2003). Reconstructing the basal thermal regime of an ice stream in a landscape of selective linear erosion: Glen Avon, Cairngorm Mountains, Scotland. *Boreas* 32**,** 191-207 https://doi.org/10.1111/j.1502-3885.2003.tb01437.x.

Hjelstuen, B.O., Elverhoi, A., and Faleide, J.I. (1996). Cenozoic erosion and sediment yield in the drainage area of the Storfjorden Fan. *Global and Planetary Change* 12**,** 95-117 doi: 10.1016/0921-8181(95)00014-3.

Hogan, K.A., Dowdeswell, J.A., Hillenbrand, C.-D., Ehrmann, W., Noormets, R., and Wacker, L. (2017). Subglacial sediment pathways and deglacial chronology of the northern Barents Sea Ice Sheet. *Boreas* 46**,** 750-771 https://doi.org/10.1111/bor.12248.

Hyodo, M., Li, Y., Yoneda, J., Nakata, Y., Yoshimoto, N., Nishimura, A., and Song, Y. (2013). Mechanical behavior of gas-saturated methane hydrate-bearing sediments. *Journal of Geophysical Research: Solid Earth* 118**,** 5185-5194 https://doi.org/10.1002/2013JB010233.

Jakobsson, M., Mayer, L., Coakley, B., Dowdeswell, J.A., Forbes, S., Fridman, B., Hodnesdal, H., Noormets, R., Pedersen, R., Rebesco, M., Schenke, H.W., Zarayskaya, Y., Accettella, D., Armstrong, A., Anderson, R.M., Bienhoff, P., Camerlenghi, A., Church, I., Edwards, M., Gardner, J.V., Hall, J.K., Hell, B., Hestvik, O., Kristoffersen, Y., Marcussen, C., Mohammad, R., Mosher, D., Nghiem, S.V., Pedrosa, M.T., Travaglini, P.G., and Weatherall, P. (2012). The International Bathymetric Chart of the Arctic Ocean (IBCAO) Version 3.0. *Geophysical Research Letters* 39**,** 6 doi: 10.1029/2012gl052219.

Jakobsson, M., Mayer, L.A., Bringensparr, C., Castro, C.F., Mohammad, R., Johnson, P., Ketter, T., Accettella, D., Amblas, D., An, L., Arndt, J.E., Canals, M., Casamor, J.L., Chauché, N., Coakley, B., Danielson, S., Demarte, M., Dickson, M.-L., Dorschel, B., Dowdeswell, J.A., Dreutter, S., Fremand, A.C., Gallant, D., Hall, J.K., Hehemann, L., Hodnesdal, H., Hong, J., Ivaldi, R., Kane, E., Klaucke, I., Krawczyk, D.W., Kristoffersen, Y., Kuipers, B.R., Millan, R., Masetti, G., Morlighem, M., Noormets, R., Prescott, M.M., Rebesco, M., Rignot, E., Semiletov, I., Tate, A.J., Travaglini, P., Velicogna, I., Weatherall, P., Weinrebe, W., Willis, J.K., Wood, M., Zarayskaya, Y., Zhang, T., Zimmermann, M., and Zinglersen, K.B. (2020). The International Bathymetric Chart of the Arctic Ocean Version 4.0. *Scientific Data* 7**,** 176 10.1038/s41597-020-0520-9.

Jansen, E., Fronval, T., Rack, F., and Channell, J.E.T. (2000). Pliocene-Pleistocene ice rafting history and cyclicity in the Nordic Seas during the last 3.5 Myr. *Paleoceanography* 15**,** 709-721 doi: 10.1029/1999pa000435.

Jansen, E., Raymo, M.E., and Blum, P. (1996). "The Leg 162 Shipboard Scientific Party, 1996.", in: *Proceedings of the Ocean Drilling Program, Initial Reports.*).

Joughin, I., and Alley, R.B. (2011). Stability of the West Antarctic ice sheet in a warming world. *Nature Geoscience* 4**,** 506-513 10.1038/ngeo1194.

Kleman, J., and Glasser, N.F. (2007). The subglacial thermal organisation (STO) of ice sheets. *Quaternary Science Reviews* 26**,** 585-597 10.1016/j.quascirev.2006.12.010.

Kleman, J., and Hättestrand, C. (1999). Frozen-bed Fennoscandian and Laurentide ice sheets during the Last Glacial Maximum. *Nature* 402**,** 63-66 10.1038/47005.

Knies, J., Köseoğlu, D., Rise, L., Baeten, N., Bellec, V.K., Bøe, R., Klug, M., Panieri, G., Jernas, P.E., and Belt, S.T. (2018). Nordic Seas polynyas and their role in preconditioning marine productivity during the Last Glacial Maximum. *Nature Communications* 9**,** 3959 doi: 10.1038/s41467-018-06252-8.

Knies, J., Matthiessen, J., Mackensen, A., Stein, R., Vogt, C., Frederichs, T., and Nam, S.-I. (2007). Effects of Arctic freshwater forcing on thermohaline circulation during the Pleistocene. *Geology* 35**,** 1075-1078 doi: 10.1130/G23966A.1.

Knies, J., Matthiessen, J., Vogt, C., Laberg, J.S., Hjelstuen, B.O., Smelror, M., Larsen, E., Andreassen, K., Eidvin, T., and Vorren, T.O. (2009). The Plio-Pleistocene glaciation of the Barents Sea-Svalbard region: a new model based on revised chronostratigraphy. *Quaternary Science Reviews* 28**,** 812-829 doi: 10.1016/j.quascirev.2008.12.002.

Knies, J., Mattingsdal, R., Fabian, K., Grøsfjeld, K., Baranwal, S., Husum, K., De Schepper, S., Vogt, C., Andersen, N., Matthiessen, J., Andreassen, K., Jokat, W., Nam, S.-I., and Gaina, C. (2014). Effect of early Pliocene uplift on late Pliocene cooling in the Arctic–Atlantic gateway. *Earth and Planetary Science Letters* 387**,** 132-144 https://doi.org/10.1016/j.epsl.2013.11.007.

Laberg, J.S., Andreassen, K., Knies, J., Vorren, T.O., and Winsborrow, M. (2010). Late Pliocene-Pleistocene development of the Barents Sea Ice Sheet. *Geology* 38**,** 107-110 doi: 10.1130/g30193.1.

Laberg, J.S., Andreassen, K., and Vorren, T.O. (2012). Late Cenozoic erosion of the high-latitude southwestern Barents Sea shelf revisited. *Geological Society of America Bulletin* 124**,** 77-88 doi: 10.1130/b30340.1.

Laberg, J.S., and Vorren, T.O. (1996a). The glacier-fed fan at the mouth of Storfjorden trough, western Barents Sea: a comparative study. *Geologische Rundschau* 85**,** 338-349 doi: 10.1007/bf02422239.

Laberg, J.S., and Vorren, T.O. (1996b). The Middle and Late Pleistocene evolution of the Bear Island Trough Mouth Fan. *Global and Planetary Change* 12**,** 309-330 doi: 10.1016/0921-8181(95)00026-7.

Lambeck, K., Purcell, A., Funder, S., Kjær, K.H., Larsen, E., and Moller, P. (2006). Constraints on the Late Saalian to early Middle Weichselian ice sheet of Eurasia from field data and rebound modelling. *Boreas* 35**,** 539-575 https://doi.org/10.1080/03009480600781875.

Lambeck, K., Purcell, A., Zhao, J., and Svensson, N.-O. (2010). The Scandinavian Ice Sheet: from MIS 4 to the end of the Last Glacial Maximum. *Boreas* 39**,** 410-435 https://doi.org/10.1111/j.1502-3885.2010.00140.x.

Landvik, J.Y., Bondevik, S., Elverhøi, A., Fjeldskaar, W., Mangerud, J.a.N., Salvigsen, O., Siegert, M.J., Svendsen, J.-I., and Vorren, T.O. (1998). The Last Glacial Maximum of Svalbard and the Barents Sea area: Ice Sheet extent and configuration. *Quaternary Science Reviews* 17**,** 43-75 https://doi.org/10.1016/S0277-3791(97)00066-8.

Liakka, J., Löfverström, M., and Colleoni, F. (2016). The impact of the North American glacial topography on the evolution of the Eurasian ice sheet over the last glacial cycle. *Climate of the past* 12**,** 1225-1241 10.5194/cp-12-1225-2016.

Lien, Ø.F., Hjelstuen, B.O., Zhang, X., and Sejrup, H.P. (2022). Late Plio-Pleistocene evolution of the Eurasian Ice Sheets inferred from sediment input along the northeastern Atlantic continental margin. *Quaternary Science Reviews* 282**,** 107433 https://doi.org/10.1016/j.quascirev.2022.107433.

Lucchi, R.G., St. John, K., and And Ronge, T.A. (2023). Expedition 403 Scientific Prospectus: Eastern Fram Strait PaleoArchive (FRAME). . *International Ocean Discovery Program.*

Macayeal, D.R., Bindschadler, R.A., and Scambos, T.A. (1995). Basal friction of Ice Stream E, West Antarctica. *Journal of Glaciology* 41**,** 247-262 10.3189/S0022143000016154.

Mattingsdal, R., Knies, J., Andreassen, K., Fabian, K., Husum, K., Grosfjeld, K., and De Schepper, S. (2014). A new 6 Myr stratigraphic framework for the Atlantic-Arctic Gateway. *Quaternary Science Reviews* 92**,** 170-178 doi: 10.1016/j.quascirev.2013.08.022.

Mitchum, J.R.M., and Vail, P.R. (1977). Seismic stratigraphy and global changes of sea level; Part 7, Seismic stratigraphic interpretation procedure (in Seismic stratigraphy; applications to hydrocarbon exploration, C. E. Payton, editor). *Memoir - American Association of Petroleum Geologists* 26**,** 135-143.

Mitchum, J.R.M., Vail, P.R., and Sangree, J.B. (1977). Seismic stratigraphy and global changes of sea level; Part 6, Stratigraphic interpretation of seismic reflection patterns in depositional sequences (in Seismic stratigraphy; applications to hydrocarbon exploration, C. E. Payton, editor). *Memoir - American Association of Petroleum Geologists* 26**,** 117-133.

Montelli, A., Solovyeva, M., Akhmanov, G., Mazzini, A., Piatilova, A., Bakay, E., and Dowdeswell, J.A. (2023). The geomorphic record of marine-based ice dome decay: Final collapse of the Barents Sea ice sheet. *Quaternary Science Reviews* 303**,** 107973 https://doi.org/10.1016/j.quascirev.2023.107973.

Myhre, A., Thiede, J., and Firth, J.A. (1995). Proceedings of the Ocean Drilling Program. Initial Reports, Leg 151. *Ocean Drilling Program, College Station, Texas, USA* 151**,** 39-59.

Newton, A.M.W., and Huuse, M. (2017). Glacial geomorphology of the central Barents Sea: Implications for the dynamic deglaciation of the Barents Sea Ice Sheet. *Marine Geology* 387**,** 114-131 http://dx.doi.org/10.1016/j.margeo.2017.04.001.

Obrochta, S.P., Crowley, T.J., Channell, J.E.T., Hodell, D.A., Baker, P.A., Seki, A., and Yokoyama, Y. (2014). Climate variability and ice-sheet dynamics during the last three glaciations. *Earth and Planetary Science Letters* 406**,** 198-212 https://doi.org/10.1016/j.epsl.2014.09.004.

Ottesen, D., Stokes, C.R., Rise, L., and Olsen, L. (2008). Ice-sheet dynamics and ice streaming along the coastal parts of northern Norway. *Quaternary Science Reviews* 27**,** 922-940 doi: 10.1016/j.quascirev.2008.01.014.

Patton, H., Alexandropoulou, N., Lasabuda, A.P.E., Knies, J., Andreassen, K., Winsborrow, M., Laberg, J.S., and Hubbard, A. (in review). Glacial erosion and Quaternary landscape development of the Eurasian Arctic. *Earth-Science Reviews*.

Patton, H., Andreassen, K., Bjarnadottir, L.R., Dowdeswell, J.A., Winsborrow, M.C.M., Noormets, R., Polyak, L., Auriac, A., and Hubbard, A. (2015). Geophysical constraints on the dynamics and retreat of the Barents Sea ice sheet as a paleobenchmark for models of marine ice sheet deglaciation. *Reviews of Geophysics* 53**,** 1051-1098 10.1191/095968398677085532; 10.1002/2015rg000495.

Patton, H., Hubbard, A., Andreassen, K., Winsborrow, M., and Stroeven, A.P. (2016). The build-up, configuration, and dynamical sensitivity of the Eurasian ice-sheet complex to Late Weichselian climatic and oceanic forcing. *Quaternary Science Reviews* 153**,** 97-121 10.1016/j.quascirev.2016.10.009.

Patton, H., Hubbard, A., Heyman, J., Alexandropoulou, N., Lasabuda, A.P.E., Stroeven, A.P., Hall, A.M., Winsborrow, M., Sugden, D.E., Kleman, J., and Andreassen, K. (2022). The extreme yet transient nature of glacial erosion. *Nature Communications* 13**,** 7377 10.1038/s41467-022-35072-0.

Piasecka, E.D., Winsborrow, M.C.M., Andreassen, K., and Stokes, C.R. (2016). Reconstructing the retreat dynamics of the Bjørnøyrenna Ice Stream based on new 3D seismic data from the central Barents Sea. *Quaternary Science Reviews* 151**,** 212-227 http://dx.doi.org/10.1016/j.quascirev.2016.09.003.

Pope, E.L., Talling, P.J., Hunt, J.E., Dowdeswell, J.A., Allin, J.R., Cartigny, M.J.B., Long, D., Mozzato, A., Stanford, J.D., Tappin, D.R., and Watts, M. (2016). Long-term record of Barents Sea Ice Sheet advance to the shelf edge from a 140,000 year record. *Quaternary Science Reviews* 150**,** 55-66 http://dx.doi.org/10.1016/j.quascirev.2016.08.014.

Pope, E.L., Talling, P.J., and Ó Cofaigh, C. (2018). The relationship between ice sheets and submarine mass movements in the Nordic Seas during the Quaternary. *Earth-Science Reviews* 178**,** 208-256 https://doi.org/10.1016/j.earscirev.2018.01.007.

Rebesco, M., Laberg, J.S., Pedrosa, M.T., Camerlenghi, A., Lucchi, R.G., Zgur, F., and Wardell, N. (2014). Onset and growth of Trough-Mouth Fans on the North-Western Barents Sea margin – implications for the evolution of the Barents Sea/Svalbard Ice Sheet. *Quaternary Science Reviews* 92**,** 227-234 https://doi.org/10.1016/j.quascirev.2013.08.015.

Rich, J.L. (1951). THREE CRITICAL ENVIRONMENTS OF DEPOSITION, AND CRITERIA FOR RECOGNITION OF ROCKS DEPOSITED IN EACH OF THEM. *GSA Bulletin* 62**,** 1-20 10.1130/0016-7606(1951)62[1:Tceoda]2.0.Co;2.

Rohling, E.J., Hibbert, F.D., Williams, F.H., Grant, K.M., Marino, G., Foster, G.L., Hennekam, R., De Lange, G.J., Roberts, A.P., Yu, J., Webster, J.M., and Yokoyama, Y. (2017). Differences between the last two glacial maxima and implications for ice-sheet, δ18O, and sea-level reconstructions. *Quaternary Science Reviews* 176**,** 1-28 https://doi.org/10.1016/j.quascirev.2017.09.009.

Ryseth, A., Augustson, J.H., Charnock, M., Haugerud, O., Knutsen, S.M., Midboe, P.S., Opsal, J.G., and Sundsbo, G. (2003). Cenozoic stratigraphy and evolution of the Sorvestsnaget Basin, southwestern Barents Sea. *Norwegian Journal of Geology* 83**,** 107-130.

Sættem, J., Poole, D.a.R., Ellingsen, L., and Sejrup, H.P. (1992). Glacial geology of outer Bjørnøyrenna, southwestern Barents Sea. *Marine Geology* 103**,** 15-51 https://doi.org/10.1016/0025-3227(92)90007-5.

Sættem, J., Rise, L., Rokoengen, K., and By, T. (1996). Soil investigations, offshore mid Norway: A case study of glacial influence on geotechnical properties. *Global and Planetary Change* 12**,** 271-285 https://doi.org/10.1016/0921-8181(95)00024-0.

Sato, T., and Kameo, K. (1996). Pliocene to Quaternary calcareous nannofossil biostratigraphy of the Arctic Ocean, with reference to late Pliocene glaciation. In: Thiede, J., Myhre, A.M., Firth, J.V., Johnson, G.L., Ruddiman, W.F. (Eds.), Proceeding of the Ocean Drilling Program, Scientific Results. *Ocean Drilling Program, College Station, Texas, USA* 151**,** 39-59.

Sejrup, H.P., Hjelstuen, B.O., Patton, H., Esteves, M., Winsborrow, M., Rasmussen, T.L., Andreassen, K., and Hubbard, A. (2022). The role of ocean and atmospheric dynamics in the marine-based collapse of the last Eurasian Ice Sheet. *Communications Earth & Environment* 3**,** 119 10.1038/s43247-022-00447-0.

Shackleton, N.J., Backman, J., Zimmerman, H., Kent, D.V., Hall, M.A., Roberts, D.G., Schnitker, D., Baldauf, J.G., Desprairies, A., Homrighausen, R., Huddlestun, P., Keene, J.B., Kaltenback, A.J., Krumsiek, K.a.O., Morton, A.C., Murray, J.W., and Westberg-Smith, J. (1984). Oxygen isotope calibration of the onset of ice-rafting and history of glaciation in the North Atlantic region. *Nature* 307**,** 620-623 10.1038/307620a0.

Sloan, E.D. (1998). Gas Hydrates: Review of Physical/Chemical Properties. *Energy & Fuels* 12**,** 191-196 10.1021/ef970164+.

Sloan Jr, E.D., and Koh, C.A. (2007). *Clathrate hydrates of natural gases.* CRC press.
Solheim, A., Faleide, J.I., Andersen, E.S., Elverhøi, A., Forsberg, C.F., Vanneste, K., Uenzelmann-Neben, G., and Channell, J.E.T. (1998). LATE CENOZOIC SEISMIC STRATIGRAPHY AND GLACIAL GEOLOGICAL DEVELOPMENT OF THE EAST GREENLAND AND SVALBARD–BARENTS SEA CONTINENTAL MARGINS. *Quaternary Science Reviews* 17**,** 155-184 https://doi.org/10.1016/S0277-3791(97)00068-1.
Stokes, C.R., Clark, C.D., Lian, O.B., and Tulaczyk, S. (2007). Ice stream sticky spots: A review of their identification and influence beneath contemporary and palaeo-ice streams. *Earth-Science Reviews* 81**,** 217-249 https://doi.org/10.1016/j.earscirev.2007.01.002.
Svendsen, J.I., Alexanderson, H., Astakhov, V.I., Demidov, I., Dowdeswell, J.A., Funder, S., Gataullin, V., Henriksen, M., Hjort, C., Houmark-Nielsen, M., Hubberten, H.W., Ingolfsson, O., Jakobsson, M., Kjaer, K.H., Larsen, E., Lokrantz, H., Lunkka, J.P., Lysa, A., Mangerud, J., Matiouchkov, A., Murray, A., Moller, P., Niessen, F., Nikolskaya, O., Polyak, L., Saarnisto, M., Siegert, C., Siegert, M.J., Spielhagen, R.F., and Stein, R. (2004). Late quaternary ice sheet history of northern Eurasia. *Quaternary Science Reviews* 23**,** 1229-1271 doi: 10.1016/j.quascirev.2003.12.008.
Torbjørn Dahlgren, K.I.T., Vorren, T.O., Stoker, M.S., Nielsen, T., Nygard, A., and Sejrup, H.P. (2005). Late Cenozoic prograding wedges on the NW European continental margin: their formation and relationship to tectonics and climate. *Marine and Petroleum Geology* 22**,** 1089-1110 doi: 10.1016/j.marpetgeo.2004.12.008.
Vorren, T.O., and Laberg, J.S. (1997). Trough mouth fans - Palaeoclimate and ice-sheet monitors. *Quaternary Science Reviews* 16**,** 865-881 doi: 10.1016/s0277-3791(97)00003-6.
Vorren, T.O., Landvik, J.Y., Andreassen, K., and Laberg, J.S. (2011). "Chapter 27 - Glacial History of the Barents Sea Region," in *Developments in Quaternary Sciences*, eds. J. Ehlers, P.L. Gibbard & P.D. Hughes. Elsevier), 361-372.
Vorren, T.O., Lebesbye, E., and Larsen, K.B. (1990). *GEOMETRY AND GENESIS OF THE GLACIGENIC SEDIMENTS IN THE SOUTHERN BARENTS SEA.* Bath: Geological Soc Publishing House.
Vorren, T.O., Richardsen, G., Knutsen, S.M., and Henriksen, E. (1991). CENOZOIC EROSION AND SEDIMENTATION IN THE WESTERN BARENTS SEA. *Marine and Petroleum Geology* 8**,** 317-340 doi: 10.1016/0264-8172(91)90086-g.
Wadham, J.L., Arndt, S., Tulaczyk, S., Stibal, M., Tranter, M., Telling, J., Lis, G.P., Lawson, E., Ridgwell, A., Dubnick, A., Sharp, M.J., Anesio, A.M., and Butler, C.E.H. (2012). Potential methane reservoirs beneath Antarctica. *Nature* 488**,** 633-637 10.1038/nature11374.
Wadham, J.L., Hawkings, J.R., Tarasov, L., Gregoire, L.J., Spencer, R.G.M., Gutjahr, M., Ridgwell, A., and Kohfeld, K.E. (2019). Ice sheets matter for the global carbon cycle. *Nature Communications* 10**,** 3567 10.1038/s41467-019-11394-4.
Wallmann, K., Pinero, E., Burwicz, E., Haeckel, M., Hensen, C., Dale, A., and Ruepke, L. (2012). The Global Inventory of Methane Hydrate in Marine Sediments: A Theoretical Approach. *Energies* 5**,** 2449-2498.
Wekerle, C., Colleoni, F., Näslund, J.-O., Brandefelt, J., and Masina, S. (2016). Numerical reconstructions of the penultimate glacial maximum Northern Hemisphere ice sheets: sensitivity to climate forcing and model parameters. *Journal of Glaciology* 62**,** 607-622 10.1017/jog.2016.45.
Whillans, I.M., Bentley, C.R., and Van Der Veen, C.J. (2001). "Ice Streams B and C," in *The West Antarctic Ice Sheet: Behavior and Environment*.), 257-281.
Whillans, I.M., and Van Der Veen, C.J. (1993). New and improved determinations of velocity of Ice Streams B and C, West Antarctica. *Journal of Glaciology* 39**,** 483-590 10.3189/S0022143000016373.
Winsborrow, M., Andreassen, K., Hubbard, A., Plaza-Faverola, A., Gudlaugsson, E., and Patton, H. (2016). Regulation of ice stream flow through subglacial formation of gas hydrates. *Nature Geosci* 9**,** 370-374 http://www.nature.com/ngeo/journal/v9/n5/abs/ngeo2696.html#supplementary-information.
Winsborrow, M.C.M., Andreassen, K., Corner, G.D., and Laberg, J.S. (2010). Deglaciation of a marine-based ice sheet: Late Weichselian palaeo-ice dynamics and retreat in the southern

Barents Sea reconstructed from onshore and offshore glacial geomorphology. *Quaternary Science Reviews* 29**,** 424-442 https://doi.org/10.1016/j.quascirev.2009.10.001.

Winsborrow, M.C.M., Patton, H., Esteves, M., and Alexandropoulou, N. (2022). "Chapter 32 - The Eurasian Arctic: glacial landforms prior to the Last Glacial Maximum (before 29ka)," in *European Glacial Landscapes*, eds. D. Palacios, P.D. Hughes, J.M. García-Ruiz & N. Andrés. Elsevier), 233-240.

Winters, W.J., Pecher, I.A., Waite, W.F., and Mason, D.H. (2004). Physical properties and rock physics models of sediment containing natural and laboratory-formed methane gas hydrate. *American Mineralogist* 89**,** 1221-1227 10.2138/am-2004-8-909.

9. Research papers

Paper 1

frontiers in Earth Science

ORIGINAL RESEARCH
published: 14 May 2021
doi: 10.3389/feart.2021.656732

A Continuous Seismostratigraphic Framework for the Western Svalbard-Barents Sea Margin Over the Last 2.7 Ma: Implications for the Late Cenozoic Glacial History of the Svalbard-Barents Sea Ice Sheet

Nikolitsa Alexandropoulou[1], Monica Winsborrow[1], Karin Andreassen[1], Andreia Plaza-Faverola[1], Pierre-Antoine Dessandier[1,2], Rune Mattingsdal[3], Nicole Baeten[4] and Jochen Knies[1,4]*

[1] Centre for Arctic Gas Hydrate, Environment and Climate (CAGE), Department of Geosciences, UiT The Arctic University of Norway, Tromsø, Norway, [2] Laboratoire Environnement Profond, IFREMER—Centre de Bretagne, Plouzané, France, [3] Norwegian Petroleum Directorate, Harstad, Norway, [4] Geological Survey of Norway, Trondheim, Norway

OPEN ACCESS

Edited by:
Ivar Midtkandal, University of Oslo, Norway

Reviewed by:
Brian W. Romans, Virginia Tech, United States
Giacomo Dalla Valle, National Research Council, Consiglio Nazionale delle Ricerche (CNR), Italy

***Correspondence:**
Nikolitsa Alexandropoulou
nikolitsa.alexandropoulou@uit.no

Specialty section:
This article was submitted to Sedimentology, Stratigraphy and Diagenesis, a section of the journal Frontiers in Earth Science

Received: *21 January 2021*
Accepted: *16 April 2021*
Published: *14 May 2021*

Citation:
Alexandropoulou N, Winsborrow M, Andreassen K, Plaza-Faverola A, Dessandier P-A, Mattingsdal R, Baeten N and Knies J (2021) A Continuous Seismostratigraphic Framework for the Western Svalbard-Barents Sea Margin Over the Last 2.7 Ma: Implications for the Late Cenozoic Glacial History of the Svalbard-Barents Sea Ice Sheet. Front. Earth Sci. 9:656732. doi: 10.3389/feart.2021.656732

Here we present a high-resolution, continuous seismostratigraphic framework that for the first time, connects the over 1,000 km long western Svalbard-Barents Sea margin and covers the last ∼2.7 million years (Ma). By exploiting recent improvements in chronology, we establish a set of reliable age fix-points from available boreholes along the margin. We then use a large 2-D seismic database to extend this consistent chronology from the Yermak Plateau and offshore western Svalbard, southwards to the Bear Island Trough-Mouth Fan. Based on this new stratigraphic framework we divide the seismic stratigraphy along the continental margin into three seismic units, and 12 regionally correlated seismic reflections, each with an estimated age assignment. We demonstrate one potential application of this framework by reconstructing the Svalbard-Barents Sea Ice Sheet evolution from the intensification of the northern hemisphere glaciation at ∼2.7 Ma to the Weichselian glaciations. Through seismic facies distribution and sedimentation rate fluctuations along the margin we distinguish three phases of glacial development. The higher temporal resolution provided by this new framework, allows us to document a clear two-step onset to glacial intensification in the region during phase 1, between ∼2.7 and 1.5 Ma. The initial step, between ∼2.7 and 2.58 Ma shows glacial expansion across Svalbard. The first indication of shelf-edge glaciation is on the Sjubrebanken Trough-Mouth Fan, northwestern Barents Sea after ∼2.58 Ma; whilst the second step, between ∼1.95 and 1.78 Ma shows glacial advances beyond Svalbard to the northwestern Barents Sea. Phase 2 is characterized by variations in sedimentation rates and the seismic facies are indicative for a regional glacial intensification for the whole Barents Sea-Svalbard region with widespread shelf-edge glaciations recorded at around ∼1.5 Ma. During Phase 3, the western Barents Sea margin is characterized by a dramatic increase in sedimentation rates, inferring once

again a regional glacial intensification. Our new stratigraphic framework allows for the first time differentiation of the sediments deposited on the slope during Early Saalian (∼0.4 and 0.2 Ma), Late Saalian (∼0.2 and 0.13 Ma), and Weichselian (<∼0.123 Ma) periods, providing new insights into the Barents Sea glaciations over the last ∼0.42 Ma.

Keywords: chronostratigraphy, quaternary, glacial intensification, palaeo-ice streams, Trough-Mouth Fan, sedimentation rates, Saalian, Weichselian

INTRODUCTION

The western Svalbard-Barents Sea continental margin (**Figure 1**) is over 1,000 km long and is characterized by thick glacigenic sediments that have been deposited over the last ∼2.7 Ma. These represent a valuable archive of Late Cenozoic environmental change, in particular, the waxing and waning of ice sheets across the adjacent continental shelf. However, the use of this archive to study and compare the sedimentological and glaciological evolution along the entire margin, and place this in a wider regional perspective, has been limited due to the lack of a unifying chronostratigraphic framework.

In the past, there have been several attempts to establish chronostratigraphic frameworks for both the western (Vorren et al., 1991; Faleide et al., 1996; Fiedler and Faleide, 1996; Hjelstuen et al., 1996; Laberg and Vorren, 1996a,b; Ryseth et al., 2003; Rebesco et al., 2014) and northern (e.g., Geissler and Jokat, 2004). Barents Sea and Svalbard margins. These attempts have been hampered by inconsistent chronologies between the sparse boreholes along the margin and limited seismic surveys necessary to by-pass problematic areas and correlate between the available boreholes. This lack of a continuous chronostratigraphic framework has also hindered attempts to provide a coherent reconstruction of paleoenvironmental variations along the entire western Svalbard-Barents Sea margin based on paleontological studies from the ODP sites on Yermak Plateau (ODP Site 910, 911, 912) and offshore west Svalbard (ODP 986). The interpretation of these proxies form the basis for the individual stratigraphic frameworks for each site (e.g., Cronin and Whatley, 1996; Hull et al., 1996; Matthiessen and Brenner, 1996; Spiegler, 1996; Eidvin and Nagy, 1999; Smelror, 1999; Grøsfjeld et al., 2014).

New age assignments for the Ocean Drilling Program (ODP) Sites 910, 911, 912 on Yermak Plateau (e.g., Knies et al., 2009; Mattingsdal et al., 2014) and ODP Site 986 west of Svalbard (e.g., Channell et al., 1999; Knies et al., 2009; **Figure 1**) now provide a robust, consistent chronology for the north and western Svalbard margin. Additionally, a new seafloor drill rig MeBo (Meeresboden-Bohrgerät) site (MeBo Site 126) on Vestnesa Ridge (Dessandier et al., 2021), and a piston core site (GS14-190-01PC; hereafter referred to as GS14-190) on the Bear Island (Bjørnøya) Trough-Mouth Fan (TMF) (**Supplementary Figure 1** and **Figure 1**), have yielded dates for the youngest (< ∼0.42 Ma) part of the sequence based on stable isotope data. These now offer the possibility to identify a consistent chronology along the entire margin and the potential to correlate between age fix-points, given a suitable seismic dataset.

In this paper, we exploit these recent improvements in chronology to establish a set of reliable age fix-points from available boreholes along the margin and then use a large dataset compiled of both conventional and high-resolution (e.g., Andreassen, 2017) 2D seismic data to extend this consistent chronology from the Yermak Plateau and offshore western Svalbard, southwards to the Bear Island TMF. This provides a continuous seismostratigraphic framework that extends along the entire 1,000 km long western Svalbard-Barents Sea margin (**Figures 2**, **3**) and includes seismic reflections corresponding to the widely used R7-R1 seismic stratigraphy proposed by Faleide et al. (1996) and additional seismic reflections tied to the new age fix-points. This yields 12 regionally correlated seismic reflections (including R7-R1), each with an estimated age assignment (**Figures 4**, **5**). Finally, we demonstrate one potential application of this new stratigraphic framework by reconstructing the Late Cenozoic glacial history of the Svalbard-Barents Sea Ice Sheet (SBIS), based on seismic facies distribution (**Figures 6**, **7**) and sedimentation rate trends along the margin (**Figure 8**).

REGIONAL SETTING

The Barents Sea is today an epicontinental sea characterized by relatively shallow banks separated by deep troughs (**Figure 1**). With water depths ranging from 100 to 200 m in the banks to around 400 m in the troughs, the Barents Sea shelf extends from the Norwegian-Greenland Sea and the Svalbard Archipelago in the west to Novaya Zemlya in the east.

The evolution of the western Barents Sea margin is closely related to the gradual opening of the Norwegian-Greenland Sea (e.g., Faleide et al., 2008). The western Barents Sea and Svalbard continental margin extends about 1,000 km in a north-south direction. Yermak Plateau is located on the eastern flank of the Fram Strait in the marginal Arctic Ocean (**Figure 1**). It forms the northwestern part of the Barents Sea shelf and is bounded by the Arctic Ocean to the north and the Svalbard archipelago to the south. The southern Yermak Plateau has water depths of about 600–800 m, but shallows to less than 500 m in the southernmost part.

Rift flank uplift, inferred to have been most pronounced in the Svalbard area and caused by a thermal anomaly (Dimakis et al., 1998), was a consequence of the tectonic evolution of the area during early-middle Cenozoic. Farther south in the shear zone area of the southwestern Barents Sea, the uplift was less pronounced and was the result of thermomechanical coupling (e.g., Dimakis et al., 1998; Faleide et al., 2008). The uplifted northern Barents Sea shelf areas experienced severe erosion during Eocene to Miocene times, feeding sediment to the southern and eastern Barents Sea shelf, which were low-relief areas close to sea level at that time (e.g., Butt et al., 2002),

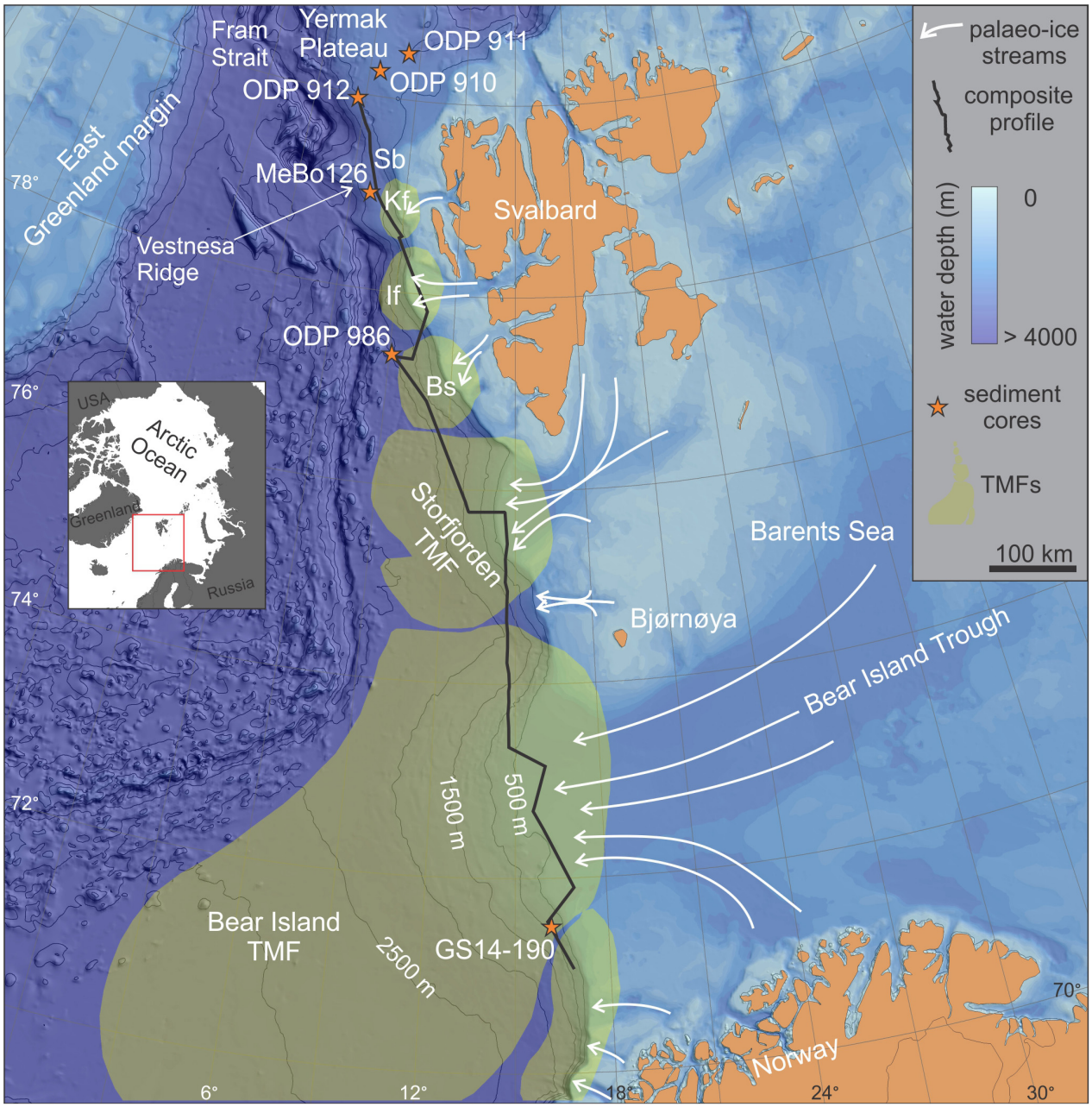

FIGURE 1 | Basemap shows the composite profile along the western Svalbard-Barents Sea margin. Sb: Sjubrebanken TMF; Kf: Kongsfjorden TMF; If: Isfjorden TMF; Bs: Bellsund TMF. Background bathymetry from International Bathymetric Chart of the Arctic Ocean (IBCAO, version 3.0) (Jakobsson et al., 2012). TMFs: trough-mouth fans (Vorren and Laberg, 1997; Dahlgren et al., 2005).

contributing to the composition of the sedimentary bedrock across the Barents Sea shelf (Sættem et al., 1992, 1994; Sigmond, 1992). The uplifted Barents Sea region (Dimakis et al., 1998; Faleide et al., 2008) subsequently became the site of nucleation of very large ice masses during several glaciations (e.g., Eidvin et al., 1993).

Butt et al. (2002) and Zieba et al. (2017) based on numerical modeling, suggested that the Barents Sea was subaerial during the earliest Late Pliocene, becoming a submarine platform around ∼1 Ma ago. Both the preglacial and glacial history is reflected in the present-day topography of the Barents Sea region (e.g., Faleide et al., 1996; Ottesen et al., 2008; Andreassen and Winsborrow, 2009; Laberg et al., 2012). An upper regional unconformity (URU) defines the base of the glacigenic sediments across the continental shelf (Solheim and Kristoffersen, 1984; Vorren et al., 1986).

The Plio-Pleistocene sedimentary succession of the Svalbard-Barents Sea margin consists of successive glacial-interglacial

western Svalbard-Barents Sea Margin				Yermak Plateau	
Seismic stratigraphy and age (Ma)[1]		Age (Ma) ODP Site 986[2]	Revised age (Ma)[3]	Seismic stratigraphy[4]	Age (Ma) ODP Sites 910,911,912[5]
GIII					
	R1 -0.44	0.2	0.2		
	R2	0.5	0.4		
GII	R3	0.78	0.75		0.78
	R4	0.99	1.1	YP-3	0.99
	R4A		1.3		
	R5 -1.0	1.3 - 1.5	1.5		1.5
GI	R6	1.6 - 1.7	2.1		
	R7 -2.3	2.7			2.7
G0				YP-2	

FIGURE 2 | Previous correlation between the seismic stratigraphy of the western Barents Sea-Svalbard margin and Yermak Plateau together with the published age estimates for the seismic reflections. G0: preglacial strata. [1]Faleide et al. (1996); [2]Jansen et al. (1996); Channell et al. (1999); Eidvin and Nagy (1999); Forsberg et al. (1999); Butt et al. (2000); Knies et al. (2009); [3]Rebesco et al. (2014); [4]Geissler and Jokat (2004); [5]Myhre et al. (1995); Knies et al. (2009); Mattingsdal et al. (2014).

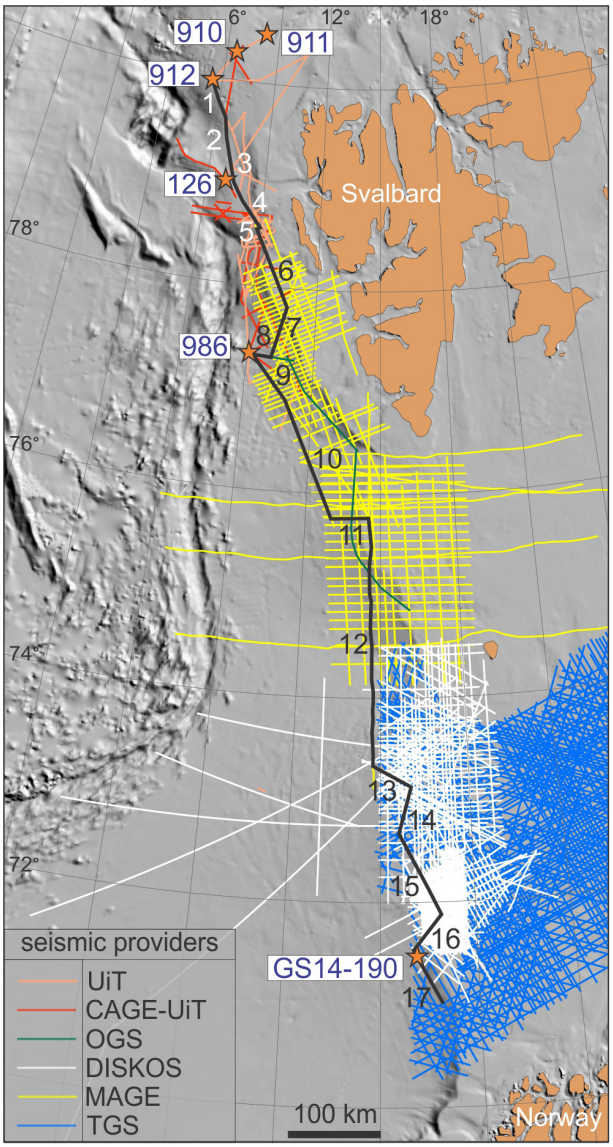

FIGURE 3 | 2D seismic dataset and composite seismic profile used to derive the new seismic stratigraphic framework. Basemap presenting the 2D seismic datasets and the composite seismic profile. Orange stars: location of the core sites. ODP Sites: 910, 911, 912, 986. Piston core: GS14-190. CAGE-Centre for Arctic Gas Hydrate, Environment and Climate-UiT The Arctic University of Norway in Tromsø. EGLACOM provided by the National Institute of Oceanography and Applied Geophysics (OGS), Trieste, Italy. Diskos: Norwegian Diskos National Data Repository (NDR) database. MAGE: Russian Joint Stock Company 'Marine Arctic Geological Expedition'. TGS: TGS-NOPEC Geophysical Company Pty Ltd.

sedimentary sequences, including several large submarine trough mouth fans, forming the morphological shelf edge along the passive continental margin of the European plate. The size of the individual TMFs reflects both the size of the troughs and their corresponding drainage area. The Bear Island TMF is by far the largest, and the TMFs along the Svalbard margin the smallest (e.g., Faleide et al., 1996; Vorren and Laberg, 1997; Pope et al., 2018). The TMFs are depocenters accumulated in front of ice streams draining the former large ice sheets, representing an excellent source of information on past glacial fluctuations (e.g., Faleide et al., 1996; Hjelstuen et al., 1996, 2007; Solheim et al., 1996; Vorren and Laberg, 1997; Taylor et al., 2002; Dowdeswell et al., 2008; Montelli et al., 2018; Ó Cofaigh et al., 2018; Pope et al., 2018). More specifically, during glacial maxima, sediments transported by the advancing ice sheet attain the shelf break and are delivered directly to the upper slope producing glacigenic debris flow deposits (e.g., Dowdeswell et al., 2008; Ottesen et al., 2016; Camerlenghi, 2018; Knies et al., 2018).

PREVIOUS SEISMIC FRAMEWORKS AND AGE CONTROL ALONG THE NORTHERN AND WESTERN SVALBARD-BARENTS SEA CONTINENTAL MARGIN

The first attempt to combine the local seismic stratigraphies from different TMFs along the western Barents Sea margin into one, was made by Faleide et al. (1996). In their seismic framework, three main seismic units GI-GIII, and seven regional seismic reflections R7-R1 were identified along the western margin, of which the deepest, R7, was interpreted to mark the base of the glacial deposits (**Figure 2**). Chronological constraints on the proposed seismic stratigraphy were sparse, and a likely age of R7 was proposed by Faleide et al. (1996) to be 2.3 Ma, derived from the chronostratigraphic framework of shallow boreholes and exploration wells from the southwestern Barents Sea (e.g., Sættem et al., 1992, 1994; Eidvin et al., 1993; Mørk and Duncan, 1993). R1 was considered to be between 440 and 200 ka based

Seismic units	Seismic horizons	Assigned Age (Ma)	Datum	Sediment cores
GIII		0.074	MIS 5/4 boundary	MeBo 126[1], GS14- 190[2]
		0.13	MIS 6/5 boundary	MeBo 126[1]
	R1	0.2	Seismic horizon[7]	
GII	R2	0.42	MIS 12/11 boundary	MeBo 126[1]
	R3	0.78	Brunhes/Matuyama	ODP 910A[5], 911A[3], 912A[3], 986[4]
	R4	0.99	Top Jaramillo	ODP 986C[4], 912A[3]
	R4A	1.2	Cobb Mountain Top	ODP 912A[3], 910A[5], 910C[9]
	R5	1.5	Seismic horizon[6, 7]	
GI	R6	1.78	Olduvai Top	ODP 911A[3], 912A[3]
		1.95	Olduvai Base	ODP 911A[3], 912A[3], 910A/C[6]
		2.58	Matuyama/Gauss	ODP 910A/C[6], 911A[3]
	R7	2.7	"Datum A"	ODP 911A[8], 910A/C[6], 986[9]

FIGURE 4 | Age-fix points on which seismostratigraphic framework is based. Seismic units and seismic reflections along the western Svalbard-Barents Sea margin correlated with the seismic stratigraphy, R7-R1 (Faleide et al., 1996; Jansen et al., 1996), age fix-points and their datums, used to constrain the seismic stratigraphy from the available core sites along the margin. [1]Dessandier et al., 2021 [2]This study [3]Myhre et al. (1995) [4]Channell et al. (1999) [5]Knies et al. (2007) [6]Mattingsdal et al. (2014); [7]Faleide et al. (1996); Fiedler and Faleide (1996) [8]Sato and Kameo (1996) [9]Smelror (1999); Knies et al. (2009).

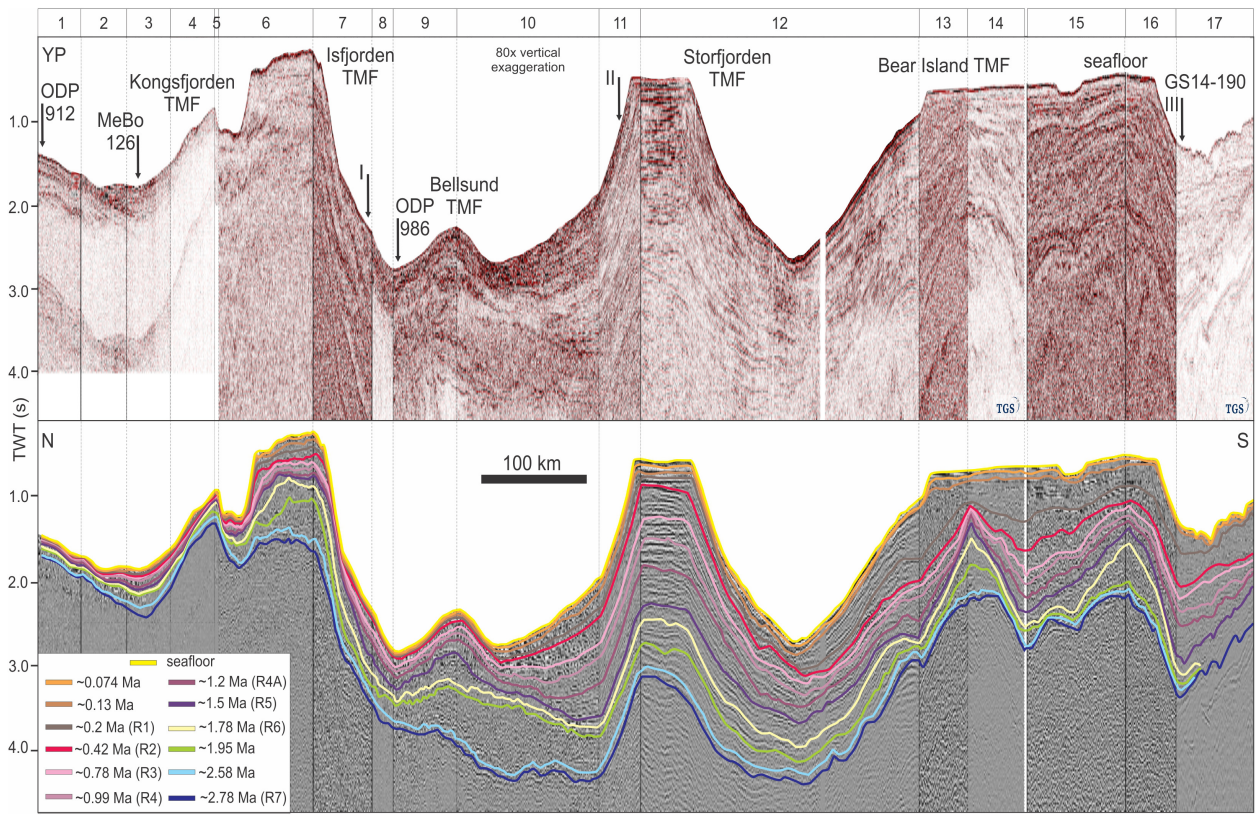

FIGURE 5 | Composite profile along the western Svalbard-Barents Sea margin showing the new seismic stratigraphy (see **Figures 1**, **3** for location). R1-R7: seismic reflections corresponding to this study seismic stratigraphy. I–III: selected points along the composite profile for estimating the sedimentation rates. 1–17: seismic lines that comprise the composite profile (the names of the seismic lines are displayed in **Supplementary Table 1**). Sections 14 and 17 courtesy TGS.

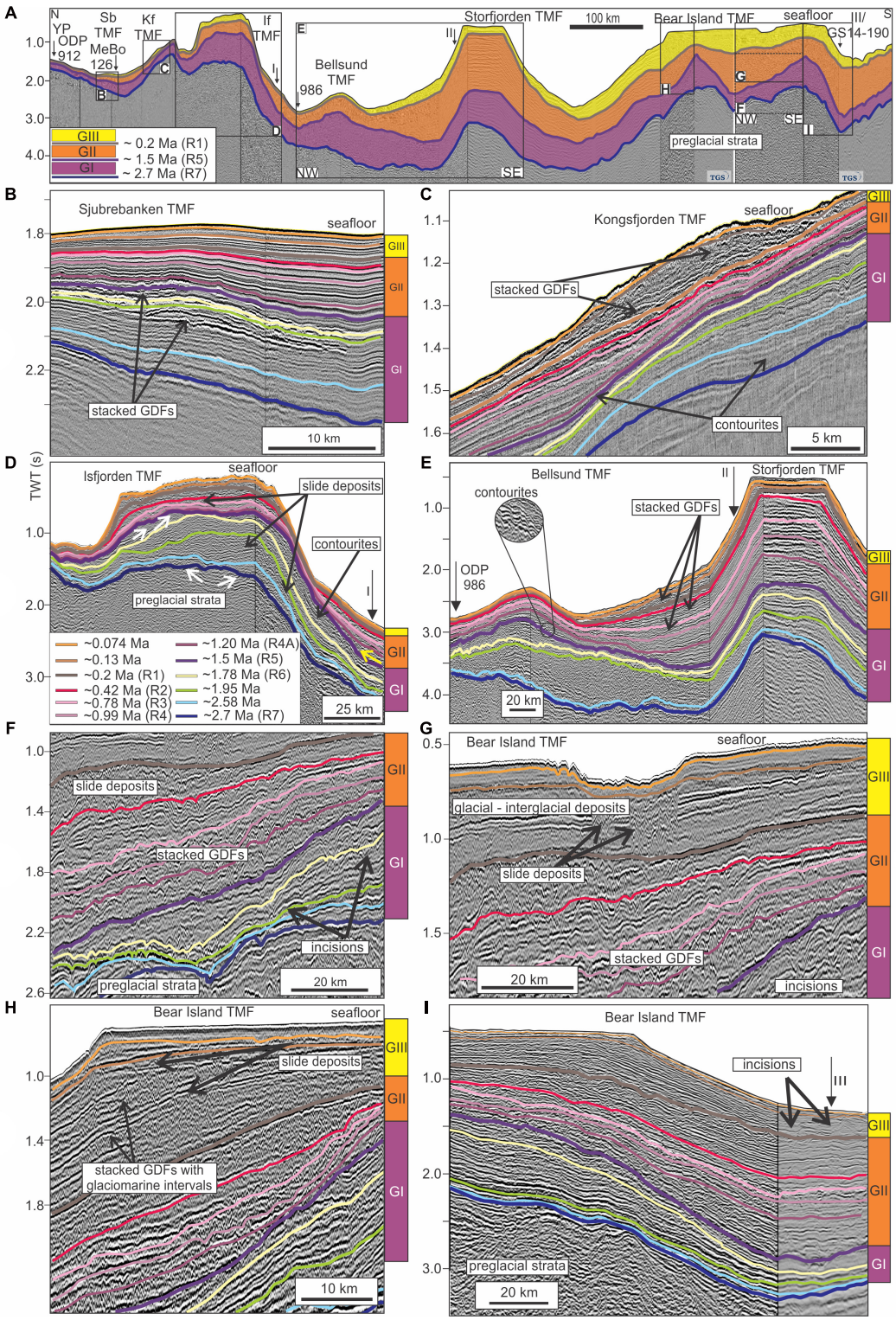

FIGURE 6 | Variations in seismic facies and sediment thickness along the margin. **(A)** Seismic stratigraphy of the western Svalbard-Barents Sea margin divided into three main seismic units GI-GIII and 12 regionally correlatable seismic reflections. **(B–I)** Characteristic seismic facies along the margin are presented in selected closed-up views. **(B)** Sjubrebanken TMF (Sb). **(C)** Kongsfjorden TMF (Kf). **(D)** Isfjorden TMF (If). White arrows: truncated reflections; yellow arrows: onlapping reflections. **(E)** Bellsund and Storfjorden TMF. **(F–I)** Bear Island TMF, southwestern Barents Sea margin. GDFs: glacigenic debris flow deposits. I–III: selected points along the composite profile for estimating the sedimentation rates. Part of the seismic data including in **(A,I)** courtesy TGS. R1-R7: seismic reflections corresponding to this study seismic stratigraphy.

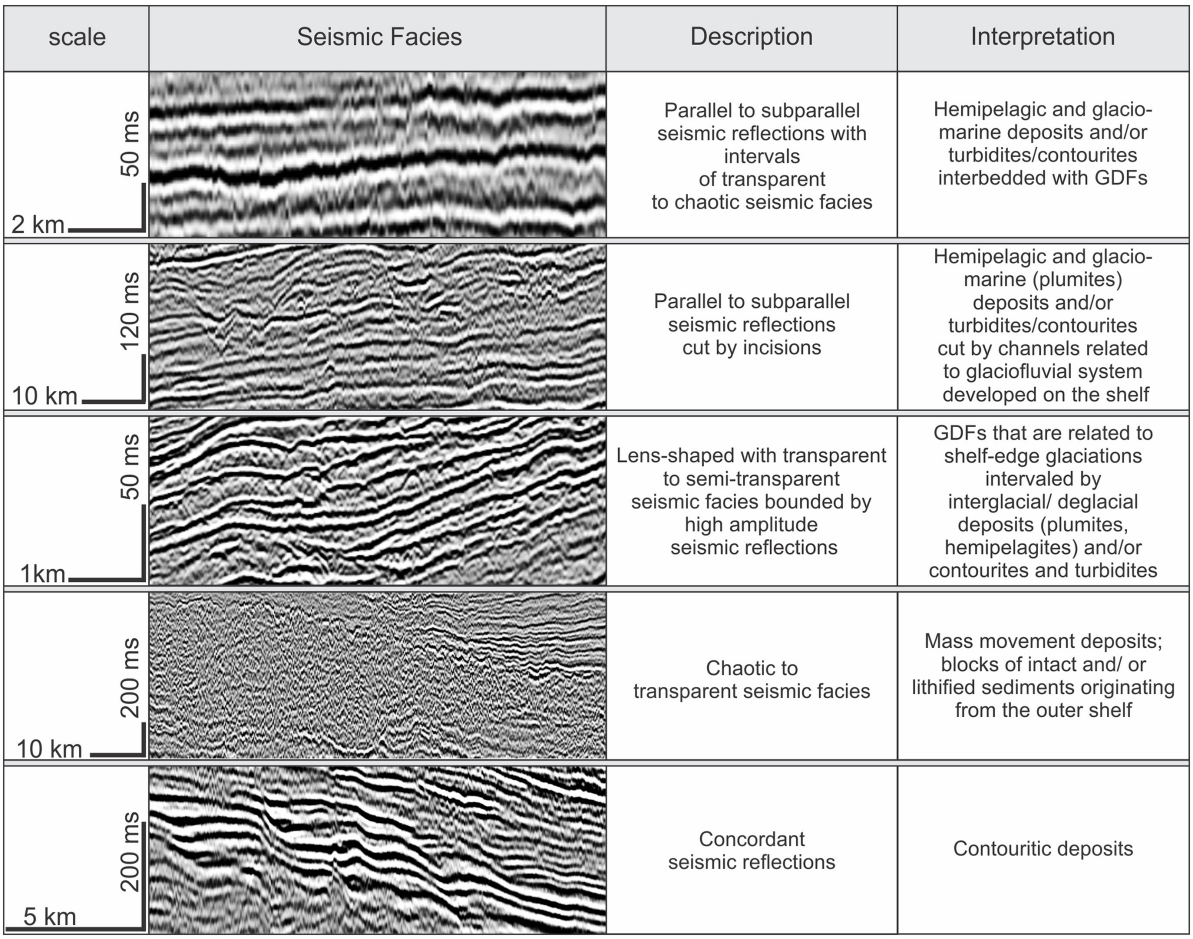

FIGURE 7 | Characteristic seismic facies that are observed along the western Svalbard-Barents Sea margin over the last ∼2.7 Ma together with their interpretation. GDFs: glacigenic debris flow deposits.

on shallow boreholes in the outer Bear Island Trough (Sættem et al., 1992), amino acid analyses (Sættem et al., 1992) and extrapolation of calculated sedimentation rates in piston cores on the Svalbard margin (Elverhoi et al., 1995). The age of R5 was estimated to be ∼1.0 Ma by correlation with increased amounts of ice-rafted detritus (IRD) and oxygen-isotope measurements (Faleide et al., 1996).

In 1995 ODP Site 986 west of Svalbard was drilled (Jansen et al., 1996) and a key objective for this site was to improve the age control of the R7-R1 seismic stratigraphy. Initial age estimates for ODP Site 986 were made using paleomagnetic (Channell et al., 1999), biostratigraphic (Eidvin and Nagy, 1999) and Sr-isotope data (Forsberg et al., 1999), with much emphasis placed on the magnetic stratigraphy due to poor biostratigraphic constraints. This yielded the following age estimates (**Figure 2**): ∼0.5 Ma for R2 (interpolation, supported by biostratigraphic data; Butt et al., 2000). ∼0.78 Ma (Brunhes/Matuyama palaeomagnetic datum; Channell et al., 1999) for R3. ∼0.99 Ma for R4 (Top Jaramillo palaeomagnetic datum; Channell et al., 1999). 1.3–1.5 Ma was estimated for R5 (interpolated age, supported by biostratigraphic and Sr-data; Butt et al., 2000), ∼1.6–1.7 Ma for R6 (interpolated age, supported by biostratigraphic and Sr-data; Butt et al., 2000), and 2.3–2.5 Ma for R7 based on linear interpolation between the maximum age of 2.6 Ma at the base of ODP Site 986, supported by biostratigraphic and Sr data (Butt et al., 2000). The biostratigraphy of Site 986 was re-evaluated later by Knies et al. (2009) who suggested the additional biostratigraphic datums of ∼2.41 and 2.76 Ma. They further found that the age of the base of ODP Hole 986D dates to ∼3.2 Ma and together with the additional biostratigraphic datums they revised the age of R7 to ∼2.7 Ma (**Figure 2**).

Later Rebesco et al. (2014) revised the ages of reflections R6, R5, R4, R3, R2, and R1 and assigned for the first time an age for R4A reflection by linear interpolation between the palaeomagnetic datums, the Brunhes/Matuyama boundary and the top of the Jaramillo Subchron (Channell et al., 1999). The respectively, given ages of those reflections are about 2.1 Ma (R6), 1.5 Ma (R5), 1.3 Ma (R4A), 1.1 Ma (R4), 0.75 Ma (R3), 0.4 Ma (R2), and 0.2 Ma (R1) (**Figure 2**).

The northern Barents Sea margin stratigraphy (Geissler and Jokat, 2004) relies on the three ODP sites (910, 911, 912) on the Yermak Plateau (**Figure 3**) and is divided into three seismic

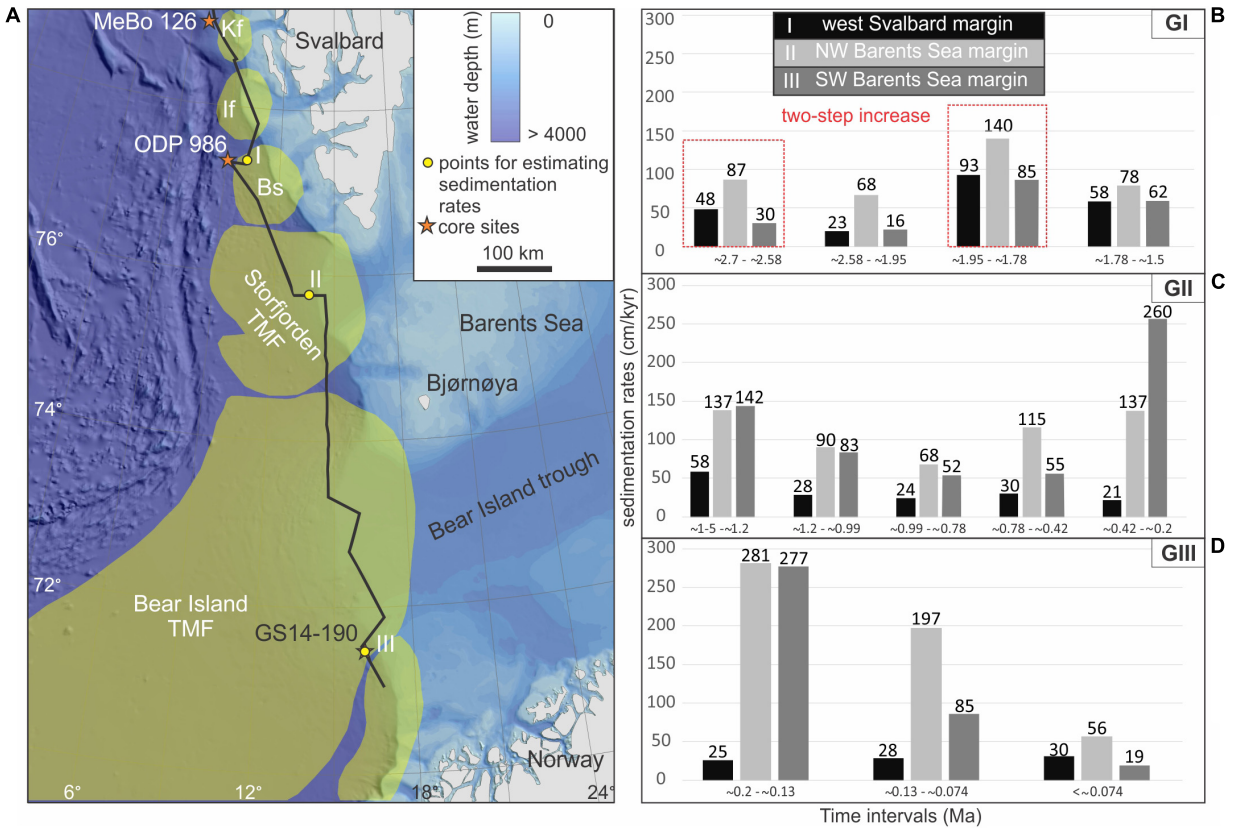

FIGURE 8 | Sedimentation rate estimates along the margin. **(A)** Basemap shows the location of the selected points along the composite profile for estimating the sedimentation rates (I–III) and the available core sites along the western Svalbard-Barents Sea margin. **(B–D)** Sedimentation rate plot shows variations on selected points I–III. Kf: Kongsfjorden TMF; If: Isfjorden TMF; Bs: Bellsund TMF.

units YP-1, YP-2, and YP-3 (Eiken and Hinz, 1993; Geissler and Jokat, 2004). The base of unit YP-3 represents the base of the glacial deposits and has been assigned an age of ∼2.7 Ma based on the chronostratigraphic framework of ODP Site 911 (Myhre et al., 1995: palaeomagnetic data; Sato and Kameo, 1996: biostratigraphic data). The ages of YP2-YP3 boundary on the Yermak Plateau and R7 seismic reflection on the western Barents Sea margin are similar, indicating a close correspondence of both seismic units GI-GIII (west) and YP-3 (north). Mattingsdal et al. (2014) further identified additional seismic horizons within YP-3 unit and assigned ages to these by ties to the three ODP sites on Yermak Plateau (910, 911, 912). Today, therefore two separated seismic stratigraphic frameworks have been established covering different parts of the continental margin, one for the northern Barents Sea margin (ODP Site 910, 911, 912), and one for the western Barents Sea margin (ODP Site 986).

MATERIALS AND METHODS

Dataset

Our dataset consists of 2D seismic reflection profiles, acquired over the last 34 years, both from industry and academia, that extends along the entire western Barents Sea-Svalbard margin, covering the continental slope and outer shelf (**Figure 3**). The vertical resolution (∼1/4 of the dominant wavelength, λ) of the existing seismic datasets varies considerably. In the western Barents Sea, the vertical resolution varies from 10 to 15 m close to the seafloor and up to 25–30 m near the base of the glacigenic sediments. The high-resolution 2D seismic data acquired by CAGE-Centre for Arctic Gas Hydrate, Environment and Climate -UiT The Arctic University of Norway in Tromsø (e.g., Andreassen, 2017), are located along the western Svalbard margin, and have a vertical resolution of ∼3–5 m at the seafloor, and ∼11–15 m at the base of the glacigenic sediments.

Methodology

The following workflow was implemented:

1. Compile all available 2D seismic datasets (**Figure 3**).
2. Correlate selected age fix-points from the available boreholes along the margin (**Figure 1** and **Supplementary Figures 2, 3**). The conversion of the age fix-points from depth to time at each core site was based on the velocity constraints from various studies (a) ODP 912: Mattingsdal et al. (2014), (b) MeBo Site 126: Plaza-Faverola et al. (2017), (c) ODP 986: Jansen et al. (1996), (d) GS14-190 piston core: Fiedler and Faleide (1996). Using the

2D seismic dataset we extend the chronostratigraphic framework from southern Yermak Plateau (ODP Sites 910, 911, 912) across a composite profile, toward Vestnesa Ridge, northern-western Svalbard margin (MeBo Site 126), Isfjorden TMF, west of Svalbard (ODP Site 986), and finally to the Bear Island TMF on the southwestern Barents Sea margin (piston core GS14-190) (**Figures 1**, **3** and **Table 1**). An overview of the 2D seismic profiles that comprise the composite profile are available in **Supplementary Table 1**. It is important to note that these seismic horizons extending along the margin are not necessarily timelines, as their character varies from depositional, continuous sedimentary reflections to erosional unconformities. We acknowledge the sparse availability of age fix-points and the fact that their uncertainty likely increases as these are extended along the margin, away from the core sites. However, the number and reliability of age fix-points, and the coverage and quality of the seismic database, represents a considerable improvement on previous frameworks used to calibrate the glacial seismic stratigraphy along the western Svalbard-Barents Sea margin. We anticipate that future scientific drillings in the study area, will test, modify, and further refine this framework.

3. Identify the most pronounced seismic reflections along the margin and divide the seismic stratigraphy into three main seismic units, GI-GIII.
4. Estimate sedimentation rates at selected points along the margin. The margin was divided into three sections representing the broad changes in source area and depositional environments along the margin: western Svalbard, northwestern Barents Sea and southwestern Barents Sea. Within each sector, sedimentation rates were estimated at a point along the composite seismic line selected as representative for that section based on visual inspection of the seismic datasets. Particular attention was given to avoid areas of mass wasting deposits and sediment bypass, and we consider these estimates to be representative of broad, regional changes in sedimentation rate despite the complex and varied depositional settings along the margin. The conversion of the seismic reflections from time to depth where there were no available age fix-points was based on the velocity constraints from various studies: Jansen et al. (1996) was used for the western Svalbard section (I), Hjelstuen et al. (1996) for the northwestern Barents Sea section (II), and Fiedler and Faleide (1996) for the southwestern Barents Sea section (III). We assume constant sedimentation rates during the selected time intervals.

TABLE 1 | Details of core sites displayed in **Figure 1**.

Core sites	Longitude	Latitude	Location	Water depth (m)
ODP 910A[a]	80°15.882 N	6°35.405 E	Yermak Plateau	556.4
ODP 911A[a]	80°28.466 N	8°13.640 E	Yermak Plateau	901.6
ODP 912A[a]	79°57.557′ N	5°27.360′E	Yermak Plateau	556.4
ODP 986C[b]	77°20.431′ N	9°04.664′ E	west Svalbard	2051.5
MeBo 126[c]	78°59.806′N	6°57.808′ E	Vestnesa Ridge	1207
GS14-190[d]	71°28.53′N	16°9.9′ E	SW Barents Sea	949

[a]*Myhre et al. (1995);* [b]*Jansen et al. (1996);* [c]*Bohrmann et al. (2017);* [d]*Knies et al. (2018).*

RESULTS

Chronology

Figure 4 shows the age fix-points that we have used to constrain the seismic stratigraphic framework on the southern Yermak Plateau (ODP Sites 910, 911, 912), Vestnesa Ridge (MeBo Site 126), west of Svalbard (ODP Site 986) and southwestern Barents Sea (GS14-190PC).

On the Yermak Plateau, ODP Site 912 covers sediments that extend only over the last 1.95 Ma (Myhre et al., 1995), and the seismic horizons older than 1.95 Ma are constrained by the age model for ODP Holes 910C and 911A established by Mattingsdal et al. (2014). The seismic reflection that correspond to ∼0.78 Ma is constrained by the ODP Sites 910, 911, and 912 (Yermak Plateau) and 986 (west of Svalbard), ∼0.99 Ma is constrained by the ODP Site 912 (Yermak Plateau) and 986 (west of Svalbard) and the seismic reflection that corresponds to ∼2.7 Ma age is constrained by the ODP Sites 910 and 911 (Yermak Plateau) and 986 (west of Svalbard), corresponding to R3, R4, and R7 of Faleide et al. (1996) seismic stratigraphy, respectively. The seismic horizons ∼1.2, 1.78, 1.95, and ∼2.58 Ma are calibrated only by the ODP Sites on the Yermak Plateau, however, they are characterized by moderate- to high-amplitude seismic reflections, allowing them to be correlated along the whole margin. The seismic reflection that corresponds to ∼1.5 Ma is equivalent to the R5 reflection by Faleide et al. (1996) and is constrained by the ODP Site 912 (Yermak Plateau) and Site 986 (west of Svalbard). The younger age estimates, ∼0.074, 0.13, and 0.42 Ma, are based on the MeBo Site 126 borehole from the Vestnesa Ridge (Dessandier et al., 2021). Based on the depth at which the seismic horizons corresponding to ∼0.42, 1.2, and 1.78 Ma ages cross the ODP Site 986 we correlate them to the R7-R1 seismic stratigraphy (Faleide et al., 1996; Jansen et al., 1996; **Figure 2** and **Supplementary Figure 3**). The respectively given ages of those reflections are about ∼0.42 Ma (R2), ∼1.2 Ma (R4A), and ∼1.78 Ma (R6). At the ODP Site 986, R1 reflection lies between the seismic reflections that correspond to ∼0.13 and 0.42 Ma ages (**Figure 2**). Based on the published ages for R1 reflection and its position at the ODP Site 986, we apply here ∼0.2 Ma as the age of R1.

On the southwestern Barents Sea margin, the GS14-190 Piston Core was used to provide additional confirmation of one age fix point. Specifically, the age of the core base (1,380 cm) in GS14-190 was estimated by linear interpolation to be ∼74 ka (**Supplementary Figure 1**) and correlates well with the seismic reflection that corresponds to ∼74 ka age fix-point on the MeBo Site 126 (Dessandier et al., 2021). Beyond this age fix-point, we rely on the R7-R1 seismic stratigraphy (Faleide et al., 1996; Fiedler and Faleide, 1996; Jansen et al., 1996; Hjelstuen et al., 2007) to constrain the stratigraphic framework in this area.

Seismostratigraphic Correlation

The continuous seismostratigraphic framework for the entire western Svalbard-Barents Sea margin developed in this study is presented in **Figure 5**. The framework comprises 12 seismic horizons, correlated along a composite seismic profile, between Yermak Plateau and the Bear Island TMF, with age assignments from ∼0.074 to 2.7 Ma, derived from selected age fix-points from available core sites (**Figure 4** and **Table 1**). All the seismic reflections are pronounced and can be traced along the whole margin. The location of the composite seismic profile (**Figure 1**) was selected to avoid challenging areas for the interpretation, such as steep slopes and areas with abundant slides and glacigenic debris flows.

An overview of the depth in two-way travel time (ms) for all the seismic reflections is given for all the key core sites in **Table 2** (see location of the sediment cores in **Table 1**), providing useful age estimates along the margin.

In line with the existing nomenclature, we separate the seismic stratigraphy of the last ∼2.7 Ma, into three seismic units, GI-GIII (Faleide et al., 1996). These units are bounded by the three most pronounced seismic reflections: R7 (∼2.7 Ma) (base of GI unit), R5 (∼1.5 Ma) (GI-GII boundary), and R1 (∼0. 2 Ma) (GII-GIII boundary) (**Figure 6A**), providing constraints on their age. These three seismic reflections represent important depositional sequence boundaries along the entire Barents Sea-Svalbard margin (e.g., Faleide et al., 1996; Butt et al., 2000; Hjelstuen et al., 2007; Mattingsdal et al., 2014; Rebesco et al., 2014).

Seismic Facies, Sedimentation Rates, and Interpretation

In the following sections, we describe the internal seismic facies distribution and variations in the sedimentation rates within each seismic unit (GI-GIII) and then interpret this with respect to palaeo-environmental conditions during the deposition of each unit. The thicknesses of the three seismic units vary along the continental margin and the internal seismic reflection patterns vary from stratified to chaotic. The characteristic seismic facies for the glacigenic sediments along the western Svalbard-Barents Sea margin are shown in **Figure 7**, together with their interpretation.

Along the composite profile we select three points (I–III) to calculate the sedimentation rates (**Figures 6**, **8A**). These points are located on: (I) western Svalbard margin section with sedimentation rates assumed to reflect a source area covering western Svalbard; (II) northwestern Barents Sea margin section with sedimentation rates assumed to reflect a source area encompassing both southern and central Svalbard, and the northwestern Barents Sea draining out the Storfjorden Trough; and (III) southwestern Barents Sea margin section with sedimentation rates assumed to reflect a source area encompassing a broad extent of the central and southern Barents Sea and northern Fennoscandia.

Seismic Unit GI (∼2.7–1.5 Ma)

The base of GI, reflection R7, is characterized by moderate to high amplitude and it represents a clear erosional unconformity (**Figure 6D**). However, near ODP Site 986 west of Svalbard, that is located on the deeper part of the continental margin, it forms a group of low-amplitude discontinuous reflections (**Figure 5**).

Overall, along the western Svalbard and northwestern Barents Sea margins, unit GI is characterized by subparallel seismic reflections of high amplitude interbedded with transparent to semi-transparent seismic reflections, interrupted by chaotic seismic facies (**Figures 6B–E**). From ∼2.7 to 2.58 Ma the whole margin is characterized by subparallel seismic reflections. Between ∼2.58 and 1.95 Ma on the Bellsund and Storfjorden TMFs there are intervals of chaotic seismic facies (**Figures 6D,E**), while, the Sjubrebanken TMF is characterized by lens-shaped

TABLE 2 | Correlation of the seismic stratigraphic framework proposed in this study to the three main seismic units, GI-GIII and R7-R1 seismic stratigraphy (Faleide et al., 1996).

Seismic units[a]	Seismic reflections R7-R1[a]	Assigned age (Ma)	ODP 912 (ms)	MeBo 126 (ms)	ODP 986 (ms)	GS14-190 (ms)
GIII		0	1,411	1,633	2,791	1,333
		∼0.074	1,421	**1,647**	2,806	**1,353**
		∼0.13	1,428	**1,654**	2,819	1,403
	R1	∼0.2	1,435	1,688	**2,827**	1,612
GII	R2	∼0.424	1,439	**1,717**	2,875	2,035
	R3	∼0.78	**1,444**	1,735	**2,947**	2,212
	R4	∼0.99	**1,450**	1,764	**2,988**	2,299
	R4A	∼1.2	**1,476**	1,822	3,066	2,463
	R5	∼1.5	**1,499**	1,867	**3,189**	2,871
GI	R6	∼1.78	**1,541**	1,939	3,370	3,006
		∼1.95	**1,560**	1,990	3,399	3,115
		∼2.58	**1,638**	2,124	3,625	3,186
	R7	∼2.7	**1,658**	2,268	**3,660**	3,220

*Two-way travel time in milliseconds (ms) at which the different seismic reflections derived from our seismostratigraphic framework cross the location of key core sites. In bold: actual depths of age fix-points from the key core sites (see **Table 1**) converted to two-way travel time.*

[a] *Faleide et al. (1996).*

R1-base of GIII unit and top of GII unit; R5-base of GII unit and top of GI unit; R7-base of GI unit.

bodies with a homogeneous interval, bounded by high-amplitude seismic reflections from ∼2.58 Ma and above (**Figure 6B**). Concordant seismic reflections are seen within the entire GI unit of Kongsfjorden TMF (**Figure 6C**), and in intervals from ∼1.78 Ma and above on the Bellsund TMF (**Figure 6E**). These seismic facies contrast strongly with those observed on the southwestern Barents Sea margin where unit GI is characterized by subparallel seismic reflections, cut by multiple incisions (**Figures 6F–H**).

Sedimentation rates during GI show a prominent two-step increase (**Figure 8B**). The first step (∼2.7 and ∼2.58 Ma), is marked by increased sedimentation rates compared to preglacial period (G0: 2–3 cm kyr^{-1}) (Faleide et al., 1996; Fiedler and Faleide, 1996; Hjelstuen et al., 1996, 2007; Mattingsdal et al., 2014; Lasabuda et al., 2018), in particular along the west Svalbard (48 cm kyr^{-1}) and northwestern Barents Sea (87 cm kyr^{-1}) margin (**Figure 8B**). This is followed by a significant drop in sedimentation rates, halved on both the western Svalbard and southwestern Barents Sea margin (down to 23 and 16 cm kyr^{-1}, respectively) and reducing by nearly a third on the northwestern Barents Sea margin (68 cm kyr^{-1}). Between ∼1.95 and 1.78 Ma a second period of peak sedimentation rates occurs, during which the sedimentation rates along the entire margin are characterized by a distinct increase reaching 93 cm kyr^{-1} on the western Svalbard, 85 cm kyr^{-1} on the southwestern Barents Sea margin and 140 cm kyr^{-1} on the northwestern Barents Sea margin (**Figure 8B**). This second increase is again followed by a reduction along the entire margin, with all three sections of the margin showing broadly uniform rates, varying from 58 to 78 cm kyr^{-1} (**Figure 8B**).

We interpret the variations in seismic facies distribution and sedimentation rates within GI to reflect a proximal ice margin on the western Svalbard and northwestern Barents Sea margin. The two-step increase in sedimentation rates suggests two periods of glacial expansion in these northern parts of the margin. During the first step meltwater discharges prevail inferred from the seismic facies and there is no indication of shelf-edge glaciations. The first indication of shelf-edge glaciation is on the Sjubrebanken TMF (northwestern Svalbard margin) where glacigenic debris flows are identified above ∼2.58 Ma. At the same time, mass wasting deposits become more widespread, especially on the Bellsund TMF (western Svalbard margin) and the Storfjorden TMF (northwestern Barents Sea margin), and parts of the western Svalbard margin are characterized also by contouritic/turbitidic deposits (Kongsfjorden and Bellsund TMF). The increase in mass wasting deposits related to megaslides/mass wasting may have been triggered by high sedimentation rates during the first step of glacial intensification (from ∼2.7 to 2.58 Ma), in combination with low eustatic sea-level and the presence of weak layers-contourites (Amundsen et al., 2011; Safronova et al., 2017). On the southwestern Barents Sea margin distal glaciomarine deposits prevail, interbedded with hemipelagic and/or turbiditic/contouritic deposits (e.g., Rydningen et al., 2020), cut by channels, which we relate to a glaciofluvial system developed on the shelf, in accordance with Laberg et al. (2010). Apart from the northwestern Svalbard margin, we see no evidence for shelf edge glaciation on the rest of the western Svalbard-Barents Sea margin during GI period.

Seismic Unit GII (∼1.5–0.2 Ma)

The base of GII, reflection R5, is one of the most pronounced seismic reflections along the margin. It clearly has an erosional character, truncating the underlying reflections (**Figures 6D,F,G**).

The internal seismic signature of unit GII on the western Svalbard-Barents Sea margin is lens-shaped bodies with a homogeneous internal structure bounded by high-amplitude seismic reflections and in places interrupted by chaotic seismic reflections (**Figures 6C,E–G,I**). Around ∼0.99 Ma we observe a change in seismic facies on the Sjubrebanken TMF from lens-shaped bodies with a homogeneous internal structure bounded by high-amplitude seismic reflections, to high-amplitude parallel to subparallel seismic reflections interbedded with layers of semi-transparent to transparent seismic facies. While at that time seismic facies of lens-shaped bodies with a homogeneous internal structure start to prevail on the Kongsfjorden TMF (**Figure 6C**) and these seismic facies increase in frequency on the Storfjorden TMF (**Figure 6E**). The Kongsfjorden and the Bellsund TMF are characterized by concordant seismic reflections up to ∼1.2 Ma (**Figures 6C,E**).

The transition from GI to GII is marked by an approximate doubling of sedimentation rates from 78 and 62 cm kyr^{-1} to 137 and 142 cm kyr^{-1} on the northwestern and southwestern Barents Sea margin, respectively, whilst they remain constant on the western Svalbard margin (58 cm kyr^{-1}) (**Figure 8C**). Sedimentation rates then gradually decrease along the northwestern (68 cm kyr^{-1}) and southwestern (52 cm kyr^{-1}) Barents Sea margin from ∼1.2 until ∼0.78 Ma. At around ∼0.78 Ma, rates once again start to rise, first on the northwestern Barents Sea margin (115 cm kyr^{-1}), followed by a dramatic increase, between ∼0.42 and ∼0.2 Ma, in the southwestern Barents Sea reaching up to 260 cm kyr^{-1}, the largest increase seen in our dataset. The western Svalbard margin has an overall decrease in sedimentation rates from 58 to 21 cm kyr^{-1} over the entire period (**Figure 8C**).

The western Svalbard margin during GII, is characterized by stable sedimentation rates and the seismic facies indicate the dominance of shelf-edge glaciations [e.g., glacigenic debris flow deposits, on the Sjubrebanken TMF (**Figure 6B**), Kongsfjorden TMF (**Figure 6C**) and the Bellsund TMF (**Figure 6E**)]. On the northwestern Svalbard margin (Sjubrebanken and Kongsfjorden TMF), changes in the seismic facies indicate an initial period of deposition focused on the Sjubrebanken TMF (**Figure 6B**) between ∼1.5 and 0.99 Ma, followed by a switch in deposition to the adjacent Kongsfjorden TMF, at around ∼0.99 Ma (**Figure 6C**). This change in depocentres has been interpreted as the expression of a switch in the location of the ice stream flowing out Kongsfjorden (Sarkar et al., 2011; Mattingsdal et al., 2014).

Along the northwestern and southwestern Barents Sea margin high sedimentation rates between ∼1.5 and 1.2 Ma (**Figure 8C**), accompanied by glacigenic debris flow and mass wasting deposits (**Figures 6E–G**), are consistent with increasing glacial cover across the Barents Sea, and shelf-edge glaciations along the

western Svalbard-Barents Sea margin. This is in agreement with the observation of megascale glacial lineations in the Bear Island Trough, indicating fast flowing ice streams reaching the shelf edge above R5 (∼1.5 Ma) (Andreassen et al., 2004).

Following this initial increase, sedimentation rates during GII generally decrease between ∼1.2 and 0.78 Ma, but the seismic facies (glacigenic debris flows and mass wasting deposits, **Figures 6C–I**) continue to indicate shelf-edge glaciations along the margin. At around ∼0.99 Ma an increase in glacigenic debris flow frequency is recorded in the western Svalbard and northwestern Barents Sea margins (**Figures 6C,E**) followed by an increase in sedimentation rates first on the northwestern Barents Sea margin around ∼0.78 Ma (**Figure 8C**) and then on the southwestern Barents Sea margin around ∼0.42 Ma (**Figure 8C**). This same time period is also associated with megaslides in the Bear Island TMF (Hjelstuen et al., 2007).

Seismic Unit GIII (< ∼0.2 Ma)

The base of GIII, reflection R1, is characterized by medium to strong amplitude and its character varies along the margin from depositional, continuous sedimentary reflection (**Figure 6B**) to erosional unconformity (**Figures 6C–E,G–I**). On the southwestern Barents Sea margin, the base of GIII corresponds to the Upper Regional Unconformity (URU) (Solheim and Kristoffersen, 1984; Vorren et al., 1986) on the shelf, that separates glacial sediments from the underlying preglacial strata (Fiedler and Faleide, 1996).

The western Svalbard and northwestern Barents Sea margins are characterized by an increase in frequency of the lens-shaped bodies with a homogeneous internal structure, bounded by high-amplitude parallel to subparallel seismic reflections compared to GII unit. This is well demonstrated on Kongsfjorden TMF (**Figure 6C**) and Storfjorden TMF (**Figure 6E**). The southwestern Barents Sea margin is characterized by lens-shaped bodies with a homogeneous internal structure bounded by high-amplitude parallel-subparallel seismic reflections (**Figures 6G–I**). Around ∼0.13 Ma a shift in seismic facies occurs along the whole margin from continued high amplitude parallel to subparallel seismic reflections to transparent to semi-transparent reflections (**Figures 6B,D,G**).

Overall, GIII is characterized by decreasing sedimentation rates, with higher and more variable sedimentation rates along the south- and north-western Barents Sea margin relative to those on the western Svalbard margin (**Figure 8D**). The first period of GIII (between ∼0.2 and 0.13 Ma) sees a maintenance of the low sedimentation rates on the western Svalbard margin, accompanied by increases on the northwestern and southwestern Barents Sea margins. The increase on the northwestern Barents Sea margin is particularly large, more than doubling from 137 to 281 cm kyr^{-1}, the highest sedimentation rate observed in our dataset. This is followed by a gradual decrease over the last ∼0.13 Ma for the northwestern and southwestern Barents Sea margins, resulting in more uniform sedimentation rates along the entire margin during the final period of GIII (< ∼0.074 Ma). The western Svalbard margin is characterized by stable sedimentation rates within GIII, varying from 25 to 30 cm kyr^{-1} (**Figure 8D**).

The western Svalbard-Barents Sea margin is characterized by glacigenic debris flows, with intervals of glaciomarine/hemipelagic deposits, disturbed by mass wasting deposits on the southwestern Barents Sea margin. Based on seismic facies distribution and the sedimentation rates, we infer shelf-edge glaciations along the entire western Svalbard-Barents Sea margin during GIII.

DISCUSSION

Reconstruction of the Svalbard – Barents Sea Ice Sheet Over the Last ∼2.7 Ma

Changes in sedimentation rates and seismic facies allow us to distinguish three phases of glacial development, each with specific characteristics in terms of ice extent and dynamics. Below we present a reconstruction of the evolution of glacial cover across the Svalbard-Barents Sea area over the past ∼2.7 Ma, and discuss these three phases in terms of palaeo-environmental and glacial dynamic changes.

Phase 1: 2-Step Glacial Intensification - (∼2.7 and 1.5 Ma)

The environmental change from G0 (preglacial period) to GI, associated with the first indications of large-scale glaciations in the northern Barents Sea around ∼2.7 Ma ago (e.g., Knies et al., 2009), is evidenced by a distinct increase in the mean sedimentation rate from 2 to 6 cm kyr^{-1} (preglacial strata; 55–2.7 Ma) (Faleide et al., 1996; Fiedler and Faleide, 1996; Hjelstuen et al., 1996, 2007; Mattingsdal et al., 2014; Lasabuda et al., 2018; Hjelstuen and Sejrup, 2020) to 38–82 cm kyr^{-1} (GI, ∼2.7–1.5 Ma). Within GI, the variations in sedimentation rate and seismic facies in our data are interpreted to indicate that across the Barents Sea-Svalbard shelf this initial glacial expansion occurred in two steps.

Intensification occurred first across Svalbard during phase 1, evidenced both by the high sedimentation rates (**Figure 8B**) and the prevalence of glacigenic debris flows (**Figure 6B**) and mass wasting deposits (**Figures 6D,E**) along the western Svalbard and northwestern Barents Sea margin. At this time on the southwestern Barents Sea margin, a more distal ice margin is inferred from the relatively lower sedimentation rates (**Figure 8B**) and the seismic facies implying channelized meltwater flows reaching the Bear Island TMF, sourced from the adjacent glaciated areas (**Figure 6D**). During the first step of intensification (from ∼2.7 to 2.58 Ma), the western Svalbard-Barents Sea margin is characterized by high sedimentation rates and glaciomarine deposits. In our data, we see no evidence for shelf-edge glaciation along the margin during the time period between ∼2.7 and ∼2.58 Ma. We therefore propose that during the first step of glacial build up, ice extent in the Barents Sea was restricted to the northernmost parts and did not reach the shelf break on the western Svalbard-Barents Sea margin (**Figure 9A**).

The high mountainous terrain of Svalbard provides a preferable location for glacial build-up, and this would have been further enhanced by additional preglacial tectonic uplift in the northwestern Barents Sea, yielding higher relief terrain compared

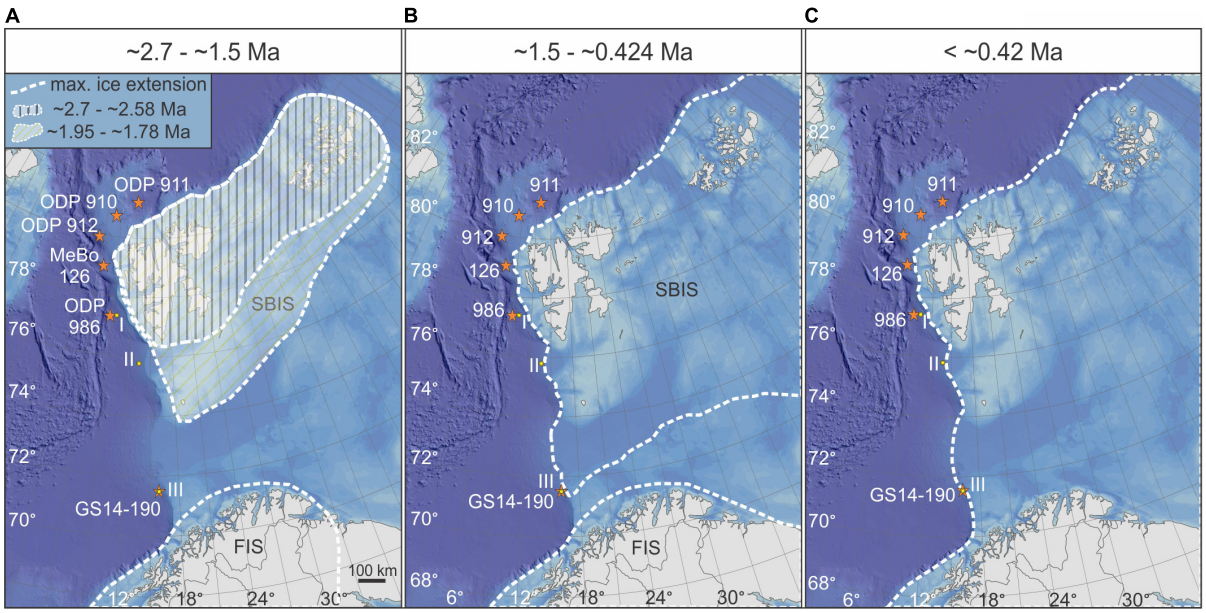

FIGURE 9 | Schematic model of lateral ice extension in the Barents Sea region (modified from Knies et al., 2009) based on our interpretation and the existing literature. **(A)** Maximum extension of the SBIS during the two steps of intensification between ~2.7 and 1.5 Ma. **(B)** Maximum extension of the SBIS and FIS between ~1.5 and 0.42 Ma. **(C)** Maximum extension of the SBIS and FIS over the last ~0.42 Ma. SBIS: Svalbard-Barents Sea Ice Sheet; FIS: Fennoscandian Ice Sheet.

with the southwestern Barents Sea and promoting more intense glaciations (e.g., Vagnes et al., 1992; Fiedler and Faleide, 1996; Henriksen et al., 2011). This interpretation of a Svalbard-focused onset to glacial expansion in the Barents Sea around ~2.7 Ma, is consistent with previous studies (e.g., Forsberg et al., 1999; Butt et al., 2000; Laberg et al., 2010; Mattingsdal et al., 2014). However, what these studies could not resolve was the subsequent pause in glacial build-up (between ~2.58 and 1.95 Ma), followed by a second period of intensification (between ~1.95 and 1.78 Ma), where ice began to extend beyond Svalbard, as indicated by the sedimentation rate and seismic facies data presented herein.

Between ~2.58 and 1.95 Ma sedimentation rates dropped along the entire margin (**Figure 8B**), however, the first observed glacigenic debris flows on the Sjubrebanken TMF indicate the first shelf-edge glaciations on the northwestern Svalbard margin and the mass wasting deposits on the Bellsund TMF and Storfjorden TMF (**Figures 6B,D,E**) may be due to the increased sedimentation rates during the first step of intensification. Meanwhile the southwestern Barents Sea margin continued to be characterized by glaciomarine sediments cut by glaciofluvial channels (**Figure 6G**). These suggest continued glacial cover, centered on Svalbard, but a halt in its expansion/intensification. This also broadly consistent with paleontological data both on Yermak Plateau (ODP Site 910) and offshore west Svalbard (ODP 986) which indicate a relatively strong influence of the North Atlantic Current during this period, bringing warmer waters to the margin (Cronin and Whatley, 1996; Osterman, 1996; Spiegler, 1996; Smelror, 1999).

The second step of glacial intensification (between ~1.95 and 1.78 Ma), is marked by simultaneously rising sedimentation rates along the entire margin (**Figure 8B**). These attest to more extensive glacial cover, extending beyond the Svalbard coastline to the wider northern and western Barents Sea, yet still not reaching the southern Barents Sea (**Figure 9A**). This is further supported by the seismic facies which shows an increase in the incisions on the southwestern Barents Sea margin (**Figure 6F**), consistent with other studies that have identified glaciofluvial drainage as the primary mode of sediment transport to the upper slope at this time (e.g., Butt et al., 2000). This is also in line with observations from ODP Site 986, where ice-rafted debris (IRD) first appears after R6 time (~1.78 Ma), suggesting that glaciers first reached the shelf break west of Svalbard after that time (Butt et al., 2000); and paleontological data in the sediments deposited directly after R6 time which indicate polar to subpolar conditions (Smelror, 1999).

The inception of large-scale North Hemisphere glaciations occurred in a stepwise fashion, with IRD records indicating initial expansion of the Greenland ice sheet at ~3.3 Ma, followed by expansion of North American and European ice sheets at ~2.72–2.75 Ma (e.g., Jansen et al., 2000; Flesche Kleiven et al., 2002). Our findings are consistent with this, showing initial Svalbard-focused glacial intensification along the western Svalbard-Barents Sea margin at the onset of the GI period (~2.7 Ma), and further show that the expansion of the Barents Sea Ice Sheet during this second period, also occurred in stepwise fashion.

A similar two-step pattern of glacial intensification is recorded in the IRD record from the circum-Atlantic region. Reduced IRD fluxes recorded between ~2.5 and 1.55 Ma (Fronval and Jansen, 1996) indicate that glacial intensification at ~2.7 Ma in Greenland and Scandinavia was followed by an interval characterized by less severe glaciations (Fronval and Jansen, 1996) and/or stabilized ice margins (Knies et al., 2009). This

is in accordance with moderate IRD supply in the Svalbard-Barents Sea region between ∼2.4 and 1.7 Ma indicating less glacial activity during that period (Knies et al., 2009). It has also been suggested that at ca. 2.4 Ma huge ice masses were probably absent from northern Greenland (Funder et al., 2001) and the western Canadian Arctic from ∼<2.0 to 1.8 Ma (Barendregt and Irving, 1998), implying a more regional climatic control of the Northern Hemisphere glaciations.

Phase 2: Glacial Expansion Across the Barents Sea and Shelf-Edge Glaciations (∼1.5 and ∼0.42 Ma)

The onset of phase 2, is marked by a clear increase in sedimentation rates along the northwestern and southwestern Barents Sea margin (**Figure 8C**), accompanied by glacigenic debris flows and mass wasting deposits (**Figure 6**). This attests to glacial expansion across the wider Barents Sea leading to shelf-edge glaciations along at least part of the western Svalbard-Barents Sea margin (**Figure 9B**), and implies a glacial intensification at around ∼1.5 Ma for the whole Barents Sea-Svalbard region (Knies et al., 2009; Mattingsdal et al., 2014; Rebesco et al., 2014). This is supported by the first signs of extensive glacial erosion on the Yermak Plateau (Mattingsdal et al., 2014) and observations of streamlined subglacial landforms and extensive glaciotectonism (deformation of rocks or sediment due to the overriding or pushing of ice) formed by ice streams reaching the shelf-edge in the southwestern Barents Sea at this time (e.g., Andreassen et al., 2004, 2007; Laberg et al., 2010). During the Middle Pleistocene Transition (MPT ∼1.3–0.7 Ma) ice sheet expansions have also been documented, both from seismic and sedimentological data, on the east Greenland margin (Laberg et al., 2018; Pérez et al., 2018), the northwestern Greenland margin (Newton et al., 2020), the mid-Norwegian margin (Montelli et al., 2017; Newton and Huuse, 2017), the North Sea (Rea et al., 2018), and North America (Balco and Rovey, 2010), implying a regional expansion of all major Northern Hemisphere ice sheets (Newton et al., 2020).

The high sedimentation rates during the initial period of glacial expansion at the onset of phase 2, and the observations of continued glacial expansion coupled with reducing sedimentation rates between ∼1.2 and 0.78 Ma along the margin, may relate to changes in the availability of erodible material for the advancing ice sheet (e.g., Clark and Pollard, 1998). Prior to the Neogene uplift and erosion, most of the Barents Sea was covered by a relatively thick succession of lower Cretaceous to Paleogene fine-grained sediments (Sigmond, 1992). This readily erodible unlithified material (regolith) would have been easily removed by the first glacial advances across the Barents Sea shelf during phase 2, depositing large volumes of fine-grained sediments to the continental slope (e.g., Hjelstuen et al., 2007) and yielding high sedimentation rates. As these preglacial unlithified sediments were eroded and not replenished, we could expect a gradual reduction in the availability of erodible material for subsequent glacial advances during phase 2, yielding diminishing sedimentation rates. As well as influencing subglacial erosion and therefore sedimentation rates, this process has also been suggested to influence ice sheet dynamics. Clark and Pollard (1998) proposed that for the Laurentide Ice Sheet, continued erosion of preglacial regolith, that was not replenished, over multiple glaciations caused a gradual change in ice sheet subglacial thermal conditions from soft-bedded (the presence of a deforming layer of basal sediment) to a mixed hard-soft bedded. Under such a scenario thin, dynamic ice sheets develop when sufficient regolith remains to provide soft-bed conditions, whilst thicker, more persistent ice sheets develop when a threshold level of regolith erosion is crossed, and the ice sheet bed is no longer predominantly soft. The refined seismic stratigraphy presented herein, reveals for the first time a decrease in average sedimentation rates within the GII seismic unit. Based on these decreasing sedimentation rates we therefore hypothesize that glacial expansion across the Barents Sea during phase 2 was characterized by a gradual progression toward thicker, less dynamic ice sheets.

Another factor that may have influenced glacial evolution during phase 2 is the topographic/bathymetric evolution of the Barents Sea at this time. Interestingly, the transition of the Barents Sea from a subaerial landmass to a submarine shelf sea is suggested to have occurred around ∼0.99 Ma (e.g., Butt et al., 2002; Zieba et al., 2017). This would have been a very gradual process, however, over time changes, such as the deepening of the Bear Island Trough, would have provided increasing topographic constraint on the ice streams operating within it. This would have led to more focused glacial erosion and more focused sediment delivery to the margin, consistent with the increase in sedimentation rates during the final period of phase 2.

A critical control on the accumulation of glacigenic sediments across the western Svalbard–Barents Sea margin is the available accommodation space, which is primarily controlled by fluctuations in relative sea level, reflecting the relative contributions of eustasy, isostasy and tectonic movement (Jervey, 1988). On the western Barents Sea margin, regional tectonics and overall shelf-slope morphology determine the accommodation space, in addition to localized controls of differential subsidence (tectonic, compaction), erosion (glacial), or mass wasting processes (landslides, etc.) (e.g., Dimakis et al., 1998; Ó Cofaigh et al., 2003; Hjelstuen et al., 2007; Faleide et al., 2008). Based on the existing literature there is evidence for large-scale intensification of Svalbard-Barents Sea glaciation at ∼1.0 Ma (Hjelstuen et al., 2007; Knies et al., 2007, 2009; Mattingsdal et al., 2014) which is consistent with the onset of a significant increase in global ice volume at ∼0.94 Ma (Mudelsee and Stattegger, 1997) associated with a distinct sea level drop of 20–30 m (Kitamura and Kawagoe, 2006). Consequently, changes in sea level could also be correlated to fluctuations in available accommodation space and therefore in sedimentation rates.

Phase 3:Saalian and Weichselian Glaciations (< ∼0.42 Ma)

The transition from phase 2 to phase 3 marks a major change in sedimentation rates along the continental margin, switching from a trend of generally declining sedimentation rates to rapidly increasing rates (**Figure 8D**). The timing of this transition is broadly consistent with the Mid-Brunhes Event, a major climate transition starting at around ∼0.4 Ma. This event was characterized by atmospheric CO_2 concentrations exceeding

300 ppm (Tzedakis et al., 2009), and sea-level highstands, sometimes above present-day global mean sea level (e.g., Dutton et al., 2015), that marked the transition from cooler to warmer interglacials (Tzedakis et al., 2009; Cronin et al., 2017). This is also supported by paleontological data that indicate a period of inflow of warmer North Atlantic surface-water masses suggesting an episode with increased influence of the North Atlantic Current and West Spitsbergen Current at around ∼0.5 Ma (Smelror, 1999). Around this time increased sedimentation rates accompanied by an increase in glacigenic debris flow deposit frequency on the western Svalbard margin (Kongsfjorden TMF, **Figure 6C**) and the northwestern Barents Sea (**Figure 6E**) are recorded in our data along the Svalbard-Barents Sea margin. Given the exceptional high increase in sedimentation rates on the western Barents Sea margin at this time, we suggest a possible interplay between this climatic event and a glacial intensification across the entire Barents Sea, resulting in coalescence of the SBIS and Fennoscandian Ice Sheet (FIS) at around ∼0.42 Ma ago (**Figure 9C**). Such a configuration would greatly enlarge the catchment area of ice masses in the southwestern Barents Sea, and specifically the source area for sediments deposited on the Bear Island TMF.

The sedimentary package deposited over the last ∼0.4 Ma corresponds to the Early Saalian (between ∼0.4 and 0.2 Ma), Late Saalian (between ∼0.2 and 0.13 Ma), and Weichselian (< ∼0.123 Ma) glaciations. This high-resolution stratigraphic framework allows for the first time the differentiation of the sediments deposited on the slope during Early Saalian, Late Saalian and Weichselian periods, representing a valuable dataset, for example for testing models of glacial erosion (e.g., Patton et al., 2015, 2016). The Saalian glaciations are characterized by the highest sedimentation rates estimated from our data on both the northwestern and southwestern Barents Sea margins, suggesting extensive, dynamic glaciations across the Barents Sea shelf. The Weichselian glaciations show a gradual decrease in rates, implying a decrease in the erosion capacity of the SBIS in comparison to Saalian SBIS. This change is also recorded in the seismic configuration where the seismic reflection corresponding to ∼0.13 Ma truncates underlying reflections and represents the base of the upper aggradational seismic facies (**Figure 6H**). In general, the presence of aggradational seismic facies is closely linked to the availability of accommodation space, resulting either from differential tectonic movements, subsidence related to topset loading with glacier-derived sediments, or eustatic changes in sea level (e.g., Dahlgren et al., 2005; Dowdeswell et al., 2007; Hofmann et al., 2016). The changes in the seismic configuration patterns between the Saalian and the Weischelian glaciations infer changes either in glacial dynamics, or/and in grounding line positions, or/and in accommodation space. For example, after several successive glaciations, and as the shelf progradation increases, the travel distance for ice-advance will be successively longer to reach the shelf break, resulting potentially in increases dominance of vertical aggradation (Solheim et al., 1998). This is in accordance with the existing literature suggesting that the dynamics and extents of the Saalian and the Weichselian SBIS were very different (e.g., Solheim et al., 1998; Pope et al., 2016) and in line with Svendsen et al. (2004) reconstructions, suggesting much more extensive late Saalian glaciations over the Kara Sea than the subsequent Weichselian glaciations. Both during Saalian and Weischelian glaciations the northwestern Barents Sea margin is characterized by relatively higher sedimentation rates compared to the southwestern Barents Sea margin implying higher erosion capacity of the SBIS on the northwestern section of the Barents Sea during the Weichselian glaciations.

CONCLUSION

A continuous high-resolution seismostratigraphic framework that connects the entire western Svalbard-Barents Sea margin and covers the last ∼2.7 Ma is presented here. We utilize recent improvements in chronology to establish a set of reliable age fix-points from available boreholes along the margin, and with the use of a large dataset composed of both, conventional and recently acquired high-resolution 2D seismic data, we extend this consistent chronology from the Yermak Plateau (north of Svalbard) and offshore western Svalbard, southwards to the Bear Island TMF. We have identified, in line with the classic nomenclature, three main seismic units, GI-GIII, along this continental margin and dated 12 regionally correlated seismic reflections, including providing age estimates for the widely used R7-R1 seismic reflections. In this study we show one potential application of this framework by reconstructing the SBIS evolution over the last ∼2.7 Ma since the intensification of northern hemisphere glaciations. The high temporal resolution provided by the proposed seismostratigraphic framework, provides new insights into the nature of the onset of Barents Sea glaciations and allows us to separate the sedimentary record deposited during the Early Saalian, Late Saalian and Weichselian glaciations on the continental slope. We identify three phases of glacial development over the last ∼2.7 Ma based on seismic facies distribution and sedimentation rate fluctuations along the margin:

Phase 1. The framework reveals a clear two-step onset to glacial intensification in the region. The initial step, between ∼2.7 and 2.58 Ma shows glacial expansion across Svalbard; whilst the second step, between ∼1.95 and 1.78 Ma indicates glacial advances beyond Svalbard to the northwestern Barents Sea. Between the two steps, the first shelf-edge glaciation is recorded on the northwestern Svalbard margin with the Sjubrebanken TMF receiving sediments from an ice stream in form of glacigenic debris flows.

Phase 2. The onset of phase 2 marks a regional glacial intensification for the whole Barents Sea-Svalbard region, with southward glacial expansion across the wider Barents Sea and the onset of shelf-edge glaciations along the western Svalbard-Barents Sea margin taking place around ∼1.5 Ma ago. This initial increase, is followed by evidence for shelf-edge glaciation but decreased sedimentation rates (∼1.2 and 0.78 Ma) indicate that as the ice masses expanded, they had diminishing erosional capacity and/or there was a gradual reduction in the availability of readily erodible unlithified material. Around ∼0.78 Ma the sedimentation rates start to increase once again along the margin, which may reflect deepening of the Bear Island Trough and increasing topographic constraint on the ice streams.

Phase 3. Around ∼0.42 Ma, the southwestern Barents Sea margin is characterized by a dramatic increase in sedimentation rates reflecting glacial expansion and enlargement of the catchment area for the sediments deposited along the margin possible related to the Svalbard-Barents Sea Ice Sheet and Fennoscandian Ice Sheet coalescence. For the first time our new stratigraphic framework allows differentiation of the sediments deposited on the slope during the Early Saalian, Late Saalian, and Weichselian periods. The Saalian glaciations are characterized by the highest sedimentation rates estimated from our dataset, suggesting extensive, dynamic glaciations across the Barents Sea. The Weichselian glaciations show a gradual decrease in rates, with the northwestern Barents Sea margin still characterized by relatively higher rates compared to the rest of the margin indicating higher erosion capacity of the SBIS in the northern Barents Sea during that period.

DATA AVAILABILITY STATEMENT

The original contributions presented in the study are included in the article/**Supplementary Material**, further inquiries can be directed to the corresponding author/s.

AUTHOR CONTRIBUTIONS

NA, KA, and MW developed the study. NA interpreted the seismic dataset and wrote the original manuscript. P-AD provided the age fix-points for the MeBo 126 core and JK the age fix-point for the GS14-190 core. NB provided the description of the logs and facies of the GS14-190 core. NA, KA, AP-F, and RM compiled the 2D seismic dataset. All authors contributed to editing of the text and figures and advised on its scope.

FUNDING

This work was supported by the Research Council of Norway (RCN) through its Centres of Excellence funding scheme, project no. 223259. P-AD contribution was supported by the IS blue program ANR-17-EURE-0015.

ACKNOWLEDGMENTS

We thank Sunil Vadakkepuliyambatta for his help with estimation of sedimentation rates, Stefan Bünz for updating the 2D seismic dataset, Jan Sverre Laberg for constructive discussions about the Svalbard-Barents Sea glacial history, and Rolf Mjelde for providing permission to publish the seismic line SVALEX2001_P11_A. We are grateful to the two reviewers BR and GV, and the editor IM for their helpful comments which improved this paper. We also appreciate the assistance provided by the Chief editor David Mark Hodgson. Norwegian Petroleum Directorate is acknowledged for providing 2D seismic data through the Diskos National Data Repository (NDR). The seismic data are available for academic purposes through NDR (http://www.diskos.no/). We thank National Institute of Oceanography and Applied Geophysics (OGS) for providing seismic data from the EGLACOM (Evolution of a GLacial Arctic COntinental Margin, July–August 2008) project. The EGLACOM seismic data are available on "Istituto Nazionale di Oceanografia e di Geofisica Sperimentale—SNAP data management system–http://snap.ogs.trieste.it." doi: 10.6092/SNAP.ea3ea207-a9ac-f9f5-cafb-2cb29deb0eaa. Information about the availability of the 2D seismic profiles acquired by CAGE-UiT are available by contacting the corresponding author. We thank TGS-NOPEC geophysical company and Russian Joint Stock Company "Russian Marine Arctic Geological Expedition" (MAGE) for providing some of the 2D seismic data. Schlumberger is acknowledged for the Petrel software under an educational license agreement to Department of Geosciences, UiT-The Arctic University of Norway.

SUPPLEMENTARY MATERIAL

The Supplementary Material for this article can be found online at: https://www.frontiersin.org/articles/10.3389/feart.2021.656732/full#supplementary-material

REFERENCES

Amundsen, I. M. H., Blinova, M., Hjelstuen, B. O., Mjelde, R., and Haflidason, H. (2011). The Cenozoic western Svalbard margin: sediment geometry and sedimentary processes in an area of ultraslow oceanic spreading. *Mar. Geophys. Res.* 32, 441–453. doi: 10.1007/s11001-011-9127-z

Andreassen, K. (2017). *Cruise report CAGE 17-5. Marine geophysical cruise to the Yermak Plateau and western Svalbard continental margin*. Norway: CAGE, 28.

Andreassen, K., Nilssen, L. C., Rafaelsen, L., and Kuilman, L. (2004). Three-dimensional seismic data from the Barents Sea margin reveal evidence of past ice streams and their dynamics. *Geology* 32, 729–732. doi: 10.1130/g20497.1

Andreassen, K., Odegaard, C. M., and Rafaelsen, B. (2007). "Imprints of former ice streams, imaged and interpreted using industry three-dimensional seismic data from the south-western Barents Sea," in *Seismic Geomorphology: Applications to Hydrocarbon Exploration and Production*, eds R. J. Davies, H. W. Posamentier, L. J. Wood, and J. A. Cartwright (London: Geological Society), 151–169.

Andreassen, K., and Winsborrow, M. (2009). Signature of ice streaming in Bjornoyrenna, Polar North Atlantic, through the Pleistocene and implications for ice-stream dynamics. *Annal. Glaciol.* 50, 17–26.

Balco, G., and Rovey, C. W. II (2010). Absolute chronology for major Pleistocene advances of the Laurentide Ice Sheet. *Geology* 38, 795–798. doi: 10.1130/g30946.1

Barendregt, R. W., and Irving, E. (1998). Changes in the extent of North American ice sheets during the late Cenozoic. *Can. J. Earth Sci.* 35, 504–509. doi: 10.1139/e97-126

Bohrmann, G., Ahrlich, F., Bergenthal, M., Bünz, S., Düßmann, R., Ferreira, C., et al. (2017). *R/V MARIA S. MERIAN Cruise Report MSM57, Gas Hydrate Dynamics at the Continental Margin of Svalbard, Reykjavik – Longyearbyen – Reykjavik, 29 July – 07 September 2016*. Universität Bremen: Berichte, MARUM – Zentrum für Marine Umweltwissenschaften, Fachbereich Geowissenschaften, 314.

Butt, F. A., Drange, H., Elverhøi, A., Otterå, O. H., and Solheim, A. (2002). Modelling Late Cenozoic isostatic elevation changes in the Barents Sea and their implications for oceanic and climatic regimes: preliminary results. *Quaternary Sci. Rev.* 21, 1643–1660. doi: 10.1016/S0277-3791(02)00018-5

Butt, F. A., Elverhoi, A., Solheim, A., and Forsberg, C. F. (2000). Deciphering late Cenozoic development of the western Svalbard margin from ODP site 986 results. *Mar. Geol.* 169, 373–390. doi: 10.1016/s0025-3227(00)00088-8

Camerlenghi, A. (2018). "Drivers of Seafloor Geomorphic Change," in *Submarine Geomorphology*, eds A. Micallef, S. Krastel, and A. Savini (Cham: Springer International Publishing), 135–159.

Channell, J. E. T., Smelror, M., Jansen, E., Higgins, S. M., Lehman, B., Eidvin, T., et al. (1999). Age models for glacial fan deposits off East Greenland and Svalbard (ODP Site 986 and Site 987). *Proc. ODP Sci. Results* 162, 149–166.

Clark, P. U., and Pollard, D. (1998). Origin of the Middle Pleistocene Transition by ice sheet erosion of regolith. *Paleoceanography* 13, 1–9. doi: 10.1029/97pa02660

Cronin, T. M., Dwyer, G. S., Caverly, E. K., Farmer, J., Deninno, L. H., Rodriguez-Lazaro, J., et al. (2017). Enhanced Arctic Amplification Began at the Mid-Brunhes Event ˜400,000 years ago. *Sci. Rep.* 7:14475. doi: 10.1038/s41598-017-13821-2

Cronin, T. M., and Whatley, R. (1996). Ostracoda from Sites 910 and 911. *Proc. ODP, Sci.* 151, 197–201. doi: 10.2973/odp.proc.sr.151.156.1996

Dahlgren, K. I. T., Vorren, T. O., Stoker, M. S., Nielsen, T., Nygard, A., and Sejrup, H. P. (2005). Late Cenozoic prograding wedges on the NW European continental margin: their formation and relationship to tectonics and climate. *Mar. Petrol. Geol.* 22, 1089–1110. doi: 10.1016/j.marpetgeo.2004.12.008

Dessandier, P.-A., Knies, J., Plaza-Faverola, A., Labrousse, C., Renoult, M., Panieri, G., et al. (2021). Ice-sheet melt drove methane emissions in the Arctic during the last two interglacials. *Geology* 49. doi: 10.1130/g48580.1 [Epub ahead of print].

Dimakis, P., Braathen, B. I, Faleide, J. I, Elverhoi, A., and Gudlaugsson, S. T. (1998). Cenozoic erosion and the preglacial uplift of the Svalbard-Barents Sea region. *Tectonophysics* 300, 311–327. doi: 10.1016/s0040-1951(98)00245-5

Dowdeswell, J. A., Ó Cofaigh, C., Noormets, R., Larter, R. D., Hillenbrand, C. D., Benetti, S., et al. (2008). A major trough-mouth fan on the continental margin of the Bellingshausen Sea, West Antarctica: The Belgica Fan. *Mar. Geol.* 252, 129–140. doi: 10.1016/j.margeo.2008.03.017

Dowdeswell, J. A., Ottesen, D., Rise, L., and Craig, J. (2007). Identification and preservation of landforms diagnostic of past ice-sheet activity on continental shelves from three-dimensional seismic evidence. *Geology* 35, 359–362. doi: 10.1130/g23200a.1

Dutton, A., Carlson, A. E., Long, A. J., Milne, G. A., Clark, P. U., Deconto, R., et al. (2015). Sea-level rise due to polar ice-sheet mass loss during past warm periods. *Science* 349:aaa4019. doi: 10.1126/science.aaa4019

Eidvin, E., and Nagy, J. (1999). "Foraminiferal biostratigraphy of Pliocene deposits at Site 986, Svalbard margin," in *Proceedings of the Ocean Drilling Program, Scientific Results*, Vol. 162, eds M. Raymo, E. Jansen, P. Blum, and T. D. Herbert (College Station, TX: Ocean Drilling Program), 3–17.

Eidvin, T., Jansen, E., and Riis, F. (1993). Chronology of Tertiary fan deposits off the western Barents Sea - Implications for the uplife and erosion history of the Barents Shelf. *Mar. Geol.* 112, 109–131. doi: 10.1016/0025-3227(93)90164-q

Eiken, O., and Hinz, K. (1993). Contourites in the Fram Strait. *Sedimen. Geol.* 82, 15–32. doi: 10.1016/0037-0738(93)90110-Q

Elverhoi, A., Svendsen, J. I, Solheim, A., Andersen, E. S., Milliman, J., Mangerud, J., et al. (1995). Late Quaternary Sediment Yield from the high Arctic Svalbard area. *J. Geol.* 103, 1–17.

Faleide, J. I., Solheim, A., Fiedler, A., Hjelstuen, B. O., Andersen, E. S., Vanneste, K., et al. (1996). Late Cenozoic evolution of the western Barents Sea-Svalbard continental margin. *Global Planet. Change* 12, 53–74. doi: 10.1016/0921-8181(95)00012-7

Faleide, J. I, Tsikalas, F., Breivik, A. J., Mjelde, R., Ritzmann, O., Engen, O., et al. (2008). Structure and evolution of the continental margin off Norway and Barents Sea. *Episodes* 31, 82–91.

Fiedler, A., and Faleide, J. I. (1996). Cenozoic sedimentation along the southwestern Barents Sea margin in relation to uplift and erosion of the shelf. *Global Planet. Change* 12, 75–93. doi: 10.1016/0921-8181(95)00013-5

Flesche Kleiven, H., Jansen, E., Fronval, T., and Smith, T. M. (2002). Intensification of Northern Hemisphere glaciations in the circum Atlantic region (3.5–2.4 Ma) – ice-rafted detritus evidence. *Palaeogeogr. Palaeoclimatol. Palaeoecol.* 184, 213–223. doi: 10.1016/S0031-0182(01)00407-2

Forsberg, C. F., Solheim, A., Elverhoi, A., Jansen, E., Channell, J. E. T., Andersen, E. S., et al. (1999). The depositional environment of the western Svalbard margin during the late Pliocene and the Pleistocene: Sedimentary facies changes at Site 986. *Proc. Ocean Drilling Prog. Sci. Results* 162, 233–246.

Fronval, T., and Jansen, E. (1996). "Late Neogene paleoclimates and paleoceanography in the Iceland-Norwegian Sea: evidence from the Iceland and Vøring Plateaus," in *Proceeding Ocean Drilling Program. Scientific Results*, Vol. 151, eds J. Thiede, A. M. Myhre, J. V. Firth, G. L. Johnson, and W. F. Ruddiman (College Station, TX: Ocean Drilling Program), 455–468.

Funder, S., Bennike, O., Bocher, J., Israelson, C., Strand, K., Símonarson, L., et al. (2001). Late Pliocene Greenland -The Kap K0benhavn Formation in North Greenland. *Bull. Geol. Soc.* 48, 117–134.

Geissler, W. H., and Jokat, W. (2004). A geophysical study of the northern Svalbard continental margin. *Geophys. J. Int.* 158, 50–66. doi: 10.1111/j.1365-246X.2004.02315.x

Grøsfjeld, K., De Schepper, S., Fabian, K., Husum, K., Baranwal, S., Andreassen, K., et al. (2014). Dating and palaeoenvironmental reconstruction of the sediments around the Miocene/Pliocene boundary in Yermak Plateau ODP Hole 911A using marine palynology. *Palaeogeogr. Palaeoclimatol. Palaeoecol.* 414, 382–402. doi: 10.1016/j.palaeo.2014.08.028

Henriksen, E., Bjørnseth, H. M., Hals, T. K., Heide, T., Kiryukhina, T., Kløvjan, O. S., et al. (2011). Chapter 17 Uplift and erosion of the greater Barents Sea: impact on prospectivity and petroleum systems. *Geol. Soc. London Mem.* 35, 271–281. doi: 10.1144/m35.17

Hjelstuen, B. O., Eldholm, O., and Faleide, J. I. (2007). Recurrent Pleistocene mega-failures on the SW Barents Sea margin. *Earth Planet. Sci. Lett.* 258, 605–618. doi: 10.1016/j.epsl.2007.04.025

Hjelstuen, B. O., Elverhoi, A., and Faleide, J. I. (1996). Cenozoic erosion and sediment yield in the drainage area of the Storfjorden Fan. *Global Planet. Change* 12, 95–117. doi: 10.1016/0921-8181(95)00014-3

Hjelstuen, B. O., and Sejrup, H. P. (2020). Latitudinal variability in the Quaternary development of the Eurasian ice sheets—Evidence from the marine domain. *Geology* 49, 346–351. doi: 10.1130/g48106.1

Hofmann, J. C., Knutz, P. C., Nielsen, T., and Kuijpers, A. (2016). Seismic architecture and evolution of the Disko Bay trough-mouth fan, central West Greenland margin. *Quaternary Sci. Rev.* 147, 69–90. doi: 10.1016/j.quascirev.2016.05.019

Hull, D. M., Osterman, L. E., and Thiede, J. (1996). Biostratigraphic synthesis of Leg 151, North Atlantic-Arctic Gateways. *Proc. ODP, Sci. Results* 151, 627–644. doi: 10.2973/odp.proc.sr.151.146.1996

Jakobsson, M., Mayer, L., Coakley, B., Dowdeswell, J. A., Forbes, S., Fridman, B., et al. (2012). The International Bathymetric Chart of the Arctic Ocean (IBCAO) Version 3.0. *Geophys. Res. Lett.* 39:L12609. doi: 10.1029/2012gl052219

Jansen, E., Fronval, T., Rack, F., and Channell, J. E. T. (2000). Pliocene-Pleistocene ice rafting history and cyclicity in the Nordic Seas during the last 3.5 Myr. *Paleoceanography* 15, 709–721. doi: 10.1029/1999pa000435

Jansen, E., Raymo, M. E., and Blum, P. (1996). "The leg 162 Shipboard Scientific Party, 1996," in *Proceedings of the Ocean Drilling Program,* Vol. 162, College Station, TX, 1182.

Jervey, M. T. (1988). "Quantitative Geological Modeling of Siliciclastic Rock Sequences and Their Seismic Expression," in *Sea-Level Changes: An Integrated Approach*, eds C. K. Wilgus, B. S. Hastings, H. Posamentier, J. V. Wagoner, C. A. Ross, and C. G. S. C. Kendall (Tulsa, USA: Society of Economic Paleontologists and Mineralogists).

Kitamura, A., and Kawagoe, T. (2006). Eustatic sea-level change at the Mid-Pleistocene climate transition: new evidence from the shallow-marine sediment record of Japan. *Quaternary Sci. Rev.* 25, 323–335. doi: 10.1016/j.quascirev.2005.02.009

Knies, J., Köseoğlu, D., Rise, L., Baeten, N., Bellec, V. K., Bøe, R., et al. (2018). Nordic Seas polynyas and their role in preconditioning marine productivity during the Last Glacial Maximum. *Nat. Commun.* 9:3959. doi: 10.1038/s41467-018-06252-8

Knies, J., Matthiessen, J., Mackensen, A., Stein, R., Vogt, C., Frederichs, T., et al. (2007). Effects of Arctic freshwater forcing on thermohaline circulation during the Pleistocene. *Geology* 35, 1075–1078. doi: 10.1130/G23966A.1

Knies, J., Matthiessen, J., Vogt, C., Laberg, J. S., Hjelstuen, B. O., Smelror, M., et al. (2009). The Plio-Pleistocene glaciation of the Barents Sea-Svalbard region: a new model based on revised chronostratigraphy. *Quaternary Sci. Rev.* 28, 812–829. doi: 10.1016/j.quascirev.2008.12.002

Laberg, J. S., Andreassen, K., Knies, J., Vorren, T. O., and Winsborrow, M. (2010). Late Pliocene-Pleistocene development of the Barents Sea Ice Sheet. *Geology* 38, 107–110. doi: 10.1130/g30193.1

Laberg, J. S., Andreassen, K., and Vorren, T. O. (2012). Late Cenozoic erosion of the high-latitude southwestern Barents Sea shelf revisited. *Geol. Soc. Am. Bull.* 124, 77–88. doi: 10.1130/b30340.1

Laberg, J. S., Rydningen, T. A., Forwick, M., and Husum, K. (2018). Depositional processes on the distal Scoresby Trough Mouth Fan (ODP Site 987): Implications for the Pleistocene evolution of the Scoresby Sund Sector of the Greenland Ice Sheet. *Mar. Geol.* 402, 51–59. doi: 10.1016/j.margeo.2017.11.018

Laberg, J. S., and Vorren, T. O. (1996a). The glacier-fed fan at the mouth of Storfjorden trough, western Barents Sea: a comparative study. *Geologische Rundschau* 85, 338–349. doi: 10.1007/bf02422239

Laberg, J. S., and Vorren, T. O. (1996b). The Middle and Late Pleistocene evolution of the Bear Island Trough Mouth Fan. *Global Planetary Change* 12, 309–330. doi: 10.1016/0921-8181(95)00026-7

Lasabuda, A., Laberg, J. S., Knutsen, S.-M., and Høgseth, G. (2018). Early to middle cenozoic paleoenvironment and erosion estimates of the southwestern Barents Sea: Insights from a regional mass-balance approach. *Mar. Petrol. Geol.* 96, 501–521. doi: 10.1016/j.marpetgeo.2018.05.039

Matthiessen, J., and Brenner, W. (1996). Dinoflagellate cyst ecostratigraphy of Pliocene–Pleistocene sediments from the Yermak Plateau (Arctic Ocean, Hole 911A). *Proc. ODP, Sci. Results* 151, 243–253. doi: 10.2973/odp.proc.sr.151.109.1996

Mattingsdal, R., Knies, J., Andreassen, K., Fabian, K., Husum, K., Grosfjeld, K., et al. (2014). A new 6 Myr stratigraphic framework for the Atlantic-Arctic Gateway. *Quaternary Sci. Rev.* 92, 170–178. doi: 10.1016/j.quascirev.2013.08.022

Montelli, A., Dowdeswell, J. A., Ottesen, D., and Johansen, S. E. (2017). Ice-sheet dynamics through the Quaternary on the mid-Norwegian continental margin inferred from 3D seismic data. *Mar. Petrol. Geol.* 80, 228–242. doi: 10.1016/j.marpetgeo.2016.12.002

Montelli, A., Dowdeswell, J. A., Ottesen, D., and Johansen, S. E. (2018). Architecture and sedimentary processes on the mid-Norwegian continental slope: A 2.7 Myr record from extensive seismic evidence. *Quaternary Sci. Rev.* 192, 185–207. doi: 10.1016/j.quascirev.2018.05.034

Mørk, M. B. E., and Duncan, R. A. (1993). Late Pliocene basaltic volcanism on the western Barents Shelf margin: implications from petrology and 40Ar-39Ar dating of volcaniclastic debris from a shallow drill core. *Norsk Geologisk Tidsskrift* 73, 209–225.

Mudelsee, M., and Stattegger, K. (1997). Exploring the structure of the mid-Pleistocene revolution with advanced methods of time-series analysis. *Geologische Rundschau* 86, 499–511. doi: 10.1007/s005310050157

Myhre, A., Thiede, J., and Firth, J. A. (1995). *Proceedings of the Ocean Drilling Program. Initial Reports, Leg 151*, College Station, TX: Ocean Drilling Program, 951.

Newton, A. M. W., and Huuse, M. (2017). Late Cenozoic environmental changes along the Norwegian margin. *Mar. Geol.* 393, 216–244. doi: 10.1016/j.margeo.2017.05.004

Newton, A. M. W., Huuse, M., Knutz, P. C., and Cox, D. R. (2020). Repeated ice streaming on the northwest Greenland continental shelf since the onset of the Middle Pleistocene Transition. *Cryosphere* 14, 2303–2312. doi: 10.5194/tc-14-2303-2020

Ó Cofaigh, C., Hogan, K. A., Jennings, A. E., Louise Callard, S., Dowdeswell, J. A., Noormets, R., et al. (2018). The role of meltwater in high-latitude trough-mouth fan development: The Disko Trough-Mouth Fan, West Greenland. *Marine Geology* 402, 17–32. doi: 10.1016/j.margeo.2018.02.001

Ó Cofaigh, C., Taylor, J., Dowdeswell, J. A., and Pudsey, C. J. (2003). Palaeo-ice streams, trough mouth fans and high-latitude continental slope sedimentation. *Boreas* 32, 37–55. doi: 10.1080/03009480310001858

Osterman, L. E. (1996). Pliocene and Quaternary benthic foraminifers from Site 910, Yermak Plateau. *Proc. ODP Sci. Results* 151, 187–195. doi: 10.2973/odp.proc.sr.151.107.1996

Ottesen, D., Dowdeswell, J. A., and Bugge, T. (2016). Deeply buried glacigenic debris-flows imaged in 3D seismic data from early Quaternary sediments of the northern North sea. *Geol. Soc. London Mem.* 46, 369–370. doi: 10.1144/m46.131

Ottesen, D., Stokes, C. R., Rise, L., and Olsen, L. (2008). Ice-sheet dynamics and ice streaming along the coastal parts of northern Norway. *Quaternary Sci. Rev.* 27, 922–940. doi: 10.1016/j.quascirev.2008.01.014

Patton, H., Andreassen, K., Bjarnadottir, L. R., Dowdeswell, J. A., Winsborrow, M. C. M., Noormets, R., et al. (2015). Geophysical constraints on the dynamics and retreat of the Barents Sea ice sheet as a paleobenchmark for models of marine ice sheet deglaciation. *Rev. Geophys.* 53, 1051–1098.

Patton, H., Hubbard, A., Andreassen, K., Winsborrow, M., and Stroeven, A. P. (2016). The build-up, configuration, and dynamical sensitivity of the Eurasian ice-sheet complex to late Weichselian climatic and oceanic forcing. *Quaternary Sci. Rev.* 153, 97–121. doi: 10.1016/j.quascirev.2016.10.009

Pérez, L. F., Nielsen, T., Knutz, P. C., Kuijpers, A., and Damm, V. (2018). Large-scale evolution of the central-east Greenland margin: New insights to the North Atlantic glaciation history. *Global Planet. Change* 163, 141–157. doi: 10.1016/j.gloplacha.2017.12.010

Plaza-Faverola, A., Vadakkepuliyambatta, S., Hong, W. L., Mienert, J., Bunz, S., Chand, S., et al. (2017). Bottom-simulating reflector dynamics at Arctic thermogenic gas provinces: An example from Vestnesa Ridge, offshore west Svalbard. *J. Geophys. Res. Solid Earth* 122, 4089–4105. doi: 10.1002/2016jb013761

Pope, E. L., Talling, P. J., Hunt, J. E., Dowdeswell, J. A., Allin, J. R., Cartigny, M. J. B., et al. (2016). Long-term record of Barents Sea Ice Sheet advance to the shelf edge from a 140,000 year record. *Quaternary Sci. Rev.* 150, 55–66. doi: 10.1016/j.quascirev.2016.08.014

Pope, E. L., Talling, P. J., and Ó Cofaigh, C. (2018). The relationship between ice sheets and submarine mass movements in the Nordic Seas during the Quaternary. *Earth-Sci. Rev.* 178, 208–256. doi: 10.1016/j.earscirev.2018.01.007

Rea, B. R., Newton, A. M. W., Lamb, R. M., Harding, R., Bigg, G. R., Rose, P., et al. (2018). Extensive marine-terminating ice sheets in Europe from 2.5 million years ago. *Sci. Adv.* 4:eaar8327. doi: 10.1126/sciadv.aar8327

Rebesco, M., Laberg, J. S., Pedrosa, M. T., Camerlenghi, A., Lucchi, R. G., Zgur, F., et al. (2014). Onset and growth of Trough-Mouth Fans on the North-Western Barents Sea margin – implications for the evolution of the Barents Sea/Svalbard Ice Sheet. *Quaternary Sci. Rev.* 92, 227–234. doi: 10.1016/j.quascirev.2013.08.015

Rydningen, T. A., Høgseth, G. V., Lasabuda, A. P. E., Laberg, J. S., Safronova, P. A., Forwick, M., et al. (2020). An Early Neogene—Early Quaternary Contourite Drift System on the SW Barents Sea Continental Margin, Norwegian Arctic. *Geochem. Geophys. Geosys.* 21:e2020GC009142. doi: 10.1029/2020GC009142

Ryseth, A., Augustson, J. H., Charnock, M., Haugerud, O., Knutsen, S. M., Midboe, P. S., et al. (2003). Cenozoic stratigraphy and evolution of the Sorvestsnaget Basin, southwestern Barents Sea. *Norwegian J. Geol.* 83, 107–130.

Sættem, J., Bugge, T., Fanavoll, S., Goll, R. M., Mørk, A., Mørk, M. B. E., et al. (1994). Cenozoic margin development and erosion of the Barents Sea: Core evidence from southwest of Bjørnøya. *Mar. Geol.* 118, 257–281.

Sættem, J., Poole, D. A. R., Ellingsen, L., and Sejrup, H. P. (1992). Glacial geology of outer Bjørnøyrenna, southwestern Barents Sea. *Mar. Geol.* 103, 15–51. doi: 10.1016/0025-3227(92)90007-5

Safronova, P. A., Laberg, J. S., Andreassen, K., Shlykova, V., Vorren, T. O., Chernikov, S., et al. (2017). Late Pliocene-early Pleistocene deep-sea basin sedimentation at high-latitudes: mega-scale submarine slides of the north-western Barents Sea margin prior to the shelf-edge glaciations. *Basin Res.* 29, 537–555. doi: 10.1111/bre.12161

Sarkar, S., Berndt, C., Chabert, A., Masson, D. G., Minshull, T. A., and Westbrook, G. K. (2011). Switching of a paleo-ice stream in northwest Svalbard. *Quaternary Sci. Rev.* 30, 1710–1725. doi: 10.1016/j.quascirev.2011.03.013

Sato, T., and Kameo, K. (1996). "Pliocene to Quaternary calcareous nannofossil biostratigraphy of the Arctic Ocean, with reference to late Pliocene glaciation," in *Proceeding Ocean Drilling Program. Scientific Results, Vol. 151*, eds J. Thiede, A. M. Myhre, J. V. Firth, G.L. Johnson, and W. F. Ruddiman (College Station, TX: Ocean Drilling Program), 39–59.

Sigmond, E. M. D. (1992). *Bedrock Map of Norway and Adjacent Ocean Areas, scale 1:3,000,000*. Trondheim: Geological Survey of Norway.

Smelror, M. (1999). Pliocene-Pleistocene and redeposited dinoflagellate cysts from the western Svalbard Margin (Site 986): Biostratigraphy, paleoenvironments, and sediment provenance. *Proc. Ocean Drilling Prog. Sci. Res.* 162, 83–97. doi: 10.2973/odp.proc.sr.162.011.1999

Solheim, A., Andersen, E. S., Elverhoi, A., and Fiedler, A. (1996). Late Cenozoic depositional history of the western Svalbard continental shelf, controlled by subsidence and climate. *Global Planet. Change* 12, 135–148. doi: 10.1016/0921-8181(95)00016-x

Solheim, A., Faleide, J. I., Andersen, E. S., Elverhøi, A., Forsberg, C. F., Vanneste, K., et al. (1998). Late Cenozoic seismic stratigraphy and glacial geological development of the East Greenland and Svalbard–Barents Sea continental margins. *Quaternary Sci. Rev.* 17, 155–184. doi: 10.1016/S0277-3791(97)00068-1

Solheim, A., and Kristoffersen, Y. (1984). The physical environment, Western Barents Sea, 1:1500000, sheet B; Sediments above the upper regional unconformity: Thickness, seismic stratigraphy and outline of the glacial history. *Norsk Polarinstitutt Skrifter* 179:26.

Spiegler, D. (1996). "Planktonic foraminifer Cenozoic biostratigraphy of the Arctic Ocean, Fram Strait (Sites 908–909), Yermak Plateau (Sites 910–912), and East Greenland Margin (Site 913)," in *Proceeding Ocean Drilling Program. Scientific Results, Vol. 151*, eds J. Thiede, A. M. Myhre, J. V. Firth, G. L. Johnson, and W. F. Ruddiman (College Station, TX: Ocean Drilling Program), 153–167. doi: 10.2973/odp.proc.sr.151.104.1996

Svendsen, J. I., Alexanderson, H., Astakhov, V. I., Demidov, I., Dowdeswell, J. A., Funder, S., et al. (2004). Late quaternary ice sheet history of northern Eurasia. *Quaternary Sci. Rev.* 23, 1229–1271. doi: 10.1016/j.quascirev.2003.12.008

Taylor, J., Dowdeswell, J. A., Kenyon, N. H., and O Cofaigh, C. (2002). "Late Quaternary architecture of trough-mouth fans: debris flows and suspended sediments on the Norwegian margin," in *Glacier-Influenced Sedimentation on High-Latitude Continental Margins*, eds J. A. Dowdeswell and C. O. Cofaigh (Bath, UK: Geological Soc Publishing House), 55–71.

Tzedakis, P. C., Raynaud, D., Mcmanus, J. F., Berger, A., Brovkin, V., and Kiefer, T. (2009). Interglacial diversity. *Nat. Geosci.* 2, 751–755. doi: 10.1038/ngeo660

Vagnes, E., Faleide, J. I, and Gudlaugsson, S. T. (1992). Glacial erosion and tectonic uplift in the Barents Sea. *Norsk Geologisk Tidsskrift* 72, 333–338.

Vorren, T. O., Kristoffersen, Y., and Andreassen, K. (1986). Geology of the inner shelf west of North Cape, Norway. *Norsk Geologisk Tidsskrift* 66, 99–105.

Vorren, T. O., and Laberg, J. S. (1997). Trough mouth fans - Palaeoclimate and ice-sheet monitors. *Quaternary Sci. Rev.* 16, 865–881. doi: 10.1016/s0277-3791(97)00003-6

Vorren, T. O., Richardsen, G., Knutsen, S. M., and Henriksen, E. (1991). Cenozoic erosion and sedimentation in the western Barents Sea. *Mar. Petrol. Geol.* 8, 317–340. doi: 10.1016/0264-8172(91)90086-g

Zieba, K. J., Omosanya, K. O., and Knies, J. (2017). A flexural isostasy model for the Pleistocene evolution of the Barents Sea bathymetry. *Norsk Geologisk Tidsskrift* 97, 1–19.

Conflict of Interest: The authors declare that the research was conducted in the absence of any commercial or financial relationships that could be construed as a potential conflict of interest.

Supplementary Material

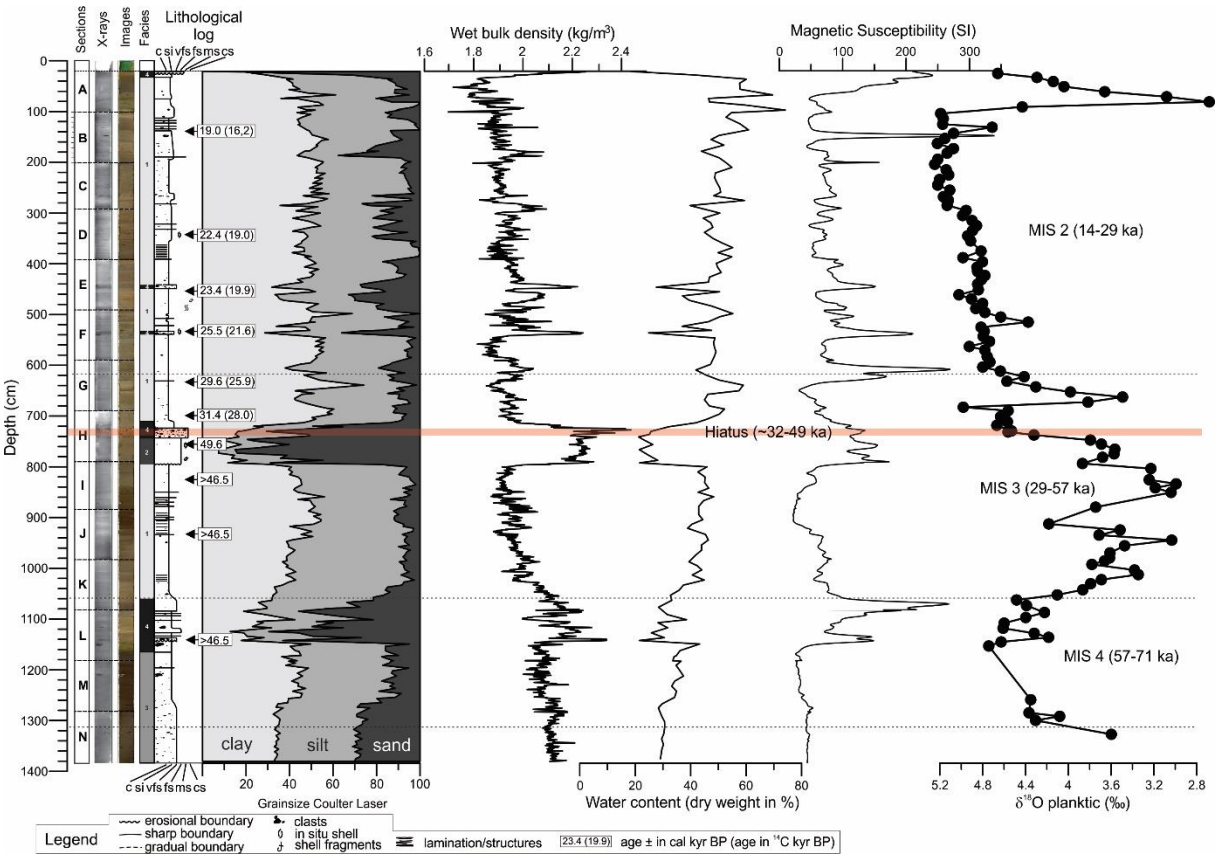

Supplementary Figure 1. Sedimentological, physical properties, and stable oxygen isotopes from planktonic foraminifera *Neoglobaquadrina pachyderma* (sin.) of GS14-190-01PC (0-1380 cm). Available calibrated radiocarbon AMS^{14}C datings (uncalibrated ages in parenthesis) between 0 and 700 cm are published in Knies et al. (2018). Below 700 cm, we present 3 infinite AMS^{14}C ages between 823 and 1140 cm measured on planktonic foraminifera *Neogloboquadrina pachyderma* (sin). An AMS^{14}C age of 49.6 ka at 758.9 cm on bivalve shell *Macoma calcarea* constrain the hiatus between ~725-740 cm corresponding to ~32-49 ka. AMS^{14}C analyses were conducted at the CHRONO Centre at Queen's University Belfast, Northern Ireland (UBA-30874-76, 21639).

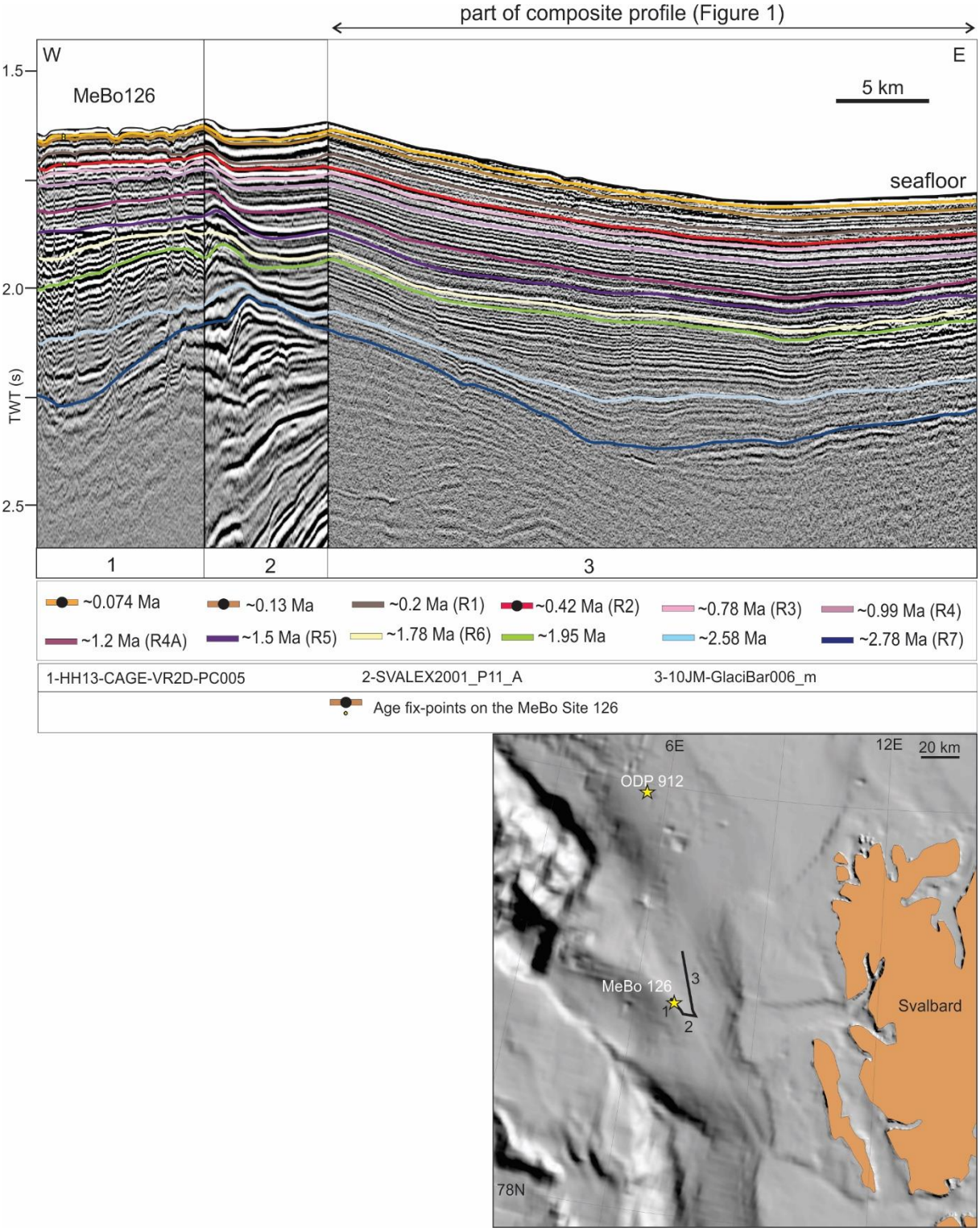

Supplementary Figure 2. shows a seismic profile crossing the Vestnesa MeBo Site 126 and connecting to the composite profile that is presented in Figure 1. The seismic reflections that are tied to MeBo Site 126 are marked with a dot. 1-3: the name of the seismic profiles.

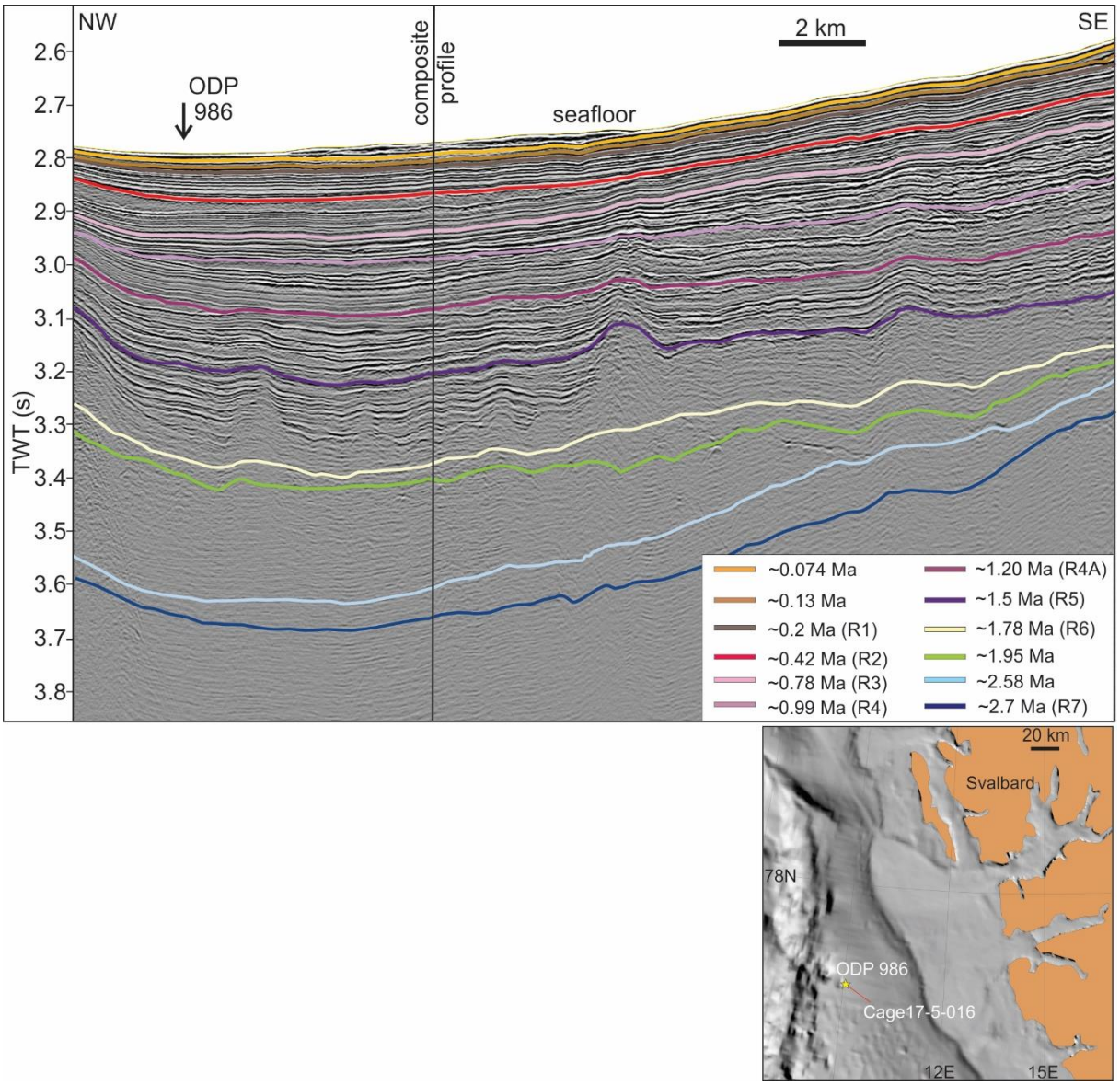

Supplementary Figure 3. shows Cage17-5-016 2D seismic line (Andreassen, 2017) crossing ODP Site 986. Based on the depth at which the seismic horizons corresponding to ~0.42 Ma, ~1.2 Ma, and ~1.78 Ma ages cross the ODP Site 986 we correlate them to the R7-R1 seismic stratigraphy (Faleide et al., 1996; Jansen et al., 1996). Composite profile: see Figure 1 and 3 for location).

Section	Seismic line	Seismic provider
1	10JM-GlaciBar 001_m-2	UiT
2	10JM-GlaciBar 0021_m	UiT
3	10JM-GlaciBar 006_m	UiT
4	09KA-JK129	UiT
5	CAGE14-2_Line01	CAGE-UiT
6	MAGE04-CM15-20-3	MAGE
7	MAGE04-CM15-42	MAGE
8	EG-02A	OGS
9	MAGE-05-06-CM15-200536-01-WGS-15	MAGE
10	MAGE-05-06-CM15-200537-WGS-15	MAGE
11	MAGE-05-06-CM15-200544-WGS-15	MAGE
12	MAGE-b89241	MAGE
13	BV-06-87	DISKOS
14	NBR09-419789	TGS
15	GVH-90-203	DISKOS
16	GVH-90-301	DISKOS
17	NBR11-215100	TGS

Supplementary Table 1. presents the seismic profiles 1-17 that comprise the composite seismic profile (see Figures 1 and 3 for location), and the seismic providers. CAGE: Centre for Arctic Gas Hydrate, Environment and Climate, UiT: The Arctic University of Norway in Tromsø. OGS: National Institute of Oceanography and Applied Geophysics, Trieste, Italy. DISKOS: Norwegian Diskos National Data Repository (NDR) database. MAGE: Russian Joint Stock Company 'Marine Arctic Geological Expedition'. TGS: TGS-NOPEC Geophysical Company Pty Ltd.